UNIVERZITA PALACKÉHO V OLOMOUCI

Přírodovědecká fakulta

Katedra biochemie

Skupina proteinů ARF v ječmeni a jejich role v zakládání a vývoji nodálních kořenů

Diplomová práce

Autor:	**Bc. Nikola Kořínková**
Studijní program:	B1406 Biochemie
Studijní obor:	Biotechnologie a genové inženýrství
Forma studia:	Prezenční
Vedoucí práce:	**Véronique Hélene Bergougnoux-Fojtík, Ph.D.**
Rok:	2019

PALACKÝ UNIVERSITY OLOMOUC

Faculty of science

Department of biochemistry

ARF family in barley (*Hordeum vulgare* L.) and their role in crown-root initiation and development

Master thesis

Author:	**Bc. Nikola Kořínková**
Study program:	B1406 Biochemistry
Field of study:	Biotechnology and Genetic Engineering
Form of study:	Full-time
Supervisor:	**Véronique Hélene Bergougnoux-Fojtík, Ph.D.**
Year:	2019

I declare that I developed this master thesis separately with showing all the sources and authorship. I agree with the publication of the thesis by Act no. 111/1998 Coll., about universities, as amended. I was awared of that the rights and obligations arising from the Act no. 121/2000 Coll., the Copyright Act, as amended, are applied to my work.

In Olomouc .....

Acknowledgments

I wish to express my sincere gratitude to my supervisor Véronique Hélene Bergougnoux-Fojtík, Ph.D. for her professional guidance throughout the study, constructive criticism and suggestions during preparation of the master thesis and the positive attitude. I also want to thank Dieu Thu Nguyen, Msc. for the continuous help during the work on the practical part of the thesis. My thanks also belong to my family and close friends for the support during the whole study.

Bibliografická identifikace

Jméno a příjmení autora	Nikola Kořínková
Název práce	Skupina proteinů ARF v ječmeni a jejich role v zakládání a vývoji nodálních kořenů
Typ práce	Diplomová
Pracoviště	Katedra biochemie
Vedoucí práce	Véronique Hélene Bergougnoux-Fojtík, Ph.D.
Rok obhajoby práce	2019

Abstrakt

AUXIN RESPONSE FACTOR (ARF) proteiny představují velkou rodinu transkripčních faktorů, jejichž funkcí je aktivace nebo represe genů primární odpovědi na auxin. ARF jako součást auxinové signální dráhy regulují mnoho vývojových procesů rostlin. Byla studována role ARF proteinů v procesu zakládání a vývoje nodálních kořenů v ječmenu. V této práci bylo identifikováno 21 ARF proteinů v ječmenu, z nichž 8 ARF byla predikována funkce aktivátorů a 13 funkce represorů. Byla vytvořena teplotní mapa exprese *ARF*, která ukazuje, že většina *ARF* genů je exprimována napříč různými pletivy ječmene a úroveň jejich exprese se mění během vývoje. U *ARF* represorů byly pozorovány změny v expresních profilech během raného vývoje báze stonku, které naznačují roli těchto ARF v procesu tvorby nodálních kořenů. Pro budoucí analýzu prostorového rozložení *ARF* transkriptů v bázi stonku byl zdokonalen protokol *in situ* PCR a byly navrženy další kroky pro optimalizaci této metody. V následující části práce byl určen kandidátní ARF na funkci hlavního inhibitoru nodálních kořenů v ječmenu. Byly připraveny konstrukty pro vypnutí kandidátního genu *HvARF13* pomocí CRISPR-Cas9. Metodou transformace nezralých embryí ječmene pomocí *Agrobacterium tumefaciens* bylo získáno 6 transgenních rostlin. Mutace v sekvenci *HvARF13* byla potvrzena u jedné rostliny. Výsledky prezentované v této práci pomohou dále charakterizovat roli ARF v ječmenu.

Klíčová slova	nodální kořeny, *Hordeum vulgare* L., ARF, auxin
Počet stran	87
Počet příloh	0
Jazyk	Anglický (český)

Bibliographical identification

Author's first name and surname	Nikola Kořínková
Title	ARF family in barley and their role in crown-root initiation and development
Type of thesis	Master
Department	Department of biochemistry
Supervisor	Véronique Hélene Bergougnoux-Fojtík, Ph.D.
The year of presentation	2019

Abstract

AUXIN RESPONSE FACTORs (ARFs) represent a large family of transcription factors, that function as either activators or repressors of the early auxin-responsive genes. As a part of the auxin signaling pathway, ARFs regulate many developmental processes in plants. The role of ARFs in the process of crown-root initiation and development in barley was studied. In this work, 21 ARF proteins were identified in barley. From these, 8 ARFs were predicted to act as activators and 13 as repressors. A heat-map of *ARF* expression was generated, showing that most *ARF* genes are expressed among different barley tissues and the level of their expression varies during development. Focusing on the ARF repressors, changes in the expression profiles during the early crown development were observed, suggesting a role of these ARFs in the process of crown-root formation. For future analysis of the spatial distribution of *ARF* transcripts in crown tissue, *in situ* PCR protocol was improved and further optimization steps were proposed. In the next part, a candidate for the main inhibitor of crown-roots in barley was determined. Constructs for the CRISPR-Cas9-mediated knock-out of the candidate *HvARF13* gene were prepared. By the method of *Agrobacterium tumefaciens*-mediated transformation of barley immature embryos, six transgenic plants were obtained. Mutation in *HvARF13* sequence was confirmed in one plant. Altogether, results presented in this thesis will help to further characterize the role of ARFs in barley.

Keywords	crown-roots, *Hordeum vulgare* L., ARF, auxin
Number of pages	87
Number of appendices	0
Language	English (Czech)

Table of contents

Aims

The aim of the theoretical part was to review the last insights concerning crown-root initiation and development in monocot plants, to establish a parallel between the crown-roots of monocots and the adventitious roots of Arabidopsis, and to determine the role of auxin and AUXIN RESPONSE FACTORs (ARFs), a specific group of transcription factors, in this process.

The main aims of the practical part included identification of ARFs in barley and expression analysis of *ARF* genes in different tissues of barley plant, as well as during the crown-root initiation and development. The goal of the thesis was to focus on a potential repressor of crown-root initiation and development, and to obtain knock-out barley lines in this repressor by the means of CRISPR-Cas9 system and *Agrobacterium tumefaciens*-mediated barley transformation.

1 INTRODUCTION

Facing nowadays environmental problems, increasing agricultural productivity became one of the most important tasks in the field of crop breeding. The main objectives of breeding programs include higher-yielding and resistance to drought and diseases. Understanding the molecular regulation of agronomically important traits allows to apply targeted approaches of molecular breeding, leading to acceleration of the whole breeding process (ICARDA, 2005).

For its high adaptability to different environmental conditions, barley is an interesting target for crop improvement. As a monocot plant, barley has a fibrous root system, which comprises embryonic primary and seminal roots, and post-embryonic crown-roots and lateral roots (Hackett and Rose, 1972). Crown-roots develop from the crown of the seedling, positioned at the junction between roots and the shoot. As an integral part of barley root system, crown-roots participate in water and nutrient acquisition, adaptability to environmental stress or anchoring the plant in the soil (Hackett, 1968). Uncovering the regulatory mechanism of crown-root initiation and development could be a key to enhancement of the barley root system.

In rice, the plant model to study root initiation in monocots, crown-roots initiate from the ground-meristem (Itoh *et al*., 2005). Generation of the auxin maxima in the cells of the ground meristem primes a specific cell towards the first division, which initiates the crown-root. The auxin cascade during crown-root initiation involves AUXIN/INDOLE-3-ACETIC ACID (Aux/IAA) proteins, AUXIN RESPONSE FACTORs (ARFs) and their target genes (Inukai *et al*., 2005). ARFs bind to the auxin-responsive element (AuxRE) present in the promoters of early auxin-responsive genes (Ulmasov *et al*., 1997). Controlling the transcription of auxin-responsive genes, ARFs can either promote or repress the development of crown-root primordia (Inukai *et al*., 2005).

However, there is still lack of information about the roles of individual ARF isoforms in the process of crown-root formation in monocot plants. Therefore, insights from the molecular mechanism of shoot-borne adventitious root development in Arabidopsis were used for our purpose. This thesis aimed to characterize members of ARF protein family in barley and to analyse their roles in crown-root formation. Also, a knock-out of the main inhibitor of crown-root formation was intended, in order to obtain barley lines with improved root system.

2 CURRENT STATE OF THE TOPIC

2.1 Barley (*Hordeum vulgare* L.)

Barley belongs to the grass family *Poaceae*. It was domesticated about ten thousand years ago in the region of the Fertile Crescent from the wild relative *Hordeum spontaneum*. While *H. spontaneum* is still present in the original habitat of Near East and secondary habitats of central and southwestern Asia, the harvested area of *H. vulgare* extends from subarctic to subtropical zones, reflecting its high adaptability and resistance to different environmental conditions, including dry heat (Badr *et al*., 2000).

Over the last ten years the average world production of barley was 141,7 million metric tons. In 2017 the world barley production reached 144,3 million metric tons, harvested from 48,1 million hectares. With 59,1 million metric tons produced, the European Union is the world number one producer of barley, followed by Russia with 20,2 million metric tons and Australia with 8,9 million metric tons (Statista, [2018]; USDA, 2018).

In the past, barley was used as a bread plant for Hebrews, Greeks, Romans and later also for Europeans. Today, 65 % of barley world production is used as livestock feed and another 33 % for malting in the brewing industry (Sullivan *et al*., 2013). In the Czech Republic, barley occupies a special position among crop plants. It is an irreplaceable material in the brewing industry for its ability to produce malt, wort and dextrin-rich final product with favorable properties. As the "Czech beer" is an official Protected Geographical Indication given by the European Union, the quality of barley varieties is strictly controlled. Barley varieties used to produce Czech beer should meet certain conditions. These varieties should exhibit lower proteolytic activities, cytolytic activities and lower fermentation rate leading to residual extract. Lately, breeders focus on special Czech varieties that would combine all these required traits. But breeding such a variety is not an easy task. The quality of malting barley is based on polygenic traits that are difficult to select (Sedláček *et al*., 2017).

Only 2 % of the total barley production is used for human consumption. Barley has a very good potential to become a so-called functional food. Diplock *et al.* (1999) define functional food as: "Food products can only be considered functional if together with the basic nutritional impact it has beneficial effects on one or more functions of the human organism, thus either improving the general and physical conditions or/and decreasing the risk of the evolution of diseases." Its dietary benefit is in the high content of carbohydrates and moderate content of protein, calcium and phosphorus.

Indeed, as cereal, barley contains beneficial amount of β-glucans, which contribute to reduce the risk of heart diseases and reduce the blood glucose. Depending on the barley genotype, the content of β-glucans can vary from 2,40 to 7,42 g/100 g. Moreover, barley is a dietary source of bioactive compounds such as phenolic acids, flavonoids, lignans, tocols (both tocopherols and tocotrienols), phytosterols and folate. All these compounds combined in a healthy diet containing barley exhibit strong antioxidant, antiproliferative, and cholesterol lowering abilities. For this reason, there is an ongoing research trying to examine the role that barley could have in reducing the rate of common nutrition-related diseases, including cancer, cardiovascular disease, diabetes and obesity (Bonoli *et al*., 2004; Idehen *et al*., 2017; Martínez *et al*., 2018).

Across Europe, both six-row and two-row types of spring and winter barley are cultivated. There are several factors that farmers have to face to get satisfying yield and quality of produced barley. The abiotic factors that can be controlled include the technology of cultivation or sufficient source of nutrition. From the initial phase of growing, barley requires a huge amount of nutrients available in the upper layer of the land. The most common nutritional deficiency is caused by the lack of cadmium or magnesium in the land. Cadmium deficiency can affect the number of tillers formed, and also induce yellowing/whitening of the leaves. Plants deficient in magnesium usually exhibit typical yellow spots on their leaves. Therefore, the standard application of 5-7% solution of urea is supplemented by leaf nutrition containing P, K, Mg, S (Bezdíčková *et al*., 2005; Bittner, 2008).

In opposite, environmental factors such as cold weather, drought, high temperatures or intensive UV radiation cannot be controlled. These stress conditions usually cause drying up of tillers, necrosis and general thinning of vegetation. Of course, the biotic factors are not of less significance. The most frequent barley diseases are yellow dwarf virus, wheat dwarf virus, barley yellow mosaic virus and powdery mildew. Pests feeding on barley can be represented by *Heterodera avenae* Wollenweber, *Limothrips denticornis* or aphids (*Rhopalosiphum padi* L.) (Bittner, 2008). In order to be able to respond to these environmental conditions, breeders are constantly trying to improve the required characteristics of barley cultivars.

2.2 Root system

Root system represents an integral part of the plant body. As underground plant organs, roots facilitate not only nutritional but also structural support for the plant body. Being in close contact with the soil, roots ensure water and nutrient uptake and, in some cases, also the storage of material. By creating an extensive root system, they can fix the plant into the ground and provide stability. Apart from the main functions, roots can also form symbiotic, aerial or contractile structures (Fahn, 1990; Smith *et al*., 2010). Regarding the root anatomy, specific cell layers can be determined in the cross section of a root (Fig. 1). From the root surface, there is root epidermis, cortex cell layers (8 to 15 layers in cereals), endodermis and central cylinder. Along the longitudinal axis of a root, four different zones can be distinguished (Fig. 1). The root cap, meristematic and elongation zones are basically constant in size during plant life. In opposite, the differentiation zone expands in time (Smith *et al*., 2010). All the root cells originate in the root apex. In the root apex, there is a quiescent center, where cell cycling is strictly controlled (Clowes, 1975; Romberger *et al*., 1993). From the quiescent center, cells migrate to its boundary and become initials of root cell files. There are different initials to give rise to vascular

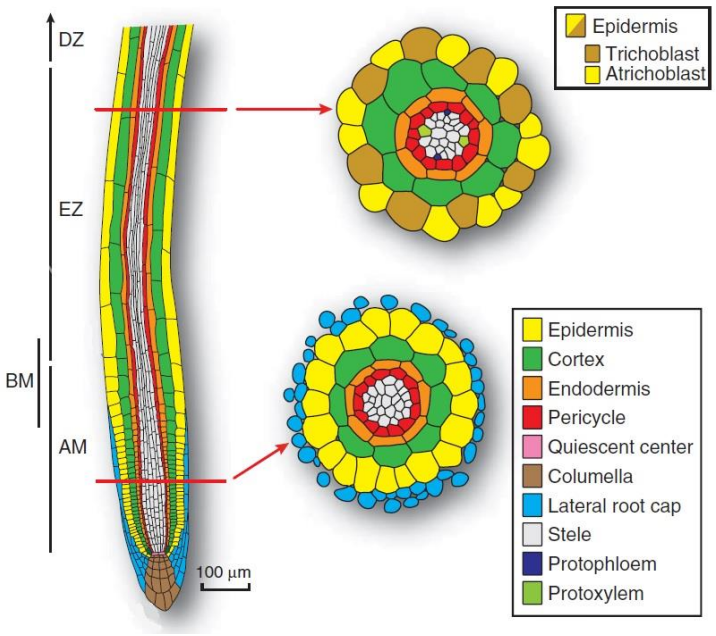

Figure 1 Schematic representation of the root anatomy. Along the longitudinal axis of the root (on the left), there are apical meristem (AM), basal meristem (BM), elongation zone (EZ) and differentiation zone (DZ). On the cross section of the root (on the right), individual cell files can be distinguished (adapted from Overvoorde *et al*., 2010).

cylinder, ground tissue (cortex/endodermis) or columella, the longitudinal axis of a root cap (Romberger *et al*., 1993). In this way, continuous growth of a root is perfectly maintained.

Generally, there are two types of root systems, the tap root system and the fibrous root system (Fig. 2). The tap root system is typical for dicotyledonous plants and it consists of the tap root and its side branches. The tap root evolves from embryonic root, radicle, and it grows deep into the soil. During development, the tap root undergoes secondary thickening and it becomes rather a storage and anchorage organ. Branching of the root system is ensured by the roots arising from the primary root, the lateral roots (LRs) and root hairs. On the contrary, the fibrous root system is typically formed by monocotyledonous plants. Most of this root system consists of post-embryonically formed nodal roots, arising from the basal part of the stem. The nodal roots can further branch to all directions and give rise to a very dense root system (Fahn, 1990).

Although the cereals also form a fibrous root system, they possess some special features. In barley, the root system consists of embryonic seminal and post-embryonic nodal roots (Hackett, 1968). In comparison, the root system of maize (*Zea mays*) comprises one additional embryonic root type, which is derived from the scutellar node of an embryo (Hochholdinger and Tuberosa, 2009). As the plant embryo develops, the radicle is formed at the basal pole, giving rise to a seminal root soon after germination (Hackett, 1968). In monocots, the seminal root is important mainly in the early

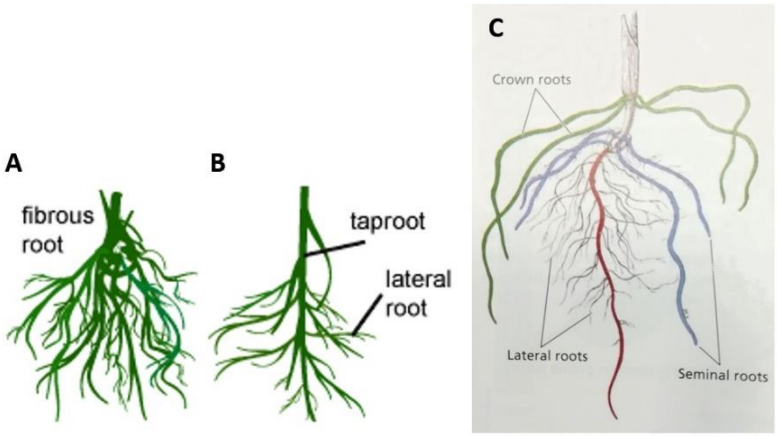

Figure 2 Schematic representation of different types of root systems. A, fibrous root system typical for monocot plants; B, taproot system typical for dicot plants; C, maize root system with the primary root (red), seminal roots (blue), crown-roots (green) and lateral roots (adapted from Hochholdinger and Tuberosa, 2009; SCQ, 2019).

development. To enlarge the overall volume of the root system, the seminal root forms a first-order, second-order or even third-order LRs (Hackett and Rose, 1972). In barley, LRs can develop either from pericycle or endodermis (Fahn, 1990). In maize, not all pericycle cells are of the same size. The pericycle cells that can initiate LR formation are bigger in size compared to the rest of pericycle cells (Jansen *et al*., 2012). LRs are formed acropetally, with the youngest primordium formed closest to the root tip in the differentiation zone of the root.

In the cereal root system, the nodal roots are of a great importance as well. The nodal roots can contribute to more than 50 percent of the root system, helping to enlarge the volume of soil explored. Number of nodal roots formed on a mature plant is highly dependent on growth conditions, including sowing density, thermal time or nutrients in the soil. In favorable conditions, mature barley plants can form up to 140 nodal roots, thus representing the majority of barley root system (Hecht *et al*., 2018). In barley, rice or other cereals, the nodal roots are also called crown-roots (CRs), for their origin in the base of the main stem, the crown (Hackett, 1968). The crown is one of the most vulnerable tissues of the plant body. It not only generates new CRs and tillers, but also ensures the translocation of water, nutrients and photosynthates between the underground and aerial parts of a plant (Fenster *et al*., 1972). Typically, CRs of a young plant are of the same length as the seminal root and make many LRs. Later, the newly formed CRs become shorter, thicker and less branched (Hackett, 1968).

The development of CRs can be demonstrated on a rice model. Rice together with barley, wheat, maize or sorghum, shares a common ancestor. Therefore, it can be assumed that they will also share some similar features. In the development of the seminal root, meristem is differentiated already in the early embryo. Unlike the seminal root, the formation of crown-root meristem must be initiated in a mature tissue. Itoh *et al*. (2005) describe 7 stages of CR development in rice (Fig. 3). (1) In the first stage, the crown-root primordium (CRP) will initiate from the ground meristem, adjacent to the peripheral cylinder of vascular bundles in the stem. Cells of the ground meristem divide to form a group of initials. (2) The inner layer of this initials group gives rise to epidermal/endodermal initial cell and central cylinder initial cell; the root-cap initial cell derives from the outer layer of the group of initial cells. (3) The meristematic activity of epidermal/endodermal initial cell produces epidermis and endodermis. At the same time, the root-cap initial and central cylinder initial differentiate into corresponding tissues.

(4) When the endodermis is established, it can undergo periclinal divisions to form cells of the cortical layer. (5) At this stage, the primordium already possesses the basic organization with the root cap. Also, the first meta-xylem vessel can be distinguished. (6) First signs of cell elongation and vacuolation can be observed in the most basal region of stele. (7) Cell elongation can be already seen in all tissues of the basal part of primordium, followed by emergence of the primordium out of the stem. Also, the vascular connection with the original tissue must be established to nourish the newly formed root.

Apart from the essential parts of a root system, whose development is strictly regulated, some plants have the ability to form so-called adventitious roots. In some plants, adventitious rooting is a natural process, while in other plants it is induced by external stress signals. Depending on the plant species, adventitious root can originate from stem/hypocotyl, leave, non-pericycle tissue of a root, cortical tissue of buds and many other types of tissue (Li *et al*., 2009). In Arabidopsis, the pericycle cells can form adventitious roots directly without external stimulus. In opposite, indirect adventitious rooting requires an external signal and establishment of a callus from pericycle and endodermal cells (Falasca and Altamura, 2003). The ability to form adventitious roots was and still is widely used in the vegetative propagation of plants.

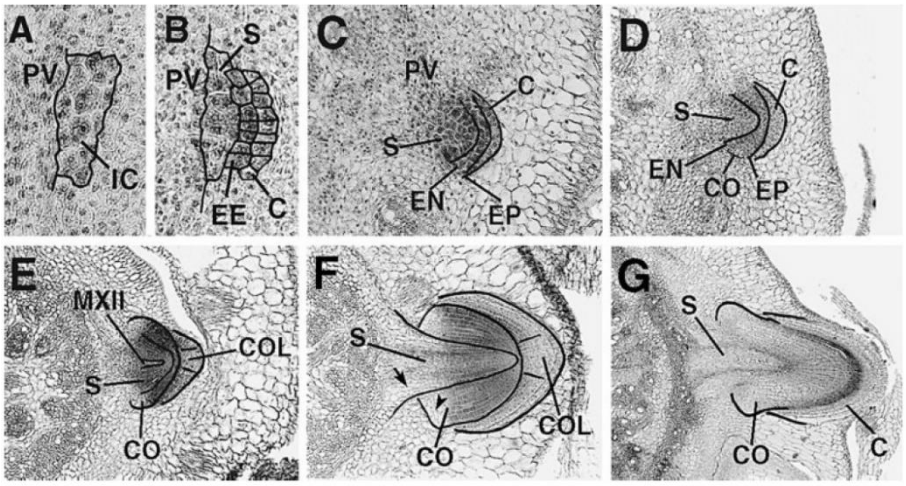

Figure 3 Initiation and development of a CRP in rice. A, initial cells are established; B, epidermis-endodermis and root-cap initials are established; C, epidermis and endodermis differentiate; D, cortex differentiates; E, general organization of a CRP is established; F, cells elongate; G, CRP emerges. IC, initial cells; PV, peripheral cylinder of vascular bundle; C, root cap or its initial; EE, epidermis–endodermis initials; S, stele; EP, epidermis; EN, endodermis; CO, cortex; COL, columella; MXII, late meta-xylem vessel (from Itoh *et al*., 2005).

2.3 Auxin in root development

Auxin is a small molecule belonging to the family of phytohormones. It participates in several processes throughout the plant life. Its impact can be observed already during the plant embryogenesis, followed by modulation of plant organogenesis, tissue patterning or tropisms (Saini *et al*., 2013). Auxin has a central role in the regulation of root system architecture, determining the root hair length, primary root length, different stages of LR development and the root response to gravity (Overvoorde *et al*., 2010).

For the great impact of auxin, plants need to ensure a precise control of auxin levels and localization in different tissues. The majority of auxin is synthesized in young leaves and cotyledons in the form of indole-3-acetic acid (IAA) (Ljung *et al*., 2001). But auxin can be generated also directly in roots, contributing to establishment of auxin gradient right in the spot (Ljung *et al*., 2005). The main precursor for IAA biosynthesis is tryptophan (Trp). Trp is converted to indole-3-pyruvate (IPA) molecule by Trp aminotransferase. Subsequently, IPA is converted to IAA in a reaction catalyzed by YUCCA flavin monooxygenase (Stepanova *et al*., 2008; Stepanova *et al*., 2011). Apart from biosynthesis, plants can increase the endogenous levels of auxin by releasing free active IAA from its conjugates with sugars, amino acids or peptides (Ljung *et al*., 2005). Release of free active IAA can also result from the conversion of the indole-3-butyric acid (IBA) through the activity of peroxisomal enzymes (Ludwig-Müller, 2000; Zolman *et al*., 2000).

Two types of transport systems cooperate to deliver auxin molecules to root. From the aerial parts of biosynthesis, auxin is transported by the bulk flow of phloem right to the root tip (Ljung *et al*., 2001). After the ionization of IAA molecules in the environment of the root tip cells, the polar auxin transport (PAT) apparatus facilitates the directional flow of auxin molecules. Two classes of transmembrane proteins control either the influx or efflux of auxin molecules by cells. To enter the plant cell, auxin must be relocated by AUXIN RESISTANT1 (AUX1) or LIKE AUX1 (LAX) transporter proteins (Bennett *et al*., 1996; Geisler and Murphy, 2006). The proteins of the PIN-FORMED (PIN) transporter family, together with a minor contribution of P-GLYCOPROTEIN ABC transporter protein family, translocate IAA out of the cells (Petrásek *et al*., 2006). These transporters set the direction of auxin flow from the root tip, through the root cap, root epidermis, cortex layers to basal region of a root (Swarup *et al*., 2001).

The PAT is primordial for the determination of the root meristem with a quiescent center. Already in the early embryo development, PAT determines the basal pole of the embryo (Smith *et al*., 2010). Later, the specific accumulation of auxin in the root tips activates the transcription of *PLETHORA* (*PLT*), *SCARECROW* and *SHORT ROOT* genes, which define the quiescent center. Especially, high levels of PLT proteins are associated with stem cell identity. With increasing distance from the quiescent center, the presence of PLT drops, allowing cell division and differentiation (Aida *et al*., 2004; Blilou *et al*., 2005).

IAA plays important role at different times during the initiation and development of the LRs. Firstly, it was observed that the position of a LR on the primary root is determined by local auxin gradients in Arabidopsis (Benková *et al*., 2003). An auxin maximum, mediated by PAT, is established in protoxylem cells; in the pericycle, the neighboring cells give rise to founder cells of the future LR primordium (LRP) (Beeckman *et al*., 2001). As the auxin maximum targets only few pericycle cells and the auxin gradient is not continuous, it leads to regular spacing of LRs. Secondly, when the position of the LRP is determined and the formation of the LRP is initiated, IAA accumulates in the initials, where it helps to promote the cell divisions by activating cell cycle-related genes (Himanen *et al*., 2002). Once the primordium is formed, IAA accumulates in the central region of the primordium, slowly relocating to the tip of the LRP (Benková *et al*., 2003). Thanks to the activity of LAX3 transporter, IAA enters endodermal and cortex cells surrounding the primordium, where it mediates their cell wall loosening, allowing the emergence of the primordium from the root (Swarup *et al*., 2008). When the process of LR development was studied in maize, some differences were discovered. In maize, the auxin maximum is rather formed in the protophloem elements, targeting the pericycle cells at phloem pole for LR initiation (Jansen *et al*., 2012).

Even though auxin plays a central role in root development, the cooperation with other phytohormones is necessary. In general, brassinosteroids and polyamines have a positive effect on a primary root, LR and root hair development; while, gibberellins, abscisic acid, jasmonic acid and cytokinins have rather negative effect on LRs. Both strigolactones and ethylene negatively affect LR development, but they can affect root hairs in a positive way (Saini *et al*., 2013). Auxin and cytokinins have antagonistic functions in the process of root growth, determination of root meristem cells and LR formation. Specifically, cytokinins influence auxin transport and homeostasis through inhibition of *PIN* genes

transcription (Benjamins and Scheres, 2008). Also, auxin and ethylene crosstalk is very important in the root development. Ethylene inhibits auxin transport and regulates its biosynthesis, hindering LR formation and root growth (Negi *et al*., 2008).

2.3.1 Auxin-induced crown-root initiation

As a model for monocot plants, much effort has been made to describe the molecular mechanisms responsible for CR initiation and development in rice. The current knowledge allowed to draw a model of the signaling pathway that integrates auxin and finally controls the CR initiation in monocot plants (Fig. 4). According to Meng *et al*. (2019), all the auxin-dependent processes involved in root development depend on the PAT, which can be either positively or negatively regulated. The positive regulation comes from CROWN ROOTLESS4 (CRL4)/OsGNOM1. This component of the pathway was discovered thanks to a *crl4* rice mutant possessing apparent defects in crown and LRs. The *CRL4/OsGNOM1* gene codes for an ADP-ribosylation factor-guanidine exchange factor and the gene is expressed at the site of CRP initiation. CRL4/OsGNOM1 is necessary for establishing the PAT, controlling the localization and recycling of OsPIN1, the auxin efflux carrier protein (Kitomi *et al*., 2008). Also, CRL4/OsGNOM1 affects the expression of other *PIN* genes, *OsPIN2*, *OsPIN5b* and *OsPIN9* in the stem base (Liu *et al*., 2009). The negative regulation of PAT is mediated by OsRPK1, a leucine-rich repeat receptor-like kinase. OsRPK1 is induced by auxin and its overexpression caused the inhibition of *PIN* genes expression and adventitious roots formation. OsRPK1 possibly acts as a link between external stimuli and auxin carriers (Zou *et al*., 2014).

PIN carriers together with AUX influx carriers are responsible for PAT. When the appropriate auxin pattern is formed, it is sensed by the auxin receptors TRANSPORT INHIBITOR RESPONSE1 (OsTIR1) or AUXIN F-BOX (OsAFB). At this point, auxin signaling is under the control of the miR393a, a microRNA molecule expressed in the CR and LR primordia. The miR393a targets *OsTIR1* transcripts, thus controlling the CR initiation. The following steps of the signaling pathway are similar to those responsible for LR formation in Arabidopsis, suggesting a high level of conservation across different plant species and root types. As in Arabidopsis, the rice OsTIR1 interacts with a member of the AUXIN/INDOLE-3-ACETIC ACID (Aux/IAA) family, OsIAA1 (Bian *et al*., 2012).

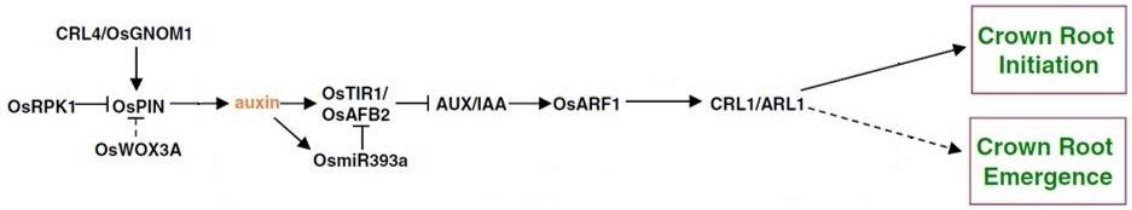

Figure 4 Signaling pathway regulating CR initiation and emergence. Lines ending with an arrowhead indicate positive regulation. Lines ending with a flat head indicate negative regulation. Regulation represented by dashed lines has not been experimentally confirmed (adapted from Meng *et al*., 2019).

There are 31 members of the Aux/IAA family in rice, which repress the transcriptional activity of AUXIN RESPONSE FACTORs (ARFs) (Jain *et al*., 2006; Wang *et al*., 2007). The detailed function of these two protein families in auxin signaling will be described in detail in Chapter 2.3.3.2. The importance of ARF transcription factors lies in the activation of target genes. In the case of CR initiation, the most important target gene of ARFs is *CROWN ROOTLESS1* (*CRL1*). The *CRL1* gene was described thanks to the *crl1* mutant, which was unable to form CRP. *CRL1* encodes an ASYMMETRIC LEAVES2/LATERAL ORGAN BOUNDARIES-domain (LBD) transcription factor, a homolog of the LOB-DOMAIN16 (LBD16) and LBD29 in Arabidopsis (Inukai *et al*., 2005; Liu *et al*., 2005). The promoter region of the *CRL1* gene possesses two auxin-responsive elements (AuxRE), AuxRE1 (TGTCTC) and AuxRE2 (GAGACA), and is a target of OsARF1 (Inukai *et al*., 2005). In general, the expression of *CRL1* colocalizes with the distribution of auxin, showing an accumulation in the ground meristem and CR meristem. It was also observed that the expression of *CRL1* can be induced by the application of exogenous auxin, with the highest accumulation of *CRL1* transcripts 1 to 3 hours after treatment (Inukai *et al*., 2005; Liu *et al*., 2005; Coudert *et al*., 2011). As a transcriptional activator, CRL1 was found to regulate up to 277 genes (Coudert *et al*., 2015). The LBD proteins bind to a specific sequence in the promoter of their target genes [5´-(G)CGGC(G)] to induce their transcription (Husbands *et al*., 2007). The significance of CRL1 is even bigger, considering that many of its target genes also code for transcription factors. The importance of auxin signaling in root development is reflected by the high degree of conservation of the final signaling targets between monocot and dicot plants. But still a number of CRL1-target genes do not have homologs in Arabidopsis. Therefore, those genes have been proposed to be involved specifically in the shoot-borne root initiation in monocot plants (Coudert *et al*., 2015).

Later, other rice mutant plants defective in CRs were discovered, revealing new factors involved in the CR initiation. For example, *CRL6* gene codes for a member of the CHD (chromodomain, helicase/ATPase, DNA-binding domain) family, representing an ortholog of *PICKLE* (*PKL*) in Arabidopsis. The *CRL6* gene is expressed in the stem base, where CRs are initiated. Even though the precise position of CRL6 in the signaling pathway is not clear, it has a very important role in the regulation of the expression of several components of the auxin signaling pathway, such as *OsIAA* genes, *CRL4/OsGNOM1*, *CRL1*, *OsPIN1* and others (Wang *et al*., 2016). But auxin is not the only plant hormone involved in the CR initiation. Both cytokinin content regulation and cytokinin-dependent signaling represent an alternative way of CR initiation (Meng *et al*., 2019).

2.3.2 Lateral roots and adventitious roots of Arabidopsis as a model for crown-root research

As CRs and LRs share several common features, the knowledge from Arabidopsis LR development can serve as a model for CR initiation research. A huge progress has been made in determining the exact molecular modules involved in certain steps of LR development in Arabidopsis. In the first step, the position of the LR must be determined and the process of LR development must be induced. LR emerge from the pericycle cells of the primary root, where the Aux/IAA28-AtARF7/AtARF19 module specifies the founder cells and promote the nuclear migration that is a pre-requisite for the division of two neighboring cells (De Rybel *et al*., 2010). After the induction of LRP, the Aux/IAA14-AtARF7/AtARF19 module is targeting *LBD16* to initiate the first asymmetrical division (Okushima *et al*., 2007). When the process of LR development is initiated, the same module also targets *LBD18*, *LBD33* and *LBD29* to regulate the following cell divisions by activation of E2F transcription factor and D-type cyclin genes (Berckmans *et al*., 2011; Feng *et al*., 2012). Then, Aux/IAA14-AtARF7/AtARF19 module works in cooperation with Aux/IAA12-AtARF5 to set the pattern of LR growth (De Smet *et al*., 2010). In the last steps, *LBD16*, *LBD18* and *LBD29* genes are the main targets of the auxin signaling. The LBD transcription factors activate genes involved in loosening and remodeling of the cell wall, thus allowing emergence and development of the LR (Lee *et al*., 2009; Lee *et al*., 2015; Porco *et al*., 2016).

Even though the mechanism of LR development in Arabidopsis highlighted auxin signaling, LRs still arise from root tissue. For that reason, the mechanism of shoot-borne adventitious rooting in Arabidopsis might represent a more suitable model for the study of CR initiation. Phenotypic analysis of Arabidopsis mutant lines affected in *ARGONAUTE1*, *AtARF6*, *AtARF8* or *AtARF17* genes suggested that lateral and adventitious rooting is controlled by distinct pathways. Indeed, mutants were altered in adventitious rooting but showed no changes in the ability to form LRs. During adventitious root initiation, AtARF6 and AtARF8 act as positive regulators and AtARF17 as a negative regulator (Sorin *et al*., 2005; Gutierrez *et al*., 2009). Both *AtARF6* and *AtARF8* genes are highly expressed in adventitious root primordia together with *miR167* which controls their accumulation. In opposite, *AtARF17* is expressed in the vascular tissues near the site of primordium initiation. The expression of ARF regulators is not only controlled by miRNA but responds also to different light conditions. Whereas light induces the accumulation of the *AtARF6* and *AtARF8* transcripts, it has an opposite effect on *AtARF17*. Most likely, AtARF17 competes with AtARF8 in regulation of *GRETCHEN HAGEN3* (*GH3*) genes which are very tightly connected to adventitious root development (Sorin *et al*., 2005; Gutierrez *et al*., 2009; Gutierrez *et al*., 2012). In this complex network, all the regulatory processes aim to set a balance between activators and repressors (Gutierrez *et al*., 2009).

2.3.3 Auxin response factors

Auxin response factors are transcription factors encoded by a multi-gene family. The first ARF transcription factor to be studied was AtARF1 in Arabidopsis, which was shown to activate transcription by binding to AuxRE-containing promoters in the yeast one-hybrid system (Ulmasov *et al*., 1997). Since then, 23 members of the ARF family have been identified in Arabidopsis. The *ARF* genes are distributed among all 5 Arabidopsis chromosomes. Near the centromere of chromosome 1, there is a cluster of 7 *ARF* genes, including *AtARF12-AtARF15* and *AtARF20-AtARF22*. The gene cluster is believed to be formed due to tandem duplications (Remington *et al*., 2004). There is also an evidence that the clustered genes may have overlapping functions as they are all expressed during embryogenesis, especially in the region surrounding the embryo (Okushima *et al*., 2005; Rademacher *et al*., 2011). Based on the phylogenetic analysis, Arabidopsis *ARF* genes are separated into three classes. Most of the family members belong to the class I, which

comprises all the genes from the cluster on chromosome 1 and also *AtARF1-AtARF4*, *AtARF9*, *AtARF11*, *AtARF18*, *AtARF23*; the class II comprises *AtARF5-AtARF8* and *AtARF19*; finally, the class III contains only three members: *AtARF10*, *AtARF16*, *AtARF17* (Okushima *et al*., 2005).

In rice, 25 *OsARF* genes were identified, coding for 19 full-length proteins and 6 truncated proteins, missing the C-terminal domain. The molecular weight of OsARFs ranged between 57 and 123 kDa (Wang *et al*., 2007). In recent years, there has been a boom in genome-wide identifications of *ARF* genes across different plant species. Most of the genome-wide studies include phylogenetic analysis, analysis of the chromosomal distribution, and scheme of the gene structure and protein domain organization. And most of the studies are enriched in gene expression analysis in different plant tissues or in different conditions. To date, about 30 different plant species were subjected to *ARF* gene identifications. Among the common model plants, 36 *ARF* genes were identified in maize, 22 in tomato (*Solanum lycopersicum*), 51 in soybean (*Glycine max*), 31 in *Brassica rapa* and 19 in grapevine (*Vitis vinifera*), as a model for berry development in fruit plants (Mun *et al*., 2012; Wang *et al*., 2012; Ha *et al*., 2013; Wan *et al*., 2014; Zouine *et al*., 2014). Recently, legume plants have attracted attention thanks to their interaction with nitrogen-fixing bacteria. In chickpea, 28 *ARF* genes were identified. The study of cis-regulatory elements of their promoter indicated a putative regulation by abiotic stress and symbiosis (Singh *et al*., 2017; Die *et al*., 2018). In *Medicago truncatula*, 24 *ARF* genes were identified and the role of ARF proteins in the process of nodule initiation will be further studied (Shen *et al*., 2015). But the genome-wide identifications of *ARF* genes are being performed also on quite unusual species, which can be important for certain branches of industry. For example, the Siberian apricot (*Prunus sibirica*) or the physic nut (*Jatropha curcas*) are potential sources of biofuels. In these species ARF families are being studied to get better insight into developmental processes and resistance to abiotic stresses (Niu *et al*., 2018; Tang *et al*., 2018). Some of the authors suggested that high number of isogenes could be important for adaptation to changing environment. Genome-wide studies can provide valuable information for future functional verification of selected candidates. Finally, this knowledge can be used in molecular breeding for specific improvement of different cultivars.

2.3.3.1 Protein structure

In Arabidopsis, over the 23 *ARF* genes, 19 encode full-length proteins, comprising all typical ARF protein domains (described below). The *AtARF13* gene contains the sequence for C-terminal domain, but due to its out-of-frame position, the final protein product is missing this domain. *AtARF3* and *AtARF17* genes are completely devoid of the C-terminal domains. Finally, the last *ARF* gene, *AtARF23*, is a pseudogene with a stop codon positioned in the sequence for the DNA-binding domain (DBD) (Guilfoyle and Hagen, 2001).

In general, ARF proteins consist of 3 different structural regions (Fig. 5). The N-terminal part of the protein is responsible for DNA-binding ability of ARFs. The DNA-binding region itself is constituted of 3 separate protein domains: B3-type domain, Dimerization domain and an ancillary domain. The B3-type domain ensures the interaction with DNA (Tiwari *et al*., 2003). The high-resolution crystal structures of Arabidopsis AtARF1 revealed a seven-stranded open β-barrel structure of B3-type domain, which comprises the residues 120 to 226 of AtARF1. The B3-type domain is surrounded by the Dimerization domain (DD) sequences on both N- and C-termini, resembling an insert of B3-type domain in the DD (Boer *et al*., 2014). The DD forms an antiparallel five-stranded central β-sheet. The name of the domain is derived from its function as the essential determinant of dimerization of ARFs after DNA binding. The role of DD was studied in an Arabidopsis *arf5* mutated in several amino acids in the DD region. The *arf5* mutant was unable to form an embryonic root and had several growth defects. These observations suggested that dimerization ensured by DD is important for the proper function of AtARF5. This can be partially explained by increased

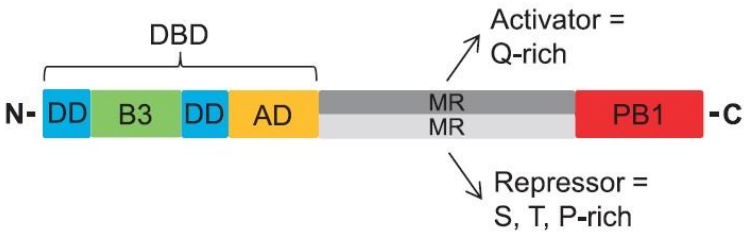

Figure 5 Schematic representation of the ARF domain composition. The N-terminal DNA-binding domain (DBD) consists of the dimerization domain (DD), B3-type domain (B3) and ancillary domain (AD). Amino acid composition of the middle region (MR) determines the regulatory function of ARFs; glutamine-rich (Q-rich); serine, threonine, proline-rich (S, T, P-rich). The C-terminus comprises the Phox and Bem1 domain (PB1) (from Chandler, 2016).

DNA-binding affinity after dimerization (Boer *et al*., 2014). The last part of DBD is called the ancillary domain (also referred to as Tudor-like ancillary domain) with five-stranded β-barrel like structure (Boer *et al*., 2014). The N-terminal part of the protein contains a lot of sequence motifs conserved among different ARF proteins, these are sometimes overally regarded as the ARF domain (Zhang *et al*., 2017).

The middle region (MR) is not of less importance. Indeed, it determines the function of ARF as activator or repressor of the transcription of auxin-responsive genes. When the amino acid composition of the MR was analysed, a specific pattern was found in the group of activator and repressor ARFs. The MR of activators is typically enriched in glutamine. On the contrary, the pattern of repressors MR is not uniform. Repressors MRs can be enriched in serine, serine and proline or serine and glycine (Tiwari *et al*., 2003). According to the specific function, these MRs are called either Activation or Repression domain (Guilfoyle, 2015).

The C-terminal part of ARF contains Phox and Bem1 (PB1) domain (also referred to as III/IV domain). The main function of PB1 is to mediate the protein-protein interactions. When this interaction is carried out with another PB1 domain protein, the dimers form in a front-to-back manner. The mechanism lies in a B-type (basic) PB1 cluster interaction with an A-type (acidic) cluster of PB1. When both A-type and B-type clusters are present in one protein, this leads to homo-polymerization (Christian *et al*., 2014). The truncated ARFs mostly lack the C-terminal domain and these proteins usually function as transcription repressors. Four truncated versions of ARF proteins have been found in the Arabidopsis genome, 6 in *O. sativa* and 13 in *M. truncatula* (Guilfoyle and Hagen, 2007; Wang *et al*., 2007; Shen *et al*., 2015). It seems that the number of truncated forms of ARFs increased during the evolution, as the number of truncated ARFs is higher in flowering plants compared to non-flowering plants. Also, it is probable that truncated ARFs are not repressed by dimerization with Aux/IAA proteins, because they are missing the dimerization PB1 domain (Ckurshumova *et al*., 2012). That would suggest an auxin-independent regulation of the truncated proteins.

2.3.3.2 Role in auxin signaling pathway

To facilitate the response to auxin signals, plants evolved a very broad network of interactions. Together, these interactions transform the hormonal signals to a sequence of gene expression events. In the middle of these are the ARFs and Aux/IAA proteins, whose

interactions ensure a proper gene transcription in response to auxin. To summarize this interaction network, a general model of ARF-Aux/IAA function has been proposed. The model of function presents two different situations according to absence or presence of auxin (Fig. 6). In the absence or low concentration of auxin, Aux/IAA proteins act as repressors of the ARF transcriptional activity by dimerization through domains III and IV, homologous to PB1 domain of ARFs (Christian *et al*., 2014). In this state, even though ARFs are still bound to auxin-response elements in the promoters of auxin-responsive genes, their activity is repressed. Therefore, ARFs interacting with Aux/IAA proteins cannot trigger transcription of auxin-responsive genes (Chapman and Estelle, 2009). Piya *et al*. (2014) proposed that only specific pairs of ARF-Aux/IAA control the auxin signaling.

The situation changes when the auxin levels are elevated. In this situation, components of the SCF (Skp1-related protein, Cullin, F-box protein) E3 ubiquitin ligase are necessary for a response to auxin. The role of the F-box protein TIR1 and the corresponding class of SCF, SCF^{TIR1}, has been already well and extensively reported (Chapman and Estelle, 2009). In high auxin concentration, the interacting proteins TIR1 and Aux/IAA create a "pocket" structure in which auxin is bound, stabilizing the interaction. TIR1 and Aux/IAA act as co-receptors for auxin (Dharmasiri *et al*., 2005; Kepinski and Leyser, 2005).

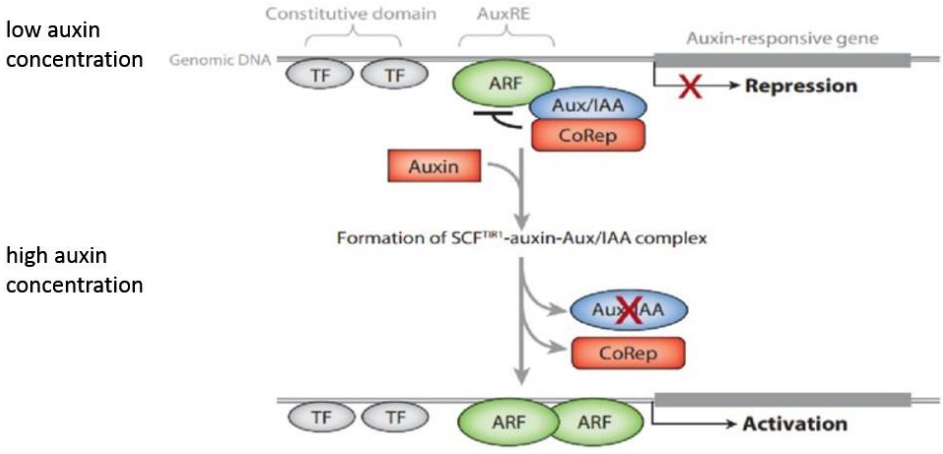

Figure 6 Auxin-dependent ARF activation. In low auxin concentration, ARFs are repressed by Aux/IAA proteins and other recruited co-repressors. In high auxin concentration, SCF^{TIR1} complex targets Aux/IAAs for degradation in proteasome, co-repressors are released and activated ARFs regulate transcription of auxin-responsive genes (adapted from Barnes, 2017).

Bound by SCF^{TIR1} complex, Aux/IAA proteins are poly-ubiquitinated and targeted to degradation by the 26S proteasome complex (Gray *et al*., 2001). In this way, the repression of ARFs is disrupted and the auxin-signaling pathway is activated. Stabilization of Aux/IAA proteins leads to very severe defects in plant development, hypocotyl elongation or tropisms (Chapman and Estelle, 2009). Aux/IAA proteins are not the only repressors affecting the transcriptional activity of ARFs. For example, the TOPLESS (TPL) proteins can act as transcriptional co-repressors of ARFs through their interaction with Aux/IAA (Tiwari *et al*., 2004). Also, chromatin-remodeling factors, such as PKL can have a co-repressor function in this process (Fukaki *et al*., 2006). However, the co-repressors dissociate from ARFs right after Aux/IAA degradation. Therefore, degradation of Aux/IAA repressors is a crucial process for auxin signaling (Chapman and Estelle, 2009).

As mentioned, this model summarizes the general aspects of ARF-Aux/IAA interaction and it can only confidently apply to a majority of ARF activators. It was already proved in different plant species that the ARF activators can directly interact with Aux/IAA proteins. In Arabidopsis, all activator ARFs interact with all the Aux/IAA proteins in the yeast two hybrid assay (Y2H) with only one exception (AtARF7 does not interact with Aux/IAA7) (Piya *et al*., 2014). ARF repressors have only limited interaction network compared to ARF activators (Vernoux *et al*., 2011). When the interactions between ARF repressors and Aux/IAA were tested, ARF repressors were found to interact with only certain Aux/IAA proteins. In the case of AtARF3 and AtARF13, the inability to interact with Aux/IAA could be caused by the absence of the C-terminal domain in their structure. Interestingly, even without the PB1 dimerization domain, the AtARF17 can still interact with 9 Aux/IAA proteins (Piya *et al*., 2014). When analyzing ARF-Aux/IAA interactions in the monocot rice plant model, the differences between activator and repressor ARFs were even more obvious. Whereas each of the eight examined OsARF activators interacted with all 15 OsIAA proteins, none of the six examined OsARF repressors interacted with OsIAA proteins (Shen *et al*., 2010).

Considering ARF repressors, the model of their regulation and function remains still quite unclear. Vert *et al.* (2008) suggested a scenario where ARF repressors are competing for a binding site in promoters of auxin-responsive genes, thus preventing transcription activation (Fig. 7). A similar mechanism was suggested also for the product of Arabidopsis pseudogene *AtARF23*. As the sequence of AtARF23 comprises only

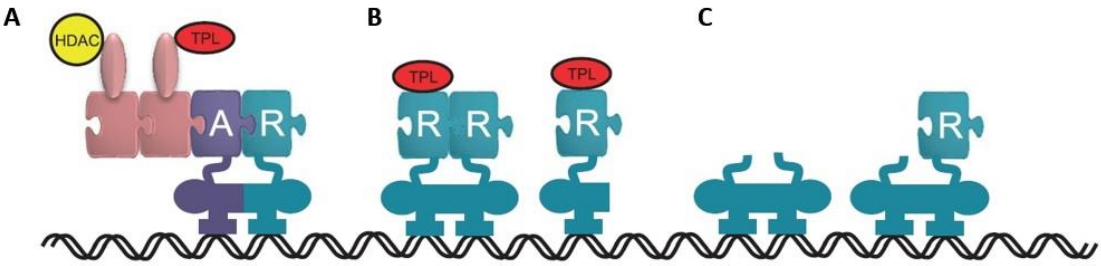

Figure 7 Hypothetical functions of ARF repressors. A, apart from inhibition by Aux/IAAs (pink) and co-repressors (yellow, red), activator ARFs (purple) may be inhibited by repressor ARFs (blue). Repressor ARFs sequester activator ARFs, leading to repression of auxin-responsive gene transcription. B, repressor ARFs may compete with activator ARFs for the binding site in gene promoters. C, truncated repressor ARFs may also form dimers and compete with activator ARFs for the binding site in promoters of genes (from Chandler, 2016).

the DBD, it could possibly interfere with the DNA-binding activity of other ARF proteins (Okushima *et al*., 2005). While bound to DNA sequences, ARF repressors could also recruit other co-repressors such as TPL and TPL-related proteins, as these interact with repressor AtARF2 and AtARF9 in Arabidopsis (Causier *et al*., 2012). But the repressors could act on more levels. Repressors can also heterodimerize with ARF activators and keep activators in an inactive state (Vernoux *et al*., 2011). Put into context, Vernoux *et al*. (2011) suggested that the auxin-induced gene expression is dependent on the absolute levels of ARF proteins and the ratio between activators and repressors.

2.3.3.3 Regulation of Auxin response factors

Effort has been made to uncover the complex regulation of gene expression. In general, gene expression can be regulated by different transcription factors or by chromatin accessibility. To understand this regulation, regulatory sequences of activator *ARF* genes were analysed. At least for the activators, it is obvious that each *ARF* gene is controlled by a specific set of transcription factors with only very little overlap between different ARFs. Transcription factors that are common for more *ARFs* include families of WRKY, ZINC FINGER PROTEIN (ZFP), SQUAMOSA PROMOTER BINDING PROTEIN-LIKE (SPL) or APETALA2/ETHYLENE RESPONSE FACTOR (AP2/ERF) (Vernoux *et al*., 2018).

At the post-transcriptional level, ARFs can be regulated by both microRNA (miRNA) and trans-acting short-interfering RNA (tasiRNA). Two families of miRNA were discovered to regulate *ARF* transcript levels. The miR160 family negatively regulates the

availability of repressor transcripts *AtARF10, AtARF16* and *AtARF17*, while the miR167 family regulates the activator genes *AtARF6* and *AtARF8* (Mallory *et al*., 2005; Wang *et al*., 2005; Wu *et al*., 2006; Liu *et al*., 2007). Control of gene expression by miRNA was shown to be essential for correct gene expression patterns and subsequent biological functions of ARFs. TasiRNAs are transcribed from the genome of land plants and further processed to form a 21-nucleotide long RNA, which is then incorporated into the RNA-induced Silencing complex (RISC). As a part of RISC, tasiRNA acts as a guide for specific mRNA cleavage. Such tasiRNA, called TAS3, shares nucleotide sequence with *AtARF2, AtARF3* and *AtARF4* targeting them for cleavage in Arabidopsis (Williams *et al*., 2005).

To show that ARFs can be also regulated at the post-translational level, the interaction and ability to phosphorylate ARFs was tested with the protein kinase BRASSINOSTEROID-INSENSITIVE2 (BIN2). First, the interaction between BIN2 and AtARF2 leading to AtARF2 phosphorylation was discovered, followed by experiments to explain the meaning of this phosphorylation. It was revealed that the stability of AtARF2 was not affected, but instead the dissociation from DNA was affected. This suggested another level of regulation of ARF repressors in favor of ARF activators, because phosphorylation would then remove ARF repressors from the AuxRE binding site (Vert *et al*., 2008). Later, phosphorylation of AtARF7 and AtARF19 by BIN2 was also discovered, supporting the hypothesis of an auxin-independent regulation of ARFs (Cho *et al*., 2014).

2.3.3.4 Specialization of different isoforms

The high number of ARF isoforms raises the question whether their functions are redundant or if there is some specialization in ARF functions. Usually, gene expression analysis provides a preliminary pattern of expression which can be potentially associated with a function in a specific tissue. One of the first studied members of the ARF family in Arabidopsis was AtARF5, also called MONOPTEROS (MP). Observing the phenotype of the *mp* single mutant, it was already obvious that MP must have an irreplaceable role in the plant development, as the mutant plants were not able to form basal organs such as hypocotyl or radicle; moreover, cotyledon positioning and formation of root meristem were also affected in the mutant (Berleth and Jürgens, 1993). The molecular mechanism of MP function was understood later, when it was found that MP controls the expression

of *PIN* genes, specifically *PIN1*, *PIN3* and *PIN7* (Schlereth *et al*., 2010; Krogan *et al*., 2016). Thanks to the regulation of PIN-dependent auxin transport, MP can control the basic processes involved in embryonal patterning, function of both shoot and root apical meristems or organogenesis. MP has been therefore proposed to be a central factor connecting auxin signal transduction and auxin transport (Krogan *et al*., 2016). The function of another member of the family, AtARF7 or NONPHOTOTROPIC HYPOCOTYL4 (NPH4), is partially overlapping with the functions of MP. *AtARF7* is expressed in different floral organs, hypocotyls, early stages of LRP, vasculature of roots and root meristem (Okushima *et al*., 2005). In the double mutant *mp nph4* the structure and function of both the apical meristems is abolished. But when only the single mutant *mp* was studied, AtARF7 could at least contribute to embryonal patterning. So even though MP is probably biochemically different from AtARF7 and has a bigger significance for the plant, AtARF7 can still substitute MP to some extent (Hardtke *et al*., 2004). Furthermore, the analysis of the *nph4* phenotype revealed reduced phototropic responses, gravitropism of the stem and severe problems with differential growth. Differential growth allows the plant to bend its organs, so enabling the plant to actively respond to changes in the environment or to overcome physical barriers in the surroundings (Harper *et al*., 2000). Further, AtARF7 together with AtARF19 control expansion of leaves and formation of auxin-induced LRs. *AtARF19* was found to be expressed in response to auxin and its transcripts accumulate in the vasculature of cotyledons and leaves, in meristems of stems and roots, in newly forming LRs or different floral organs. While *arf19* single mutants display no significant phenotype, double mutants *nph4 arf19* exhibit small leaves, less LRs compared to wild type and disrupted growth orientation (Okushima *et al*., 2005; Wilmoth *et al*., 2005). The number of LRs of the double mutants starts to increase after 2 weeks of growth (Okushima *et al*., 2005). Detailed examination of auxin-induced gene expression then indicated that AtARF7 and AtARF19 control a common set of genes (Wilmoth *et al*., 2005). It is interesting that functionally overlapping AtARF5-AtARF7 and AtARF7-AtARF19 together form one phylogenetic clade (Remington *et al*., 2004).

Another ARF phylogenetic clade comprises AtARF6 and AtARF8, which are extensively studied due to their involvement in the process of stamen and gynoecium maturation. *AtARF8* and *AtARF6* share the same expression pattern. During flower development, both genes are expressed in sepals at all stages of their development and

during very short period in different parts of stamen, petals and gynoecium. Both *arf6* and *arf8* single mutants show similar phenotypes including decreased cell expansion of stamen filaments and carpels. Flowers of such plants failed to open or to produce seeds, probably caused by longer distance between anthers and the stigma. In the double mutant, shorter petals and stamen filaments were also observed, but more importantly the processes of gynoecium maturation and release of pollen from anthers were disrupted (Nagpal *et al*., 2005). During flower development *AtARF6* and *AtARF8* need to be regulated by miR167. miR167 targets *AtARF6* and *AtARF8* transcripts *in vivo* to remove or destabilize them. Defining the pattern of *AtARF6* and *AtARF8* expression, miR167 preserves the flower fertility (Wu *et al*., 2006). A specific involvement of AtARF8 in cell proliferation in petals during early flower development stages was discovered. To have such function, AtARF8 physically interacts with BIGPETALp (BPEp) basic helix-loop-helix (bHLH) transcription factor, which limits petal growth by restricting cell expansion. The interaction between AtARF8 and BPEp is maintained by the C-terminal domain of both proteins (Varaud *et al*., 2011).

Another isoform with an important role in flower development is AtARF17. In particular, the correct post-transcriptional regulation of *AtARF17* guided by miR160 is crucial as demonstrated by the miR160-resistant version of *AtARF17* with increased number of mismatches between miR160 and *AtARF17* transcripts. Such misregulation results in abnormal stamen structure, which finally leads to reduced male fertility (Mallory *et al*., 2005). In *arf17* plants, female fertility is not affected. Further experiments revealed that AtARF17 is required for proper callose deposition around plasma membrane in the tetrad stage. AtARF17 controls the biosynthesis of callose by regulation of *CALLOSE SYNTHASE5* (*CALS5*) gene (Shi *et al*., 2015). Without sufficient callose layer, also the primexine deposition is affected. As the overall pollen wall pattern is lost, pollen does not complete development, being rather degraded. Thanks to RNA *in situ* hybridization and GFP-reporter lines, the expression profile of *AtARF17* could be observed. Both experiments proved *AtARF17* expression during anther development, especially in microsporocytes in stage 6 of anther development, and no expression in mature pollen (Yang *et al*., 2013). At the molecular level, AtARF17 affects accumulation of *GH3-like* transcripts, involved in auxin homeostasis, and controls the expression of other auxin-responsive genes and genes involved in anther development (Mallory *et al*., 2005; Shi *et al*., 2015).

The high-scale mutant analysis performed by Okushima *et al*. (2005) suggested functions for less-studied isoforms of ARF family. The *arf3* mutant displayed unusual gynoecium and increased number of sepals and carpels. The disruption of *AtARF2* gene resulted in abnormal inflorescence stem, flower morphology and large leaves. A high-scale analysis with transcriptional reporters was performed also by Rademacher *et al*. (2011) exploring the expression patterns of all *ARF* genes during embryogenesis and in the primary root meristem. Expression of most of the genes was very dynamic and it was interesting to observe that activator and repressor genes can cooperate in regulation of the same process, as in the case of *AtARF1*, *AtARF2* and *AtARF6* in the process of embryo development. Together these studies suggest a particular level of functional specialization between different ARF isoforms, dependent on the position in the phylogenetic tree.

3 PRACTICAL PART

3.1 Material

3.1.1 Biological material

Chemocompetent cells *Escherichia coli* TOP10 (NEB, USA)

Electrocompetent cells *Agrobacterium tumefaciens* (*A. tumefaciens*) strain AGL1

Hordeum vulgare L. cultivar Golden Promise

3.1.2 Vectors

p6i-d35S-TE9 (DNA-Cloning-Service, Hamburg, Germany)

pDRIVE (Qiagen, Germany)

pNB1 (Budhagatapalli *et al*., 2016)

pNB2 (Budhagatapalli *et al*., 2016)

pSH91 (Budhagatapalli *et al*., 2016)

3.1.3 Chemicals

Restriction endonucleases (NEB, USA):

*BamH*I-HF (20 000 $U \cdot ml^{-1}$)

*Bsa*I-HF (20 000 $U \cdot ml^{-1}$)

*BsiW*I (10 000 $U \cdot ml^{-1}$)

*EcoR*I-HF (20 000 $U \cdot ml^{-1}$)

*Sfi*I (20 000 $U \cdot ml^{-1}$)

Buffers for restriction endonucleases (NEB, USA):

10x CutSmart

10x NEB 3.1

Other enzymes and buffers:

DNase I (1 500 $U \cdot ml^{-1}$) (Qiagen, Germany)

GoTaq G2 Flexi DNA polymerase (5 000 $U \cdot ml^{-1}$) and 5x buffer (Promega, USA)

Phusion DNA polymerase (2 $U \cdot \mu l^{-1}$) and 5x buffer HF (Thermo Fisher Scientific, USA)

Proteinase K (400 $U \cdot ml^{-1}$) (Thermo Fisher Scientific, USA)

RevertAid H Minus transcriptase (200 $U \cdot \mu l^{-1}$) and 5x buffer (Thermo Fisher Scientific, USA)

RNase A (40 $U \cdot ml^{-1}$) (Sigma-Aldrich, USA)

RNaseOUT ribonuclease inhibitor (5 000 $U \cdot ml^{-1}$) (Thermo Fisher Scientific, USA)

T4 DNA ligase (5 $U \cdot \mu l^{-1}$) and 10x buffer (Thermo Fisher Scientific, USA)

Turbo DNase (2 000 $U \cdot ml^{-1}$) and 10x buffer (Thermo Fisher Scientific, USA)

Other chemicals and material:

Agarose (Sigma-Aldrich, USA)

Ampicillin (Sigma-Aldrich, USA)

Anti-digoxigenin-alkaline phosphatase, Fab fragments (Roche, Germany)

Benzimidazol (Merck, USA)

Biotin (Sigma-Aldrich, USA)

BM purple, substrate for alkaline phosphatase (Roche, Germany)

Bovine serum albumin (BSA; Sigma-Aldrich, USA)

Carbenicillin (Duchefa, The Netherlands)

Chloramphenicol (Duchefa, The Netherlands)

Deoxynucleoside triphosphates (dNTPs, 10 $mmol \cdot l^{-1}$) (Sigma-Aldrich, USA)

Digoxigenin-11-deoxyuridin triphosphate (Digoxigenin-11-dUTP, 1 $mmol \cdot l^{-1}$)

Dimethyl sulfoxide (DMSO) for PCR (Thermo Fisher Scientific, USA)

Ethidium Bromide (Ambion, USA)

gb SG PCR Master Mix 2x (Generi Biotech, Czech Republic)

GeneRuler 1 kb Plus DNA Ladder (Thermo Fisher Scientific, USA)

GeneRuler 50 bp DNA Ladder (Thermo Fisher Scientific, USA)

Kanamycin (Duchefa, The Netherlands)

Lithium chloride (Sigma-Aldrich, USA)

Magnesium chloride for PCR (Promega, USA)

Microcarriers, Gold (250 mg) (Bio-Rad, USA)

Nuclease-Free water (Qiagen, Germany)

Oligo dT primer (100 $\mu mol \cdot l^{-1}$) (Sigma-Aldrich, USA)

Passive Reference Dye (5 $\mu mol \cdot l^{-1}$) (Generi Biotech, Czech Republic)

Phenol/chloroform/isoamyl-alcohol (25:24:1) (Sigma-Aldrich, USA)

Rifampicin (Duchefa, The Netherlands)

Spectinomycin (Duchefa, The Netherlands)

Spermidine (Sigma-Aldrich, USA)

and other chemicals of the Department of Molecular Biology, CRH.

3.1.4 Solutions and cultivation media

Block solution 1x: the stock solution (10x) was prepared by diluting 10 mg BSA in 10x PBS. The stock solution was diluted 10 times in 1x PBS just before use.

Callus induction medium (BCIM) (1 l): 4,3 g MS mineral salts; 1 g casein hydrolysate; 0,69 g proline; 0,25 mg myoinositol; 30 g maltose·H_2O; 2,5 mg Dicamba; 1 mg thiamine-HCl; 0,25 mg $CuSO_4 \cdot 5\ H_2O$. The pH was adjusted to 5.8; 50 mg hygromycin and 150 mg timentin were added. The solution was filter-sterilized in a laminar flow hood. One volume was mixed with three volumes of 0,4% Phytagel.

Cocultivation medium (BCCM) (1 l): 4,3 g MS mineral salts; 1 g casein hydrolysate; 0,69 g proline; 0,25 mg myoinositol; 30 g maltose·H_2O; 2,5 mg Dicamba; 1 mg thiamine-HCl. The pH was adjusted to 5.8. The solution was filter-sterilized in a laminar flow hood. 800 mg L-cysteine and 500 µl 1 $mol \cdot l^{-1}$ acetosyringone in DMSO were added.

Extraction buffer for gDNA isolation: 1% N-lauroyl-sarcosine; 100 $mmol \cdot l^{-1}$ Tris-HCl; 10 $mmol \cdot l^{-1}$ EDTA; 100 $mmol \cdot l^{-1}$ NaCl; pH 8.0.

Fixative: 63% ethanol, 5% acetic acid, 2% formaldehyde, the final volume was adjusted with DEPC water.

Hoagland´s solution: Stock solution of macronutrients: 1 $mol \cdot l^{-1}$ KNO_3; 1 $mol \cdot l^{-1}$ $Ca(NO_3)_2 \cdot 4\ H_2O$; 0,2 $mol \cdot l^{-1}$ NH_4NO_3; the volume was adjusted to 500 ml with Milli-Q H_2O. Stock solution of 1 $mol \cdot l^{-1}$ $MgSO_4 \cdot 7\ H_2O$, the volume was adjusted to 500 ml with Milli-Q H_2O. Stock solution of 1 $mol \cdot l^{-1}$ KH_2PO_4, pH 6.0, the volume was adjusted to 250 ml with Milli-Q H_2O. Stock solution of Fe-EDTA: 30 $mmol \cdot l^{-1}$ EDTA-2Na·2 H_2O and 28 $mmol \cdot l^{-1}$ $FeSO_4 \cdot 7\ H_2O$ in 1 $mol \cdot l^{-1}$ KOH, the volume was adjusted to 1 l with Milli-Q H_2O. Stock solution of micronutrients: 46 $mmol \cdot l^{-1}$ H_3BO_3; 2,28 $mmol \cdot l^{-1}$ $MnCl_2 \cdot 4\ H_2O$; 0,77 $mmol \cdot l^{-1}$ $ZnSO_4 \cdot 7\ H_2O$; 0,20 $mmol \cdot l^{-1}$ $CuSO_4$; 0,50 $mmol \cdot l^{-1}$ $Na_2MoO_4 \cdot 2\ H_2O$, the volume was adjusted to 1 l with Milli-Q H_2O.

For ½ Hoagland´s solution: 2,5 ml stock solution of macronutrients; 1 ml stock solution of $MgSO_4 \cdot 7\ H_2O$; 0,25 ml stock solution of KH_2PO_4; 0,5 ml stock solution of

Fe-EDTA; 0,25 ml stock solution of micronutrients were mixed and the volume was adjusted to 1 l with Milli-Q H_2O.

K micro minerals stock solution (1 l): 84 mg $MnSO_4 \cdot H_2O$; 31 mg H_3BO_3; 72 mg $ZnSO_4 \cdot 7\ H_2O$; 1,2 mg $Na_2MoO_4 \cdot 2\ H_2O$; 0,25 mg $CuSO_4 \cdot 5\ H_2O$; 0,24 mg $CoCl_2 \cdot 6\ H_2O$; 1,7 mg KI. The solution was filter-sterilized.

K4N macro mineral stock solution (1 l): 6,4 g NH_4NO_3; 72,8 g KNO_3; 6,8 g KH_2PO_4; 8,82 g $CaCl_2 \cdot 2\ H_2O$; 4,92 g $MgSO_4 \cdot 7\ H_2O$. The solution was filter-sterilized.

Luria-Bertani (LB) medium (1 l): 15,5 g LB broth; 9,5 g NaCl; Milli-Q H_2O; pH 7.0. For solid medium: 15 g agar was added.

MG/L medium (1 l): 250 mg KH_2PO_4; 100 mg NaCl; 100 mg $MgSO_4 \cdot 7\ H_2O$; 1 g L-glutamic acid; 5 g mannitol; 5 g tryptone; 2,5 g yeast extract. The pH was adjusted to 7.0. After autoclaving of the medium, 0,1 g biotin was added. For solid medium: 12 g agar was added.

PBS (10x, 1 l): 35,8 g Na_2HPO_4 was dissolved in 800 ml of Milli-Q H_2O, pH was adjusted to 7.5 with 37% HCl. 75,9 g NaCl was added and the volume was adjusted to 1 l.

Regeneration medium (BRM) (1 l): 50 ml K4N macro mineral stock solution (above); 1 ml 75 $mmol \cdot l^{-1}$ NaFeEDTA; 1 ml K micro stock solution (above); 112 mg vitamin B5; 1 ml 1 $mmol \cdot l^{-1}$ 6-BAP; 146,4 mg L-glutamine; 36 g maltose$\cdot H_2O$; 196 µl 25 $mmol \cdot l^{-1}$ $CuSO_4 \cdot 5\ H_2O$. The pH was adjusted to 5.8. The solution was filter-sterilized in a laminar flow hood. One volume was mixed with three volumes of 0,4% Phytagel.

SOC medium: 0,5% yeast extract; 2% trypton; 10 $mmol \cdot l^{-1}$ NaCl; 2,5 $mmol \cdot l^{-1}$ KCl; 10 $mmol \cdot l^{-1}$ $MgCl_2$; 10 $mmol \cdot l^{-1}$ $MgSO_4$; 20 $mmol \cdot l^{-1}$ glucose.

TAE buffer: 1 $mol \cdot l^{-1}$ EDTA; 40 $mol \cdot l^{-1}$ Tris-acetate; Milli-Q H_2O; pH 8.0.

TE buffer: 1 $mmol \cdot l^{-1}$ EDTA; 10 $mmol \cdot l^{-1}$ Tris; Milli-Q H_2O; pH 8.0.

Wash buffer 1: 63% ethanol, 5% glacial acetic acid, the final volume was adjusted with DEPC water.

Wash buffer 2 (100 ml): 1,21 g Tris, 0,88 g NaCl, Milli-Q H_2O; pH 9.5.

3.1.5 Kits

NucleoBond Xtra Midi (Macherey-Nagel, Germany)

NucleoSpin Gel and PCR Clean-up (Macherey-Nagel, Germany)

QIAprep Spin Miniprep (Qiagen, Germany)

SuperScript IV first-strand synthesis system (including SuperScript reverse transcriptase, SSIV buffer, dithiothreitol, ribonuclease inhibitor, RNase H) (Thermo Fisher Scientific, USA)

ZR Plant RNA Miniprep (Zymo Research, USA)

3.1.6 Software

Bioedit (Hall, 1999)

Deskgen (Deskgen, [2017])

HMMER (HMMER, [2017])

Image Lab 5.1 (Bio-Rad, USA)

ImageJ (National Institutes of Health, USA)

MEGA7 (Kumar *et al*., 2016)

Phylogeny.fr (Dereeper *et al*., 2008; Dereeper *et al*., 2010)

Primer3Plus (Rozen and Skaletsky, 2000)

SnapGene Viewer (GSL Biotech, USA)

StepOnePlus (Thermo Fisher Scientific, USA)

3.1.7 Machines

Axio Imager M2 (Carl Zeiss, Germany)

BTX ECM 399 Exponential decay wave electroporator (Thermo Fisher Scientific, USA)

Electrophoretic chamber for horizontal electrophoresis (Biometra, Germany)

Environmental chamber MLR 351 (Sanyo, Japan)

Gel Doc EZ Gel Imaging System (Bio-Rad, USA)

Leica VT 1000 S vibratome (Leica, Germany)

Mixer Mill MM 200 (Retsch, Germany)

NanoDrop One^{C} Microvolume UV-Vis spectrophotometer (Thermo Fisher Scientific, USA)

PDS-1000/He Hepta^{TM} system (Bio-Rad, USA)

Spectrophotometer (Agilent, USA)

StepOnePlus Real-Time PCR thermocycler (Applied Biosystems, USA)

Stereoscopic microscope (Nikon, Japan)

and other laboratory equipment of the Department of Molecular Biology, CRH.

3.2 Methods

3.2.1 Identification and characterization of barley ARF proteins

Latest versions of Plant Transcription Factor (Plant Transcription Factor Database, [2017]) and Ensembl Plants (Ensembl Plants, [2018]) databases were searched for all potential ARF protein sequences in barley. BLAST tool of the Ensembl Plants database was used to search new potential ARF proteins based on sequence homology between annotated barley ARFs and ARFs known from rice or Arabidopsis. Domain composition of all selected protein sequences were analysed by HMMER scan. After selecting ARF sequences, a cladogram was created using MEGA7 software. Also, a cladogram was created by Phylogeny.fr online tool. In the cladogram, protein sequences of barley, rice and Arabidopsis were compared. This approach was used to identify barley closest orthologue to Arabidopsis AtARF17. Furthermore, to distinguish the HvARF repressors and activators, amino acid content of the middle region sequence was analysed by Bioedit.

3.2.2 Analysis of gene expression by semi-quantitative PCR

3.2.2.1 Sample preparation

Grains of spring barley cultivar Golden Promise were sterilized for 40 s in 70% ethanol and for 3 min in 4% sodium hypochlorite solution and extensively rinsed with sterile water. Grains were placed on a tissue paper in a Petri dish, covered with another layer of a tissue paper and supplied with water. Dishes were wrapped with parafilm and incubated at 4°C for 3 days. After vernalization, grains were transferred to a phytotron with regulated light and temperature conditions (16°C/16 h/light and 12°C/8 h/dark) for germination. From approximately 7 days after germination (DAG) seedlings were grown in a hydroponic system in a solution of half-strength Hoagland (Vlamis and Williams, 1962). For later stage of development, young plants were transferred to soil and grown in phytotron under controlled conditions until complete maturation of the plant and production of new grains. The list of samples is shown in Table 1. Samples number 1-5 and 9-11 were kindly provided by RNDr. Lenka Dzurová, Ph.D. and Bc. Barbora Hanzlíková. Each sample was collected in 3 independent biological replicates and each replicate represented a pool of explants coming from 8 different plants. Different parts of a seedling were cut with a razor blade and immediately transferred to liquid nitrogen. Using a mortar and a pestle, frozen samples were crushed into soft powder. Samples were kept at -80°C.

Table 1 List of samples for semi-quantitative PCR.

Sample number	Sample	Age of harvested plant material (after germination)
1	leaves	1 month
2	leaves	2 months
3	imbibed grains	day 0
4	grains	1 day
5	grains	2 days
6	crowns (stem base)	10 days
7	shoots	10 days
8	roots	10 days
9	inflorescence – medium milk (milky content of grains)	66 days
10	inflorescence – soft dough (wet content of grains with floury texture)	83 days
11	inflorescence – hard dough (solid content of grains)	97 days

3.2.2.2 RNA isolation and DNase treatment

RNA was isolated from plant material described in Chapter 3.2.2.1. The ZR Plant RNA Miniprep kit was used according to the manufacturer´s instructions for RNA isolation. RNA was eluted into 50 µl of nuclease-free water. The reaction mixture for DNase treatment was prepared as shown in Table 2. The mixture was incubated at 37°C for 30 min. After the first incubation, an extended step of treatment was performed by adding again 2 µl of Turbo DNase to the mixture, and further prolongating incubation at 37°C for another 30 min. To precipitate RNA, the reaction mixture was incubated with 30 µl of 7,5 $mol \cdot l^{-1}$ LiCl at -20°C for 1 h. After precipitation, the samples were centrifuged at 13 250 x *g* at 4°C for 30 min. Supernatant was discarded and the pellet was already visible at the bottom of the tube. First, the pellet was dissolved in 500 µl of 70% RNase-free ethanol. Samples were centrifuged at 13 250 x *g* at 4°C for 10 min, supernatant was discarded. Then, the pellet was dissolved in 500 µl of 96% RNase-free ethanol. Samples were centrifuged again at 13 250 x *g* at 4°C for 10 min, supernatant was discarded. Remaining ethanol was carefully removed using a tip. To let the rest of ethanol evaporate, the tubes were kept at room temperature for another 5 min. The pellet containing RNA samples was dissolved in 40 µl of nuclease-free water. Concentration of RNA samples was measured with NanoDrop One^{C}. RNA samples were kept at -80°C.

Table 2 Reaction mixture for DNase treatment.

Component	Volume [µl]
10x Turbo DNase buffer	5
Turbo DNase (2 000 U·ml^{-1})	2
RNA	50
Total volume	57

3.2.2.3 Control PCR and agarose gel electrophoresis

Polymerase chain reaction (PCR) was performed to control the purity of RNA samples. In the PCR reaction, primers designed for barley *Elongation Factor 2* (*EF2*; Primers: Fw 5′ - CCGCACTGTCATGAGCAAGT, Rv 5′ - GGGCGAGCTTCCATGTAAAG) gene were used. The reaction was prepared in 20 µl as described in Table 3 and PCR conditions were set according to Table 4. PCR was also performed with barley genomic DNA as a positive control. A sample containing water instead of RNA was used as a negative control.

Table 3 Reaction mixture for PCR.

Component	Volume [µl]	Volume [µl]	Volume [µl]
5x GoTaq Flexi buffer	2	4	8
GoTaq G2 Flexi DNA polymerase (5 000 U·ml^{-1})	0,05	0,1	0,2
Forward primer (10 µmol·l^{-1})	0,5	1	2
Reverse primer (10 µmol·l^{-1})	0,5	1	2
dNTPs (10 mmol·l^{-1})	0,5	1	2
$MgCl_2$ (25 mmol·l^{-1})	1	1,2	4
Template sample	1	1	1
Nuclease-free water	4,45	10,7	20,8
Total volume	10	20	40

Table 4 Program of the PCR thermocycler for control PCR.

Step	Temperature [°C]	Time [s]	Number of cycles
Initial denaturation	95	120	1
Denaturation	95	30	34
Primer annealing	55	30	
Elongation	72	45	
Final elongation	72	300	1
Final incubation	22	holding	-

For agarose gel electrophoresis, 1% agarose gel was prepared by dissolving agarose powder in 1x TAE buffer (w/v). To prepare one gel, 50 ml of 1% agarose were properly mixed with 10 µl of 0,5% ethidium bromide solution. The solution was poured into a gel caster and a comb was placed in the upper part of the gel. After the gel solidified, it was transferred to an electrophoresis chamber filled with 1x TAE buffer. After all the samples and a molecular standard were applied on the gel, the chamber was connected to a power supply. The electrophoresis was performed at 100 V for 45 min. The gel was transferred to a UV transilluminator to visualize the fragments of a nucleic acid on gel. The transilluminator outcome was analysed in Image Lab 5.1 software.

3.2.2.4 Reverse transcription

To synthesize cDNA by reverse transcription, 2 µg of total RNA were mixed with 1 µl of 100 $\mu mol \cdot l^{-1}$ oligo dT primers and the reaction volume was adjusted to 13 µl with nuclease-free water. The RNA-primer mix was heated to 65°C for 5 min and then immediately incubated on ice. The reaction mixture for reverse transcription was prepared by combining the components as described in Table 5. The reaction mixture was incubated at 42°C for 60 min and the reaction was inactivated at 70°C for 10 min. The samples were kept at -20°C. To check the integrity of synthesized cDNA, control PCR combined with agarose gel electrophoresis was performed as described in Chapter 3.2.2.3. PCR was also performed with barley genomic DNA as a positive control. A sample containing water instead of cDNA was used as a negative control.

Table 5 Reaction mixture for reverse transcription.

Component	**Volume [µl]**
5x Reverse transcriptase buffer	4
RevertAid H Minus transcriptase (200 $U \cdot \mu l^{-1}$)	1
dNTPs (10 $mmol \cdot l^{-1}$)	2
RNA-primer mix	13
Total volume	20

3.2.2.5 Primer design for semi-quantitative PCR and qPCR

PCR primers specific for different barley *HvARF* genes (Table 6) were designed using Primer3Plus online tool. Primers were preferentially designed for the middle region of ARFs, which is the most variable region between different orthologs. The specificity of primers was checked by the Ensembl Plants BLAST tool against barley database.

Table 6 List of *HvARF*-specific primers for semi-quantitative PCR and qPCR. Primer efficiency was analysed for repressor *ARF* genes and three selected activator *ARF* genes by qPCR in serial dilutions of 1 DAG to 4 DAG crown cDNA samples.

Gene name	Primer sequence (5´ → 3´)	Product size (bp)	Primer efficiency
HvARF1	Fw: ACTCGGTCGCAATTTGCAAC Rv: TGACGATTGCAGCAGTGTAC	101	1,95
HvARF3a	Fw: AGCAAGAGCAACGAAGAAGC Rv: ACCCGAAAAGCATGCAACTG	136	1,95
HvARF3b	Fw: TGGCGTTCAAGAAGCAATGC Rv: GCTCTACCACCTGAATTATGCG	117	1,99
HvARF4a	Fw: TCAGATGCAACAACCAACCC Rv: TCTGCCAAAGAGCAAACCAG	103	1,86
HvARF4b	Fw: AAACCATGCATCCGCGTTTC Rv: ACGCAGTTTCACATCTTCCC	74	1,94
HvARF4c	Fw: TGCAGCAACAACAACAACCC Rv: ACCAGCGGATAAACAATCGC	119	1,96
HvARF8	Fw: AGCCAGGCATTCGCAATTTG Rv: GGTCAGTGCTGATTCTTGATGC	143	1,76
HvARF9	Fw: ACATTGTGTGCGTTGCTGTG Rv: AACCAACTGGCAACGAAACG	86	1,79
HvARF11	Fw: ACTCCAAATGGCGCAACTTG Rv: GGCATTGCCGCTTTGAATTC	150	-
HvARF12	Fw: TTTGCACTTGTGGCAGTGTG Rv: TGTATTACCGAGCTCGACGAAG	149	-
HvARF13	Fw: AAGATGCTTCTGCCACAAGC Rv: TTTCTGTCGTGGCCATCATC	70	1,72
HvARF14	Fw: ACTCATTGCAACCACCAACG Rv: TTTAGCTCGCTTCGAACTGG	108	1,76
HvARF15	Fw: AAGTGGCGGCTTTCATCAAC Rv: GAATGCATGCTGTTGTTGCG	82	2,05
HvARF17a	Fw: ACAGTGCATGCAAACACCAC Rv: ACCGACAACGCATTTGGTAC	87	2,04
HvARF17b	Fw: TCCAGCAGCCACAAAACATG Rv: TGCTGCTGAAACTGAGGTTG	88	2,10
HvARF18	Fw: AGATGGCCCAATTCACCTTG Rv: TTCACATTCTGCAGCAGGTC	71	1,72
HvARF19a	Fw: TGCCCAACAACAAGTGATGC Rv: TTGCTGCTCTTGCTGAATGG	91	-
HvARF19b	Fw: ACAACCGACCAAACAAACGC Rv: ACGAGAAGCAAATGCATCCG	75	-

Table 6 List of *HvARF*-specific primers for semi-quantitative PCR and qPCR. Primer efficiency was analysed for repressor *ARF* genes and three selected activator *ARF* genes by qPCR in serial dilutions of 1 DAG to 4 DAG crown cDNA samples (*continuation*).

Gene name	Primer sequence (5′ → 3′)	Product size (bp)	Primer efficiency
HvARF21	Fw: TGTTGTCCAAGCTCAGTTCG Rv: TGTTGCTGTTGCTGCAGAAC	135	-
HvARF22	Fw: TGAAATGTGTGAGCCCATGG Rv: TTTCGTGGTGGGGAAAATGG	82	1,95
HvARF25	Fw: TGCACGTTGGCCAAATTCAC Rv: TCGGAAAGGTTGTCAATGGC	119	2,05

3.2.2.6 Semi-quantitative PCR

Expression of the 21 *HvARF* genes was analysed in 11 samples from different barley tissues in various developmental stages (Table 1). To obtain an average cDNA sample from every tissue, cDNA of 3 biological replicates were mixed to equal quantities and diluted to 1/5 with Milli-Q water. The total volume of reaction components was adjusted to 10 µl (Table 3) and the reaction conditions were set as shown in Table 7. General reference genes *EF2* (HORVU5Hr1G116710; Chapter 3.2.2.3), *Malate dehydrogenase* (HORVU1Hr1G041250; Primers: Fw 5′ - GCACTGGTGTGAATGTTGC, Rv 5′ - CTTCTCAGGGATAGATGGAGC), *E2 ubiquitin conjugating enzyme* (HORVU3Hr1G080790; Primers: Fw 5′ - CCATCCGAACATCAATAGC, Rv 5′ - CGGTAAGCAGCGAGCA) and *Elongation Factor 1-alpha* (*EF1α*, HORVU2Hr1G013680; Primers: Fw 5′ - CCAACTTCACTGCCCAGGTCA, Rv 5′ - CACAGCAACCGTCTGCCTCAT) were chosen to normalize cDNA levels. After the PCR reaction was finished, the gel electrophoresis (Chapter 3.2.2.3) was performed. As the length of amplicons ranged between 70 and 150 bp, the electrophoresis was performed with 2% agarose gel and the GeneRuler 50 bp DNA Ladder was used as a molecular standard. For electrophoresis, 8 µl from every reaction mixture were applied on gel. PCR reaction followed by gel electrophoresis were repeated 3 times for every gene.

Electrophoretic densitometry tool in ImageJ software was used to generate lane profile plots and to measure peak areas. In Excel, peak areas corresponding to analysed genes were normalized to peak areas of reference genes. Four different reference genes were used for cDNA levels normalization. The geometrical mean of normalized peak areas was calculated for every gene. Finally, obtained values were converted to a color scale, generating a heat-map.

Table 7 Program of the PCR thermocycler for semi-quantitative PCR.

Step	Temperature [°C]	Time [s]	Number of cycles
Initial denaturation	95	180	1
Denaturation	95	30	35
Primer annealing	55	30	
Elongation	72	30	
Final elongation	72	300	1
Final incubation	22	holding	-

3.2.3 Analysis of gene expression by qPCR

3.2.3.1 Sample preparation for qPCR

The procedure in Chapter 3.2.2.1 was followed for grain sterilization and cultivation. Barley crowns, the stem bases, were harvested 1 DAG, 2 DAG, 3 DAG and 4 DAG in 3 independent biological replicates. The crowns of 8 seedlings were collected for one biological replicate. The procedures in Chapter 3.2.2 were followed to obtain RNA samples and corresponding cDNA samples.

3.2.3.2 Primer efficiency analysis

Primer efficiency was measured for *HvARF* gene primers as well as for reference genes primers. *Actin* (HORVU2Hr1G004460; Fw 5′- TGTTGACCTCCAAAGGAAGCTATT, Rv 5′- GGTGCAAGACCTGCTGTTGA), *EF2* (Chapter 3.2.2.3) and *Hv5439* (HORVU5Hr1G073510; Fw 5′- GATTGAGGTGGAGAGGGTATTG, Rv 5′-CTCCTGGTCTGTTAGCAGTTT) were chosen as reference genes. To measure the primer efficiency, cDNA serial dilutions were prepared. All the cDNA samples were mixed together and diluted to 1/5, 1/10, 1/50 and 1/100. The reaction mixture for qPCR was prepared by mixing the components in Table 8. Serial dilutions of cDNA were used as a template for qPCR reaction. Negative control sample did not contain any template cDNA. Every sample was analysed in 3 technical replicates. Program of StepOnePlus Real-Time PCR thermocycler was set according to Table 9. Melting curve analysis was performed after 40 cycles to verify primer specificity.

When the C_T values were obtained, a standard curve was created, where logarithm of dilutions was plotted against C_T values. Slope value of the standard curve was used for primer efficiency calculation using the formula: $E = (10^{(-1/slope)}-1)\cdot 100$. Primer efficiency: *Actin* primers – 2,13; *EF2* – 1,97; *Hv5439* – 1,96; *HvARF* – shown in Table 6.

Table 8 Reaction mixture for qPCR.

Component	Volume [µl]
2x gb SG PCR Master Mix	5
Passive Reference Dye (5 µmol·l^{-1})	0,2
Forward primer (10 µmol·l^{-1})	0,3
Reverse primer (10 µmol·l^{-1})	0,3
Template cDNA	1,5
Nuclease-free water	2,7
Total volume	10

Table 9 Program of the StepOnePlus thermocycler for qPCR.

Temperature (°C)	Time [s]	Number of cycles
95	600	1
95	15	40
60	60	

3.2.3.3 Relative quantification by qPCR

Expression of *HvARF* repressors and three selected activators was analysed in 1 DAG, 2 DAG, 3 DAG and 4 DAG barley crown samples by qPCR. Every sample was analysed in 3 biological and 3 technical replicates. qPCR was performed as described in Chapter 3.2.3.2. C_T values of *HvARF* genes were normalized to reference genes *Actin*, *EF2* and *Hv5439*, these genes were determined as being the most stable reference genes in crowns. Normalized relative quantities were obtained using the efficiency corrected $2^{-\Delta\Delta Ct}$ method (Livak and Schmittgen, 2001; Pfaffl, 2001). To exclude the effect of biological variation on the statistical significance of results, $\log_{10}$ transformation of normalized relative quantities, mean centering and autoscalling were performed (Willems *et al*., 2008). The relative quantification was determined in comparison to the expression of 1 DAG control sample. Expression analysis in more biological replicates would be necessary to increase the statistical credibility of the results.

3.2.4 Absolute quantification of *HvARF13*

For absolute quantification of *HvARF13* in 1 DAG, 2 DAG, 3 DAG and 4 DAG crown samples, standard curve was created. Based on TA cloning approach, an amplification fragment of *HvARF13* was cloned into *pDRIVE* vector (Fig. 8). Using *pDRIVE::HvARF13* vector as a template in the qPCR reaction, standard curve for *HvARF13* quantification was obtained.

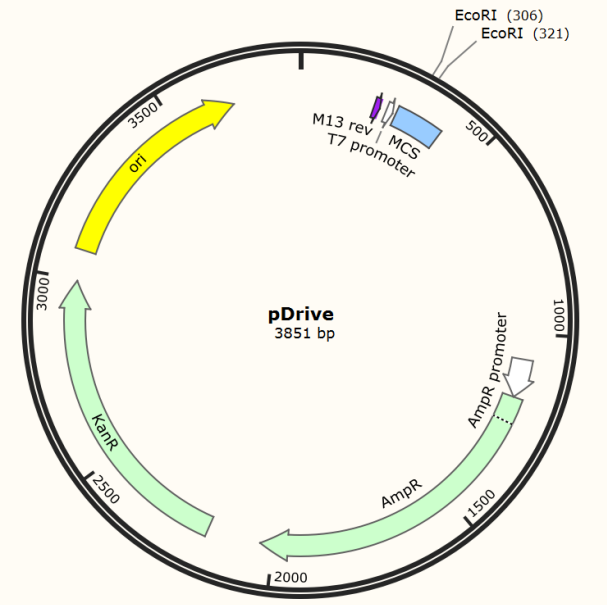

Figure 8 A map of the *pDRIVE* vector. The vector contains following features: M13 rev, a common sequencing primer; T7 promoter, promoter of bacteriophage T7 RNA polymerase; MCS, multiple cloning site; *Amp*^{R}, *β-lactamase* gene (ampicillin resistance gene); *Kan*^{R}, *Aminoglycoside Phosphotransferase* gene (kanamycin resistance gene); ori, origin of replication for bacteria.

3.2.4.1 Amplification of *HvARF13* fragment

A 70 bp fragment of *HvARF13* was amplified in a PCR reaction (Table 10, 11) using *HvARF13* specific primers (Table 6). cDNA of barley root samples was used as a template in the PCR reaction. The amplification was conducted in five separate reactions. After the PCR was finished, the content of five tubes was combined into one. PCR product was purified by NucleoSpin Gel and PCR Clean-up kit, eluted to 20 µl of sterile Milli-Q water and the concentration of purified product was measured by NanoDrop One^{C}.

Table 10 Reaction mixture for *HvARF13* amplification by Phusion DNA polymerase.

Component	**Volume [µl]**
5x Phusion buffer HF	10
Phusion DNA polymerase (2 U·µl^{-1})	0,5
Forward primer (10 µmol·l^{-1})	2,5
Reverse primer (10 µmol·l^{-1})	2,5
dNTPs (10 mmol·l^{-1})	1
DMSO (100%)	1,5
Template cDNA	2
Nuclease-free water	30
Total volume	50

Table 11 Program of the PCR thermocycler for *HvARF13* amplification.

Step	Temperature [°C]	Time [s]	Number of cycles
Initial denaturation	98	30	1
Denaturation	98	10	32
Primer annealing	63	30	
Elongation	72	15	
Final elongation	72	600	1
Final incubation	4	holding	-

In order to perform TA cloning, adenine overhangs were created at the 3´ends of *HvARF13* PCR amplification products. A single dATP was added to 3´ ends by the activity of GoTaq G2 Flexi DNA polymerase (Table 12). The reaction mixture was incubated at 70°C for 15 min. The *HvARF13* amplification product with A-overhangs was ligated with *pDRIVE* vector. The ratio of vector and insert was 1:8, respectively. The ligation mixture (Table 13) was incubated in a thermoblock at 16°C overnight. The ligation products were kept at -20°C.

Table 12 Reaction mixture for A-tailing of *HvARF13* PCR product.

Component	Volume [µl]
5x GoTaq Flexi buffer	2
GoTaq G2 Flexi DNA polymerase (5 000 $U \cdot ml^{-1}$)	1
dATP (10 $mmol \cdot l^{-1}$)	0,2
$MgCl_2$ (25 $mmol \cdot l^{-1}$)	0,6
Purified PCR product of *HvARF13*	3
Milli-Q water	3,2
Total volume	10

Table 13 Reaction mixture for ligation of *HvARF13* PCR product and *pDRIVE* vector.

Component	Volume [µl]
10x T4 DNA ligase buffer	1
T4 DNA ligase (5 $U \cdot \mu l^{-1}$)	1
pDRIVE vector (50 $ng \cdot \mu l^{-1}$)	1
Insert (*HvARF13* PCR product; 5,5 $ng \cdot \mu l^{-1}$)	1,3
Milli-Q water	5,7
Total volume	10

3.2.4.2 Transformation of *E. Coli* by heat shock

E. Coli TOP10 chemically competent cells were transformed by a heat shock. Fifty µl of *E. Coli* TOP10 were supplied with 7 µl of the ligation product. The solution was gently mixed and put on ice for 20 min. The heating shock was done at 42°C for 90 s in the dry heating machine. Immediately after that, the mixture was cooled down by putting it on ice for 2 min. The cells were supplied with 450 µl of SOC medium at room temperature. The incubation was done in a thermomixer at 37°C, shaking at 300 rpm for 60 min.

After incubation, the culture was centrifuged at 2 620 x *g* for 2 min. 400 µl of the supernatant was discarded and the pellet was resuspended in 100 µl of remaining supernatant. The bacterial culture was spread over LB agar medium containing 50 $\mu g \cdot ml^{-1}$ of kanamycin for selection of *pDRIVE*-transformed bacteria. The bacterial culture was incubated at 37°C overnight.

Separate colonies were cultured in 5 ml of liquid LB medium supplied with 50 $\mu g \cdot ml^{-1}$ kanamycin. Cultures were incubated overnight at 37°C, shaking at 180 rpm. Next day, plasmids were isolated from the bacterial cultures by QIAprep Spin Miniprep kit following the manufacturer´s instructions. Concentration of the isolated plasmids was measured using NanoDrop One^{C}.

A control PCR was performed to verify the presence of the insert in the *pDRIVE* vector. A PCR reaction mixture was prepared in 20 µl according to Table 3, using M13 reverse primer (5´ - GGAAACAGCTATGACCATGA) and M13 forward primer (5´ - TGTAAAACGAGGGCCAGTG), which are spanning the cloning site. The PCR conditions were set as in Table 4, only with 30 s for elongation. Gel electrophoresis was performed with a 1% agarose gel. The insert in *pDRIVE* vectors was also verified by sequencing. M13 reverse primer was used for sequencing of the *pDRIVE* vector.

3.2.4.3 Standard curve and *HvARF13* expression analysis

First, the copy number of *pDRIVE::HvARF13* plasmids in 1 µl was calculated using the following formula (Lee *et al*., 2006):

$$DNA\ copy = \frac{6{,}02 \cdot 10^{23}[copy \cdot mol^{-1}] \cdot DNA\ amount\ [g]}{DNA\ length\ [bp] \cdot 660\ [g \cdot mol^{-1}]}$$

Based on the calculation result, the plasmid sample was diluted to the final concentration of 10^9 copies of plasmid per µl. Diluting every following sample 10 times from the previous sample, serial dilutions of plasmid were prepared. Starting at 10^9 copies

of plasmid per µl, the plasmid sample was diluted up to 1 copy per µl. Every sample was diluted in 3 replicates. qPCR was performed as described in Chapter 3.2.3.2. The logarithm of number of DNA copies was plotted against C_T values to obtain the standard curve.

The C_T values obtained in the experiment described in Chapter 3.2.3 were used for the absolute quantification of *HvARF13*. The number of *HvARF13* copies in 1 DAG, 2 DAG, 3 DAG and 4 DAG crown samples was determined based on the standard curve.

3.2.5 Optimization of *in situ* PCR

Preliminary experiments following the protocol by Athman *et al*. (2014) for *in situ* PCR in barley crown showed a problem of unspecific signal in tested samples, including negative controls. Therefore, optimization of the protocol was necessary to eliminate the unspecific signal to minimal level.

Separate steps of *in situ* PCR protocol optimization are shown in Fig. 9. Grains of barley cultivar Golden Promise were sterilized and grown in the same conditions as described in Chapter 3.2.2.1. Crowns of 10 DAG barley seedlings were harvested to 2 ml eppendorf tubes. Immediately after harvest, crowns were fixed in 1,8 ml of formaldehyde/acetic acid/ethanol solution. The vacuum infiltration (400 mm Hg) was repeated three times for 5 min. Between infiltrations, samples were mixed properly. The time of fixation was optimized for crown and is shown in Fig. 9. During fixation, samples were kept at 4°C in the dark. After fixation, samples were washed three times with 1,8 ml of ice-cold Wash buffer 1 for 10 min. Then, samples were washed three times with ice-cold 1x PBS for 3 min. Crowns were embedded in 5% agarose in 1x PBS in a 6-well plate. The plate was sealed with parafilm and incubated at 4°C for at least 1 h.

The crown samples were sectioned with vibratome Leica VT 1000 S. Thickness of sections ranged between 30-35 µm, sections of crowns were collected in 0,2 ml eppendorf tubes with DEPC water and RNaseOUT ribonuclease inhibitor. The number of crown sections collected for one sample was also optimized and is shown in Fig. 9. During sectioning, samples were kept on ice. The pretreatment of samples was optimized and is shown in Fig. 9. In the optimized protocols, crown sections were treated with 100 µl of 2 $\mu g \cdot ml^{-1}$ proteinase K in 1x PBS at 37°C for 5 min. Proteinase K was inactivated at 95°C for 2 min. Samples were washed with 100 µl of 1x PBS and 100 µl of DEPC water. Two different DNase enzymes were tested, using either 2,5 units of Turbo DNase

(Thermo Fisher Scientific) or 10 units of DNase I (Qiagen). For both DNase enzymes, the reaction mixture was supplied with 10 µl of Turbo DNase buffer and 2,5 µl RNase-OUT inhibitor, the volume was adjusted to 100 µl with DEPC water. Samples were incubated at 37°C, the time of incubation is shown in Fig. 9. The reaction was inactivated by 3,3 µl of 0,5 mol·l^{-1} EDTA (pH 8) at 70°C for 15 min. Samples were washed twice with ice-cold DEPC water.

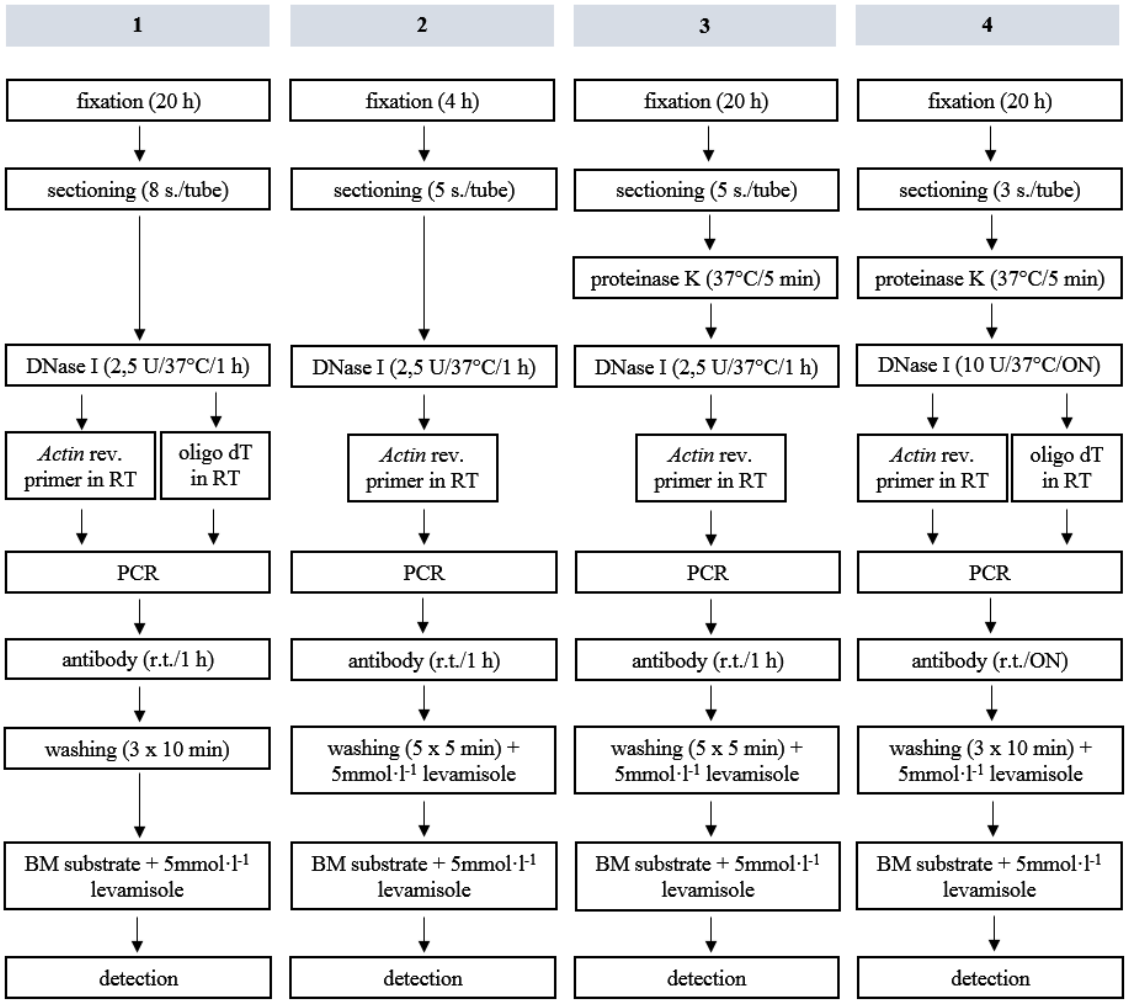

Figure 9 Individual steps of *in situ* PCR optimization for barley crown sections. Only the main steps and the optimized steps are depicted. Protocol number 1 was derived from Athman *et al.* (2014). In protocol number 2 the time of sample fixation and number of crown sections per tube were reduced. In the washing step the number of repetitions was increased, and levamisole was added to Wash buffer 2 in the last washing step. In protocol number 3 the time of fixation was prolonged to 20 h again and the treatment with proteinase K was performed. In protocol number 4 number of sample sections per tube was further reduced. The conditions for DNase treatment were changed, the incubation with antibody was prolonged and number of washing repetitions was reduced. Abbreviations: s./tube, sample sections per tube; ON, overnight; rev., reverse primer; RT, reverse transcription; r.t., room temperature.

In the next step, cDNA was synthesized from RNA via reverse transcription. One sample was completely omitted from reverse transcription and it was later used as a negative control. The rest of samples was supplied with 10 µl of DEPC water, 2 µl of 10 $mmol \cdot l^{-1}$ dNTPs, and either 1 µl of 10 $\mu mol \cdot l^{-1}$ *Actin* reverse primer (further in the text) or 1 µl of 100 $\mu mol \cdot l^{-1}$ oligo dT primer. Samples were incubated at 65°C for 5 min.

Each sample was supplied with 7 µl of the reaction mixture (Table 14). Two samples were used as negative controls, one without primers and the another without reverse transcriptase in the reaction mixture. All samples were incubated at 50°C for 30 min and at 80°C for 10 min. To each sample, 1 µl of RNase H (5 $U \cdot \mu l^{-1}$) was added and samples were further incubated at 37°C for 20 min. Then, each sample was washed twice with 200 µl of sterile water.

To each tube containing the crown sections, 50 µl of the PCR reaction solution was added (Table 15). Primers specific for *Actin* gene (Fw 5´ - ATGGGGCTTCTTTATCCTCG, Rv 5´ - TCTGGTGGGAAGCATTTGAT) were used in the PCR reaction. The PCR conditions in Table 11 were modified, the elongation time was reduced to 10 s and cycling was repeated 32 times. After the PCR reaction, samples were washed twice with 200 µl of 1x PBS.

Further, the washing solution was replaced by 100 µl of 1x BSA block solution. Samples were incubated with the block solution for 30 min on ice. After removing all the block solution, 50 µl of anti-digoxigenin antibody (Fab fragments) conjugated with alkaline phosphatase in 1x BSA solution (1:500 dilution) was added to the samples. The time of incubation with antibody was optimized and is shown in Fig. 9. After incubation with antibody, samples were washed with Wash buffer 2, the washing step was optimized as shown in Fig. 9. All crown sections in Wash buffer 2 were transferred onto a microscope slide. Wash buffer 2 was removed from the samples and 50 µl of BM purple substrate for alkaline phosphatase with 5 $mmol \cdot l^{-1}$ levamisole (an inhibitor of endogenous alkaline phosphatases) was added. Samples were incubated with the substrate for alkaline phosphatase at least 30 min in the dark. If the signal did not appear, the incubation was prolonged to maximally 1 h. Crown sections were washed three times with 100 µl of Wash buffer 2 and once with sterile water. Finally, crown sections were mounted in 40% glycerol and covered with a cover slide.

Table 14 Reaction mixture for reverse transcription in crown sections.

Component	Volume [µl]
5x SSIV buffer	4
SuperScript IV reverse transcriptase (200 $U \cdot \mu l^{-1}$)	1
Dithiothreitol (DTT, 0,1 $mol \cdot l^{-1}$)	1
Ribonuclease inhibitor (40 $U \cdot \mu l^{-1}$)	1
Total volume	7

Table 15 Reaction mixture for PCR in crown sections.

Component	Volume [µl]
5x Phusion buffer HF	10
Phusion DNA polymerase (2 $U \cdot \mu l^{-1}$)	0,5
Forward primer (10 $\mu mol \cdot l^{-1}$)	2,5
Reverse primer (10 $\mu mol \cdot l^{-1}$)	2,5
dNTPs (10 $mmol \cdot l^{-1}$)	1
Digoxigenin-11-dUTP (1 $mmol \cdot l^{-1}$)	0,2
DEPC water	33,3
Total volume	50

3.2.6 Test of Cas9 endonuclease activity

The ortholog of Arabidopsis AtARF17 was determined based on phylogenetic and HMMER analysis (Chapter 3.2.1). The ortholog *HvARF13* (HORVU2Hr1G125740, MLOC_56664) gene was chosen as a target for a CRISPR-Cas9 knock-out in barley. Based on Budhagatapalli *et al*. (2016) protocol, a test of the cleavage activity of Cas9 was performed. For this purpose, two vectors containing the Cas9-target sequences specific for *HvARF13* gene were prepared. Gene-specific gRNA was cloned into *pSH91* vector (Fig. 10) containing Cas9 sequence, resulting in gene-specific Cas9 coding vector. Also, the gRNA together with PAM sequence were cloned into *pNB1* (Fig. 11) vector, which also contains frameshift *YFP* (*Yellow fluorescent protein*) sequence. The *pSH91* and *pNB1* vectors were co-transformed into barley leaves together with *pNB2* vector, which constitutively expresses a gene coding for mCherry fluorescent protein and allows for the comparative quantification of mutation frequency. In the transformed cells, the indels caused by Cas9 activity should result in restoration of *YFP* reading frame and subsequent expression of a functional version of YFP (Fig. 12).

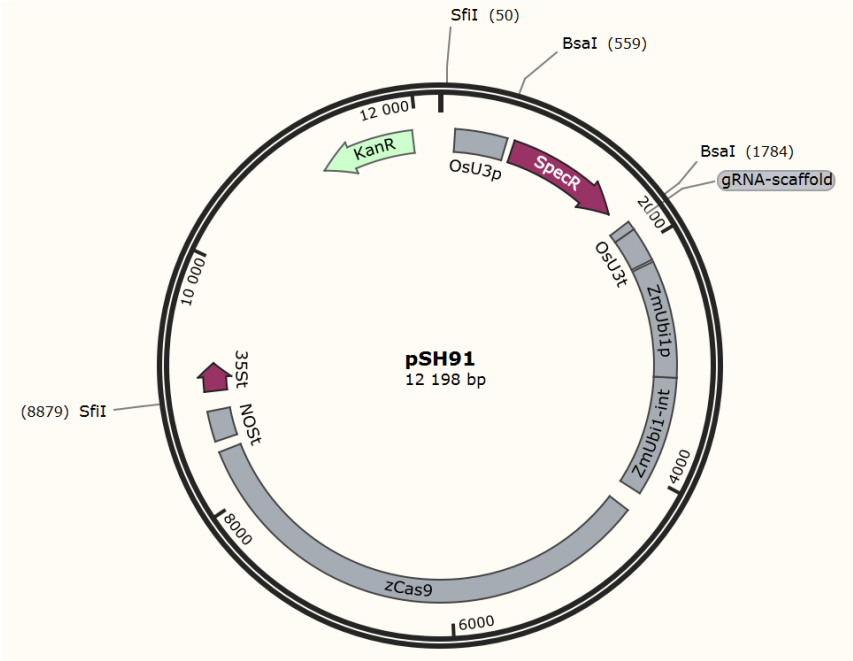

Figure 10 A map of the *pSH91* vector. The vector contains following features: OsU3p, rice snRNA U3 promoter; *Spec*^{R}, spectinomycin resistance gene; gRNA scaffold, guide RNA scaffold for CRISPR-Cas9 system; OsU3t, rice snRNA U3 terminator; ZmUbi1p and ZmUbi1-int, maize *Ubiquitin 1* promoter with first intron; *zCas9*, codon-optimized version of *Cas9*; NOSt, nopaline synthase terminator; 35St, 35S terminator; *Kan*^{R}, *Aminoglycoside Phosphotransferase* gene (kanamycin resistance gene).

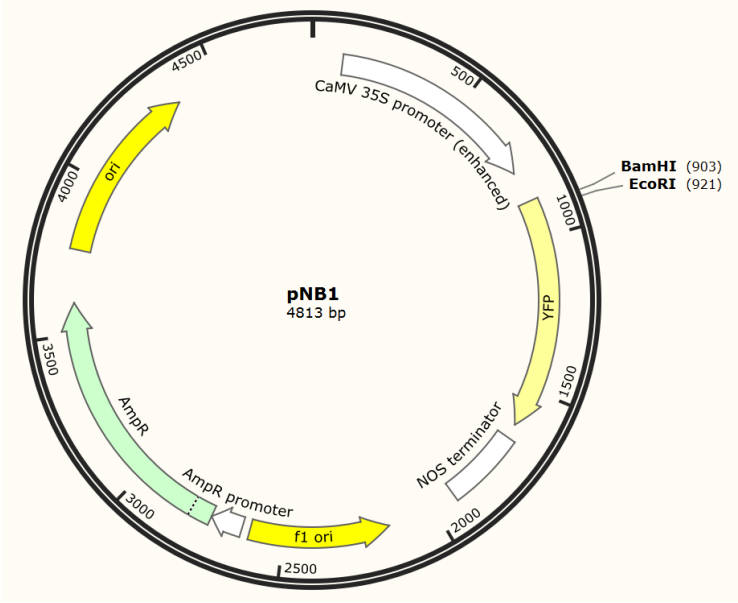

Figure 11 A map of the *pNB1* vector. The vector contains following features: CaMV 35S promoter (enhanced), Cauliflower Mosaic virus 35S promoter for enhanced gene expression in plants; *YFP*, gene for Yellow fluorescent protein; NOS terminator, nopaline synthase terminator; f1 ori, f1 bacteriophage origin of replication; *Amp*^{R} promoter, promoter of *β-lactamase* gene; *Amp*^{R}, *β-lactamase* gene (ampicillin resistance gene); ori, ColE1 origin of replication for bacteria.

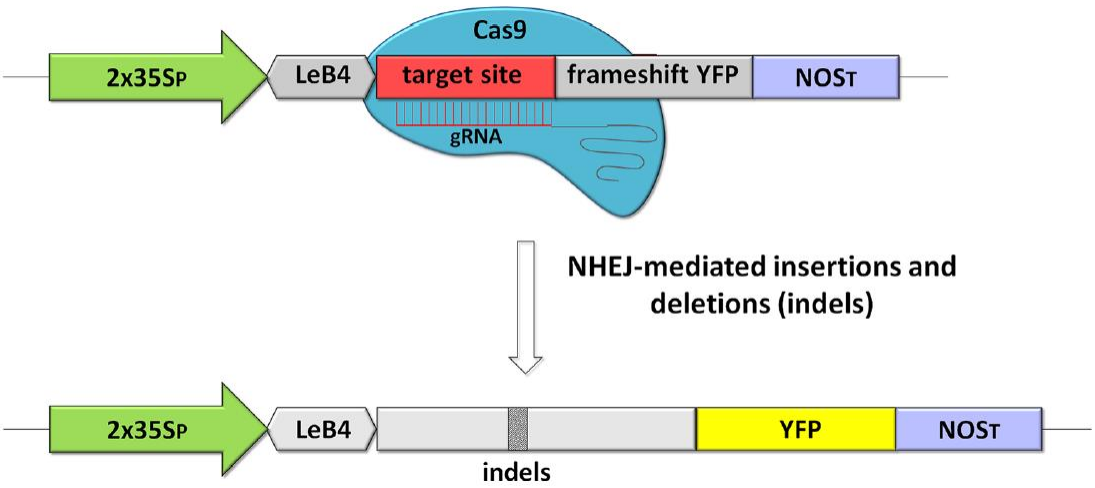

Figure 12 Diagram presenting the principal of the endonuclease cleavage activity test. Cas9 with specific gRNA recognizes target site in the construct and creates double-strand DNA breaks. Non-homologous end-joining (NHEJ) repair system creates insertions and deletions (indels) in the target site. Indels restore the functional reading frame of YFP (Budhagatapalli *et al*., 2016).

3.2.6.1 Design of the *HvARF13*-specific gRNA

The CRISPR-Cas9 knock-out experiment was designed using Deskgen Knock-out online tool. In Deskgen database, barley *HvARF13* (using MLOC_56664 code) gene was searched. gRNA sequences were designed for a coding region of *HvARF13* gene. gRNA sequences with the highest on-target activity and the least off-target activity were filtered. Target sequences with off-target activity in a coding region of the gene were excluded from the selection. Two target sequences with the best score (Table 16) were chosen for CRISPR knock-out experiment.

Table 16 gRNA designed for CRISPR-Cas9 knock-out of *HvARF13*.

gRNA sequence	PAM	Cut Site
gRNA-HvARF13_1: ACTGGGCTGAATCTGTGGCA	GGG	chromosome 2 [exon 2, position 623441040]
gRNA-HvARF13_2: CCGACATCGACGGAGCAAAG	AGG	chromosome 2 [exon 2, position 623441142]

3.2.6.2 Preparation of gRNA oligonucleotide duplex

Both gRNA-HvARF13 sequences were separately cloned into *pSH91* and *pNB1* vectors. As the restriction cloning approach was chosen, recognition sequences of specific restriction enzymes were added to gRNA oligonucleotide sequences (Table 17). For cloning into *pSH91*, *Bsa*I enzyme recognition sequence was added to the 5´ends of both forward and reverse strands of the target oligonucleotides. For cloning into *pNB1* vector, *BamH*I enzyme recognition sequence was added to the 5´end of forward oligonucleotide and *EcoR*I enzyme recognition sequence was added to the 5´end of reverse oligonucleotide. Oligonucleotides cloned into *pNB1* vector also contained the PAM sequence.

To obtain double-stranded oligonucleotide sequences, the complementary forward and reverse oligonucleotides were mixed in one reaction (Table 18). The annealing of complementary oligonucleotides was performed in a PCR thermocycler. The annealing program was set according to Table 19, with temperature dropping from 70°C to 4°C (1°C per 1 min).

Table 17 List of oligonucleotides cloned into *pSH91* and *pNB1* vectors.

Vector	gRNA type	Oligonucleotide (5´→3´)
pSH91	HvARF13_1	Fw: GGCGACTGGGCTGAATCTGTGGCA Rv: AAACTGCCACAGATTCAGCCCAGT
pSH91	HvARF13_2	Fw: GGCGCCGACATCGACGGAGCAAAG Rv: AAACCTTTGCTCCGTCGATGTCGG
pNB1	HvARF13_1	Fw: GATCCACTGGGCTGAATCTGTGGCAGGG Rv: AATTCCCTGCCACAGATTCAGCCCAGTG
pNB1	HvARF13_2	Fw: GATCCCCGACATCGACGGAGCAAAGAGG Rv: AATTCCTCTTTGCTCCGTCGATGTCGGG

Table 18 Reaction mixture for annealing of gRNA oligonucleotides.

Component	Volume [µl]
10x T4 DNA ligase buffer	5
Forward oligonucleotide (100 µmol·l^{-1})	1
Reverse oligonucleotide (100 µmol·l^{-1})	1
Nuclease-free water	43
Total volume	50

Table 19 Program of the PCR thermocycler for gRNA oligonucleotide annealing.

Step	Temperature [°C]	Time [min]
Denaturation	95	4
Oligonucleotide annealing	70	10
Oligonucleotide annealing	from 70 to 4 (1°C/min)	66
Final incubation	4	10

3.2.6.3 Cloning of gRNA into *pSH91* and *pNB1* vectors

For the cloning of gRNA oligonucleotide duplex into *pSH91*, the vector was linearized by *Bsa*I enzyme. The *Bsa*I enzyme cuts in two positions in the *pSH91* sequence. The restriction removes 1 225 bp from the vector together with the sequence for spectinomycin resistance gene ($Spec^R$). The restriction conditions were set according to Table 20. The reaction mix was incubated at 37°C for 2 h. After the restriction was done, the plasmid was purified with NucleoSpin Gel and PCR Clean-up kit following the PCR Clean-up protocol.

For the cloning of gRNA oligonucleotide duplex into *pNB1*, the vector was linearized by *BamH*I and *Eco*RI enzymes. The *BamH*I enzyme cuts in position 903 in the *pNB1* sequence and *Eco*RI enzyme cuts in position 921 in the sequence. Together, these enzymes linearize the *pNB1* vector while cutting out only 18 bp of the vector. The restriction conditions were set according to Table 21. The reaction mix was incubated

Table 20 Reaction mixture for *pSH91* restriction by *Bsa*I.

Component	Volume [µl]
10x CutSmart buffer	5
*Bsa*I-HF (20 000 U·ml^{-1})	1
pSH91 vector (400 ng·µl^{-1})	5
Nuclease-free water	39
Total volume	50

Table 21 Reaction mixture for *pNB1* restriction by *BamH*I and *Eco*RI.

Component	Volume [µl]
10x CutSmart buffer	5
*BamH*I-HF (20 000 U·ml^{-1})	1
*Eco*RI-HF (20 000 U·ml^{-1})	1
pNB1 vector (400 ng·µl^{-1})	5
Nuclease-free water	38
Total volume	50

Table 22 Reaction mixture for ligation of gRNA oligonucleotide duplex with corresponding vectors.

Component	Volume [µl]
10x T4 DNA ligase buffer	1
T4 DNA ligase (5 U·µl^{-1})	1
Digested vector *pSH91*/*pNB1*	1
Corresponding oligonucleotide duplex	7
Total volume	10

at 37°C for 2 h. After the restriction was done, the plasmid was purified with NucleoSpin Gel and PCR Clean-up kit following the PCR Clean-up protocol.

After the gRNA oligonucleotide duplex and digested plasmids were prepared, the ligation reaction was done to join the two sequences by phosphodiester bond. The reaction conditions are described in Table 22 and the mixture was incubated at 16°C overnight.

E. Coli TOP10 chemically competent cells were transformed by heat shock (Chapter 3.2.4.2). The bacterial culture was spread over LB agar medium containing corresponding antibiotic, 50 µg·ml^{-1} of kanamycin for selection of *pSH91*-transformed bacteria or 100 µg·ml^{-1} ampicillin for the selection of *pNB1*-transformed bacteria. The bacterial culture was incubated at 37°C overnight.

3.2.6.4 Verification of an insert

After overnight incubation of the bacterial culture, several bacterial colonies were visible on the LB agar plates. To check transformation products, colony PCR was performed. For every construct, five colonies were screened by colony PCR. Every bacterial colony was picked by a sterile toothpick and dissolved in 20 µl of sterile water. The culture was heated up to 99°C and incubated for 15 min.

The reaction mixture for colony PCR was prepared in 20 µl according to Table 3 (1 µl of bacterial culture was used instead of DNA template) and the PCR program was set according to Table 23. To check whether the cloning of gRNA oligonucleotide in *pSH91* vector and following transformation were successful, PCR was performed using primers spanning the cloning site (*pSH91* Fw: *5′* - CAGGGACCATAGCACAAGAC, Rv: *5′* - TCAGCGGGTCACCAGTGTTG). In the case of successful cloning of *pSH91::gRNA-HvARF13*, the PCR product was 600 bp long. In the colony PCR reaction for *pNB1::gRNA-HvARF13* control, the forward primer was annealing to the oligonucleotide duplex and the reverse primer was annealing to the NOS terminator

Table 23 Program of the PCR thermocycler for colony PCR.

Step	Temperature [°C]	Time [s]	Number of cycles
Initial denaturation	95	120	1
Denaturation	95	30	
Primer annealing	60	30	34
Elongation	72	50	
Final elongation	72	600	1
Final incubation	22	holding	-

sequence (*pNB1* Reverse primer: 5´- TAACATAGATGACACCGCGC). The bacterial cultures carrying *pNB1::gRNA-HvARF13* showed 950 bp PCR products. Agarose gel electrophoresis was performed to check the PCR product length.

When a PCR product of the correct length was obtained, the corresponding bacterial colony was cultured overnight in 5 ml of liquid LB medium supplied with corresponding antibiotic, 50 $\mu g \cdot ml^{-1}$ of kanamycin for selection of *pSH91*-transformed bacteria or 100 $\mu g \cdot ml^{-1}$ ampicillin for the selection of *pNB1*-transformed bacteria. Bacterial cultures were incubated overnight at 37°C, shaking at 180 rpm. Next day, plasmids were isolated from the bacterial cultures by QIAprep Spin Miniprep kit following the manufacturer´s instructions. Concentration of the isolated plasmids was measured using NanoDrop One^{C}. The isolated plasmids were prepared for Sanger sequencing. For the sequencing of *pSH91* plasmids, the *pSH91*-reverse primer (5´- AATGTGGCGCCGTAAATAAG) was used. To sequence the *pNB1* plasmids, the 35S-*pNB1* forward primer (5´- CCACTATCCTTCGCAAAGACC) was used.

3.2.6.5 Preparation of plasmid DNA

The concentration of *pNB1* and *pSH91* plasmids was increased using NucleoBond Xtra Midi kit. The protocol for low-copy plasmid purification was followed according to manufacturer´s instructions. In the final step, the plasmids were eluted to 300 µl of TE buffer. Concentration of plasmids was measured by NanoDrop One^{C}.

3.2.6.6 Biolistic transformation of barley leaves

Barley seedlings were grown in soil for ten days. Primary leaves were cut with a sterile razor blade. Leaves from 6-8 plants were placed on 1% agar medium containing 20 $\mu g \cdot ml^{-1}$ benzimidazol and 20 $\mu g \cdot ml^{-1}$ chloramphenicol in a sterile Petri dish.

The leaves were fastened to the Petri dish with a tape to prevent them from moving during particle bombardment.

At the beginning of the experiment, mixture of plasmid DNA was prepared. The total amount of DNA used for biolistic transformation was 60 μg. The ratio between *pNB1*, *pSH91* and *pNB2* was 2:2:1 (24 μg:24 μg:12 μg), respectively.

Suspension of 1,5 mg gold particles (microcarriers) in 50 μl of Nuclease-free water was centrifuged at 14 270 x *g* for 2 min, the supernatant was discarded. Washing with 100 μl of Nuclease-free water and centrifugation were repeated 3 times. After last centrifugation, gold particles were resuspended in 20 μl of Nuclease-free water. The suspension of gold particles was sonicated until the suspension was homogenous (without any clumps). While vortexing the suspension of gold particles, mixture of plasmid DNA was added. The mixture of gold particles and plasmid DNA was vortexed for 1 min. Still vortexing the mixture, 10 μl of 0,1 $mol \cdot l^{-1}$ spermidine and 25 μl of 2,5 $mol \cdot l^{-1}$ $CaCl_2$ were added to the mixture. Vortexing proceeded for another 2 min. The gold particles covered with DNA were washed one time with 500 μl of 70% ethanol. After short centrifugation and discarding the supernatant, gold particles were washed also with 100% ethanol. Finally, gold particles were resuspended in 140 μl of 100% ethanol.

The PDS-1000/He Hepta^{TM} system was used for biolistic transformation of barley leaves. Before use, all components of biolistic particle delivery system (especially macrocarriers, rupture disc, stopping screen) were sterilized in 70% ethanol for 15 min. The suspension of gold particles covered with plasmid DNA was sonicated until all clumps were removed. 20 μl of the gold suspension were spread over one macrocarrier. In total, seven macrocarriers were used for one bombardment. The rupture disc holder, macrocarrier adapter and the Petri dish with barley leaves were placed into the bombardment chamber. After closing the chamber firmly, it was evacuated to 23 Hg. The bombardment was conducted under 1 100 psi helium pressure. Immediately after bombardment, vacuum was released. This procedure was repeated twice for every construct. Barley leaves were incubated in the dark at room temperature for 24 to 72 h. The presence of fluorescent signal of mCherry and YFP was checked every 24 h with epifluorescent microscope Axio Imager M2.

3.2.7 Stable transformation of barley

The stable transformation of barley was performed according to the protocol introduced by Marthe *et al*. (2015). In order to obtain *HvARF13*-knock-out barley plants, the *p6i-d35S-TE9* vector (Fig. 13) containing CRISPR-Cas9-gRNA-HvARF13 cassette was transformed into barley. The vector was introduced into barley immature embryos by *A. tumefaciens*-mediated transformation.

3.2.7.1 Preparation of the binary vector for barley transformation

To obtain the final vector for barley stable transformation, a fragment of the *pSH91::gRNA-HvARF13* vector was cloned into *p6i-d35S-TE9* vector. First, both vectors were digested with *Sfi*I enzyme. The *Sfi*I enzyme cuts at two positions in the *pSH91::gRNA-HvARF13* vector, creating fragments of 3 300 bp and 7 600 bp. While the digestion of the *p6i-d35S-TE9* vector with *Sfi*I enzyme removes only 64 bp fragment. The restriction mixture was prepared according to Table 24 and it was incubated at 50°C for 4 h. Then, the digested plasmids were purified by PCR Clean-up kit and the plasmid concentration was measured by NanoDrop One^{C}. Also, the agarose gel electrophoresis was performed to check the length of restriction products.

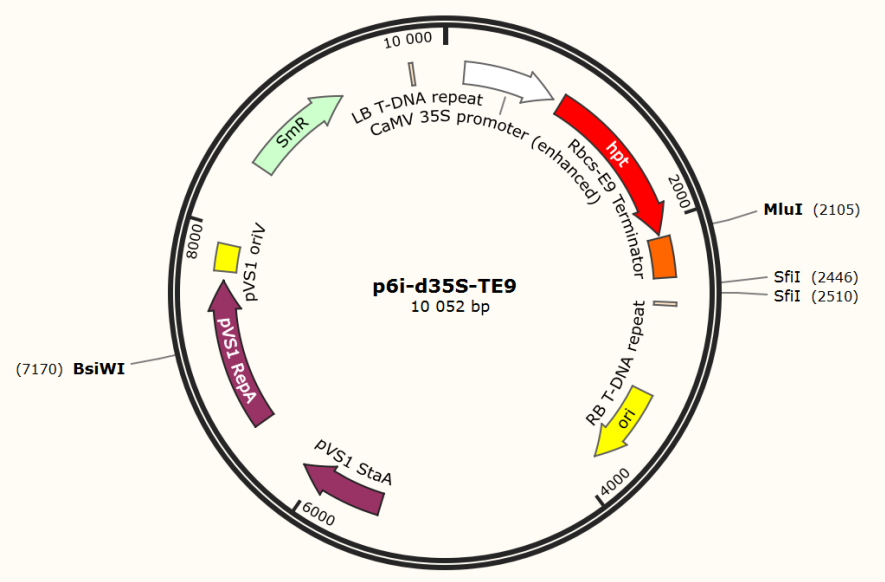

Figure 13 A map of the *p6i-d35S-TE9* vector. The vector contains following features: CaMV 35S promoter (enhanced), Cauliflower Mosaic virus 35S promoter for enhanced gene expression in plants; *Hpt*, *Hygromycin Phosphotransferase* gene; Rbcs-E9 terminator; LB (left border) and RB (right border) T-DNA repeats; ori, ColE1 origin of replication for bacteria; pVS1 StaA, pVS1 oriV, pVS1 RepA, cassette for plasmid replication and stability in *Agrobacterium*; *Sm*^{R}, streptomycin/spectinomycin resistance gene.

Table 24 Reaction mixture for restriction of *pSH91* and *p6i-d35S-TE9* vectors by *Sfi*I.

Component	Volume [µl]
10x CutSmart buffer	5
*Sfi*I (20 000 U·ml^{-1})	1
pSH91::gRNA-HvARF13/*p6i-d35S-TE9*	according to the plasmid concentration (3 µg)
Milli-Q water	up to 50
Total volume	50

As the longer fragment of *pSH91::gRNA-HvARF13* contained the CRISPR-Cas9 cassette and the gRNA sequence, it was necessary to clone that fragment into the *p6i-d35S-TE9* vector. To increase the probability of correct ligation, the ratio between vector and insert in the reaction mixture was 1:10 (Table 25). The ligation mixture was incubated at 16°C overnight.

The product of ligation was transformed into *E. Coli* TOP10 following the same protocol as in Chapter 3.2.4.2. The transformed bacteria were cultured on solid LB agar medium containing 50 µg·ml^{-1} spectinomycin to select bacteria transformed with *p6i-d35S-TE9::gRNA-HvARF13.* Verification of the insert was performed the same way as for vector *pSH91* in Chapter 3.2.6.4, with the difference that every cultivation medium was supplied with spectinomycin antibiotic.

Before sending the plasmids for sequencing, control restriction of the *p6i-d35S-TE9::gRNA-HvARF13* vector was performed. The *BsiW*I enzyme was chosen, because it cuts in only one position in the vector sequence and in one position in the insert sequence. The reaction mixture (Table 26) was incubated at 55°C for 2 h. The restriction results were subsequently checked by agarose gel electrophoresis.

Table 25 Reaction mixture for ligation of *pSH91* fragment and *p6i-d35S-TE9.*

Component	Volume [µl]
10x T4 DNA ligase buffer	1
T4 DNA ligase (5 U·µl^{-1})	1
Digested vector *p6i-d35S-TE9* (50 ng·µl^{-1})	1
Digested vector *pSH91::gRNA-HvARF13* (140 ng·µl^{-1})	2,6
Milli-Q water	4,4
Total volume	10

Table 26 Reaction mixture for control restriction of *p6i-d35S-TE9::gRNA-HvARF13*.

Component	Volume [µl]
10x NEB 3.1 buffer	5
*BsiW*I (10 000 U·ml^{-1})	1
p6i-d35S-TE9::gRNA-HvARF13 vector (330 ng·µl^{-1})	3
Milli-Q water	41
Total volume	50

3.2.7.2 Preparation and culture of *Agrobacterium tumefaciens*

The protocol of Marthe *et al*. (2015) was followed to prepare and culture the *A. tumefaciens* strain AGL1 for barley transformation. AGL1 is a hypervirulent strain of *A. tumefaciens*, which carries chromosomal marker genes for rifampicin and carbenicillin resistance (Lazo *et al*., 1991).

Electroporation was carried out to transform *A. tumefaciens* strain AGL1 with *p6i-d35S-TE9::gRNA-HvARF13*. The electroporation cuvette was cooled down on ice before use. Also, the plasmid DNA and *A. tumefaciens* cells were kept on ice before the electroporation. 2 µl of the plasmid DNA were added to *A. tumefaciens* electrocompetent cells, mixed gently and incubated for 2 min on ice. Then, the sample was transferred to the electroporation cuvette and put into the electroporation chamber in BTX ECM 399 electroporator. A high voltage (1 800 V) was applied to the samples. Immediately after the pulse, 200 µl of SOC medium (prewarmed to 28°C) was added to the cells. Cells were transferred to a new eppendorf tube and incubated in a thermomixer at 4°C, shaking at 300 rpm for 1 h. After the incubation, 25 µl of the culture was spread over MG/L agar medium supplied with 100 µg·ml^{-1} spectinomycin, 100 µg·ml^{-1} carbenicillin, 50 µg·ml^{-1} rifampicin and 1 µg·l^{-1} biotin. The cultivation time was approximately 48 h. Separate *A. tumefaciens* colonies were cultured in 5 ml of liquid MG/L medium supplied with antibiotics and biotin. Bacterial cultures were incubated overnight at 28°C, shaking at 180 rpm. After the cultivation, plasmid isolation was performed using double amount of P1, P2 and N3 buffers of QIAprep Spin Miniprep kit. Then, the isolated plasmids were checked by restriction with *BsiW*I restriction enzyme. The restriction reaction mixture was prepared according to Table 26 and it was incubated at 55°C for 2 h. The plasmid fragments were separated by agarose gel electrophoresis.

A. tumefaciens culture, in which the *p6i-d35S-TE9::gRNA-HvARF13* vector was confirmed, was used for preparation of stock bacterial culture. The overnight cultivation

in liquid MG/L medium was performed as described above. The cultivation was stopped when the optical density (OD_{600}) of the culture reached OD_{600} = 2, the OD_{600} was measured by spectrophotometer. Two hundred µl of the culture was mixed with 200 µl of 15% glycerol. The mixture was incubated at room temperature for 2 h. The stock bacterial cultures were kept at -80°C.

3.2.7.3 Barley immature embryo transformation

Barley immature embryos were transformed according to the protocol by Marthe *et al*. (2015). The process of barley transformation and regeneration was done in cooperation with Mgr. Kateřina Střelcová and Bc. Vendula Svobodová. A day before the transformation, *A. tumefaciens* culture was prepared. The stock culture of *A. tumefaciens* in glycerol was dissolved in 10 ml of MG/L liquid medium in a 100 ml Erlenmeyer flask. The culture was incubated overnight at 28°C, shaking at 180 rpm.

The immature caryopses were harvested and collected in a 500 ml bottle in an ice bath. The caryopses were sterilized first with 70% ethanol for 3 min and then with 4% sodium hypochlorite for 15 min. All other manipulation with caryopses were done in the laminar flow cabinet. The caryopses were washed five times with sterile water. For collecting barley embryos, the six-well plate was prepared. Each well was filled with 3 ml of liquid cocultivation medium (BCCM). Manipulation with barley caryopses were done under a stereo zoom microscope. Also, the light in the laminar flow cabinet was turned off, as the embryos are light-sensitive. After exposing the embryo inside the caryopses, the embryo axis was removed. The excised embryo was transferred to the six-well plate containing liquid BCCM medium. In total, 250 immature embryos were collected.

For the barley transformation, the OD_{600} of *A. tumefaciens* culture was measured and adjusted to OD_{600} = 2,5. The BCCM medium was removed from the wells and it was replaced by 600 µl of *A. tumefaciens* culture. The plate with barley embryos was placed in a desiccator and the 500 mbar vacuum was applied for 1 min. After 10 min of incubation at room temperature, the barley embryos were washed two times with 3 ml of BCCM medium for 15 min. Finally, the wells were filled with 3 ml of BCCM. The plate was sealed with parafilm and covered with aluminum foil. Barley embryos were incubated at 21°C for 2 days.

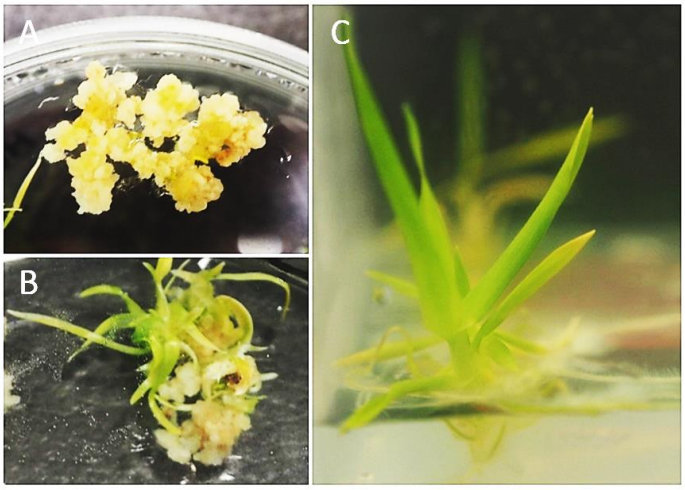

Figure 14 Regeneration of transgenic plants from callus. A, callus on the regeneration medium; B, regeneration of a shoot from callus; C, barley plantlet after regeneration from callus.

After 2 days, the barley embryos were transferred to solid callus induction medium (BCIM) with the scutellum side down. The Petri dish was sealed with parafilm and it was incubated in the dark at 24°C for 2 weeks. Then, embryos were transferred to fresh BCIM for another three weeks. Callusing embryos were transferred to regeneration medium (BRM) and incubated in an environmental chamber with the photoperiod of 24°C/16 h/light (160 $\mu mol \cdot m^{-2} \cdot s \cdot^{-1}$) and 22°C/8 h/dark (Fig. 14). Callusing embryos were transferred to fresh BRM every two weeks until shoots reached about 3 cm. Then, shoots were transferred to a plastic box containing BRM and incubated in the conditions of the environmental chamber. After the plantlets developed roots, they were transferred to soil and grown in high humidity conditions (covered with a plastic hood) in a phytotron (16°C/16 h/light and 12°C/8 h/dark).

3.2.7.4 Screening of the transgenic plants

To analyse transgenic plants by PCR, genomic DNA (gDNA) was isolated from leaves of T_0 barley plants. The phenol/chloroform/isoamyl-alcohol method for gDNA isolation was followed according to Pallotta *et al*. (2000). A young leaf was cut, placed in a tube with metal beads and it was immediately frozen by liquid nitrogen. The samples were homogenized by Mixer Mill at 20 Hz for 1 min. To each sample, 800 µl of extraction buffer was added and the samples were vortexed. Working in an air hood, 800 µl of a phenol/chloroform/isoamyl-alcohol (25:24:1) mixture was added. The samples were

vortexed and centrifuged at 1 820 x *g* for 3 min. Supernatant containing gDNA was carefully transferred to a new tube. Then, 80 µl of 3 $mol \cdot l^{-1}$ sodium acetate (pH 5.2) and 800 µl of isopropanol were added. The tubes were shaken until a precipitate was observed. The samples were centrifuged at 12 300 x *g* at 4°C for 5 min. Supernatant was discarded, and the pellet was dried at room temperature. The pellet was resuspended in 100 µl of RNase A (40 $\mu g \cdot ml^{-1}$) in TE buffer (pH 8.0). The solution was incubated at 37°C for 1 h. Samples were kept at 4°C.

First, T_0 transgenic plants were screened for presence of CRISPR-Cas9 cassette (Fig. 15), specifically the *Hygromycin Phosphotransferase* (*Hpt*) gene, *Cas9* gene and gRNA scaffold. Genomic DNA was used as a template in a 10 µl PCR reaction (Table 3). The PCR conditions were adjusted to primers used in the reaction (Table 27, 28). The annealing temperature was set to 63°C for *Cas9* and gRNA scaffold primers, 59°C for *Hpt* primers. The time of elongation was set to 40 s for *Hpt*, 45 s for gRNA scaffold gene and 100 s for *Cas9*. To analyse the results, agarose gel electrophoresis was performed.

Next, T_0 plants positive for all three genes were further screened for presence of a mutation in *HvARF13* gene sequence. PCR was performed in 40 µl (Table 3) in two separate PCR tubes (to obtain the final volume of 80 µl for one sample) with genomic DNA of T_0 plants as a template and with *HvARF13*-specific primers (Table 28). The PCR conditions (Table 27) were again adjusted to the primers used and to the length of amplified region. The annealing temperature was set to 60°C and the time of elongation was set to 105 s. The PCR product was purified with NucleoSpin Gel and PCR Clean-up kit and sequenced by Sanger sequencing method.

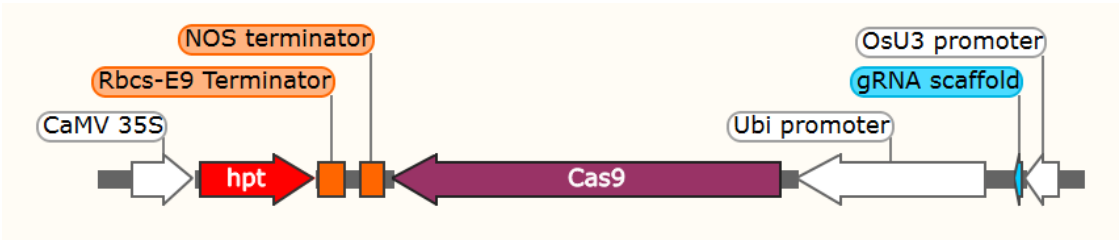

Figure 15 A CRISPR-Cas9 construct in the *p6i-d35S-TE9* vector. The construct contains following features: CaMV 35S, Cauliflower Mosaic virus 35S promoter for enhanced gene expression in plants; *Hpt*, *Hygromycin Phosphotransferase* gene; Rbcs-E9 terminator; NOS terminator, nopaline synthase terminator; *Cas9*, *Cas9* endonuclease; Ubi promoter, maize polyubiquitin promoter; gRNA scaffold, guide RNA scaffold for CRISPR-Cas9 system; OsU3 promoter, rice snRNA U3 promoter.

Table 27 Program of the PCR thermocycler for control PCR. The primer annealing temperature varies according to the primer, 63°C for *Cas9* and gRNA scaffold, 59°C for *Hpt*, 60°C for *HvARF13*. The time for elongation varies according to the PCR product length, 40 s for *Hpt*, 45 s for gRNA scaffold, 100 s for *Cas9*, 105 s for *HvARF13*.

Step	Temperature [°C]	Time [s]	Number of cycles
Initial denaturation	98	300	1
Denaturation	98	45	34
Primer annealing	x	30	
Elongation	72	y	
Final elongation	72	300	1
Final incubation	4	holding	-

Table 28 Primers used for screening of transgenic plants.

Target	Primer sequence (5´ → 3´)	Product size (bp)
Hpt	Fw: GAATTCAGCGAGAGCCTGAC Rv: ACATTGTTGGAGCCGAAATC	557
gRNA scaffold	Fw: CAGGGACCATAGCACAAGAC Rv: TCAGCGGGTCACCAGTGTTG	594
Cas9	Fw: TGGTTAGGGCCCGGTAGTTC Rv: TTAATCATGTGGGCCAGAGC	1 595
HvARF13	Fw: TTCTGAATGAATGAGGGAGTGG Rv: TGGAGCTAGGTGGGAAGAA	1 449

4 RESULTS

4.1 Identification and characterization of barley ARF proteins

In general, plant genomes comprise a high number of ARF family members. At the time of starting work on this topic, only few members of ARF family were described in barley. For that reason, barley databases were searched for new potential ARFs.

First, only protein sequences longer than 100 amino acids were selected. Then, the domain composition of pre-selected candidates was analysed by HMMER.

Table 29 List of putative ARF family members in barley. ID, identification code; CDS, coding sequence; Aux/IAA, PB1 domain facilitating dimerization with Aux/IAAs; B3, B3-type domain; Auxin-resp, a domain specific for ARFs.

Gene name	Gene ID	MLOC ID	Activator/ Repressor	CDS length/bp	Protein domains	Predicted protein/aa
HvARF1	HORVU3Hr1G032230.6	MLOC_65945	R	2 771	Aux/IAA, B3, Auxin-resp	800
HvARF3a	HORVU3Hr1G072340.1	MLOC_66439	R	2 963	B3, Auxin-resp	648
HvARF3b	HORVU3Hr1G064590.1	MLOC_44012	R	1 184	B3, Auxin-resp	194
HvARF4a	HORVU3Hr1G097200.1	MLOC_18401	R	3 092	Aux/IAA, B3, Auxin-resp	826
HvARF4b	HORVU3Hr1G096410.4	MLOC_68907	R	2 415	Aux/IAA, B3, Auxin-resp	804
HvARF4c	HORVU3Hr1G096510.5	MLOC_68907	R	3 172	Aux/IAA, B3, Auxin-resp	801
HvARF8	HORVU6Hr1G058890.1	MLOC_77438	R	2 561	B3, Auxin-resp	759
HvARF9	HORVU2Hr1G076920.1	MLOC_64596	R	2 806	Aux/IAA, B3, Auxin-resp	658
HvARF11	HORVU2Hr1G109650.4	MLOC_55345	A	4 131	Aux/IAA, B3, Auxin-resp	955
HvARF12	HORVU2Hr1G121110.32	MLOC_74570	A	2 517	Aux/IAA, B3, Auxin-resp	838
HvARF13	HORVU2Hr1G125740.1	MLOC_56664	R	1 170	B3, Auxin-resp	389
HvARF14	HORVU1Hr1G076690.7	MLOC_38232	R	2 301	B3, Auxin-resp	600
HvARF15	HORVU1Hr1G087460.5	MLOC_17721	R	2 150	B3, Auxin-resp	615
HvARF17a	HORVU6Hr1G026730.8	MLOC_66152	A	3 731	Aux/IAA, B3, Auxin-resp	927
HvARF17b	HORVU7Hr1G106280.1	MLOC_58330	A	4 255	Aux/IAA, B3, Auxin-resp	938
HvARF18	HORVU7Hr1G101270.3	MLOC_69988	R	3 178	B3, Auxin-resp	697
HvARF19a	HORVU6Hr1G020330.9	MLOC_73144	A	4 297	Aux/IAA, B3, Auxin-resp	1 129
HvARF19b	HORVU7Hr1G096460.14	MLOC_63193	A	3 531	Aux/IAA, B3, Auxin-resp	1 176
HvARF21	HORVU7Hr1G051930.4	MLOC_14584	A	3 737	Aux/IAA, B3, Auxin-resp	1 083
HvARF22	HORVU1Hr1G041770.1	MLOC_64795	R	2 900	B3, Auxin-resp	688
HvARF25	HORVU5Hr1G009650.17	MLOC_63938	A	3 895	Aux/IAA, B3, Auxin-resp	575

Only sequences containing the typical ARF protein domains (PB1 domain for dimerization with Aux/IAAs, B3-type domain or ARF domain) were considered as putative barley ARFs.

In total, 21 *ARF* genes (Table 29) were identified in barley. Names of barley ARF proteins were assigned based on their orthology with rice ARF proteins. For each gene, one representative splicing variant was chosen, and the corresponding protein sequence was further examined. When the amino acid composition of the middle region of protein sequences was analysed, 8 of the ARF proteins were rich in glutamine. These 8 ARF proteins potentially have a function of activator transcription factors. The remaining 13 ARF proteins could function as repressor transcription factors. Eight of the putative ARF repressors are truncated, lacking the PB1 domain necessary for dimerization with Aux/IAA proteins. The phylogenetic analysis of the barley ARF family members (Fig. 16) indicates that ARFs separate into three classes. While class Ia comprises full-length ARF repressors, classes Ib and III group only truncated ARF proteins. All activator ARF proteins associated in class II.

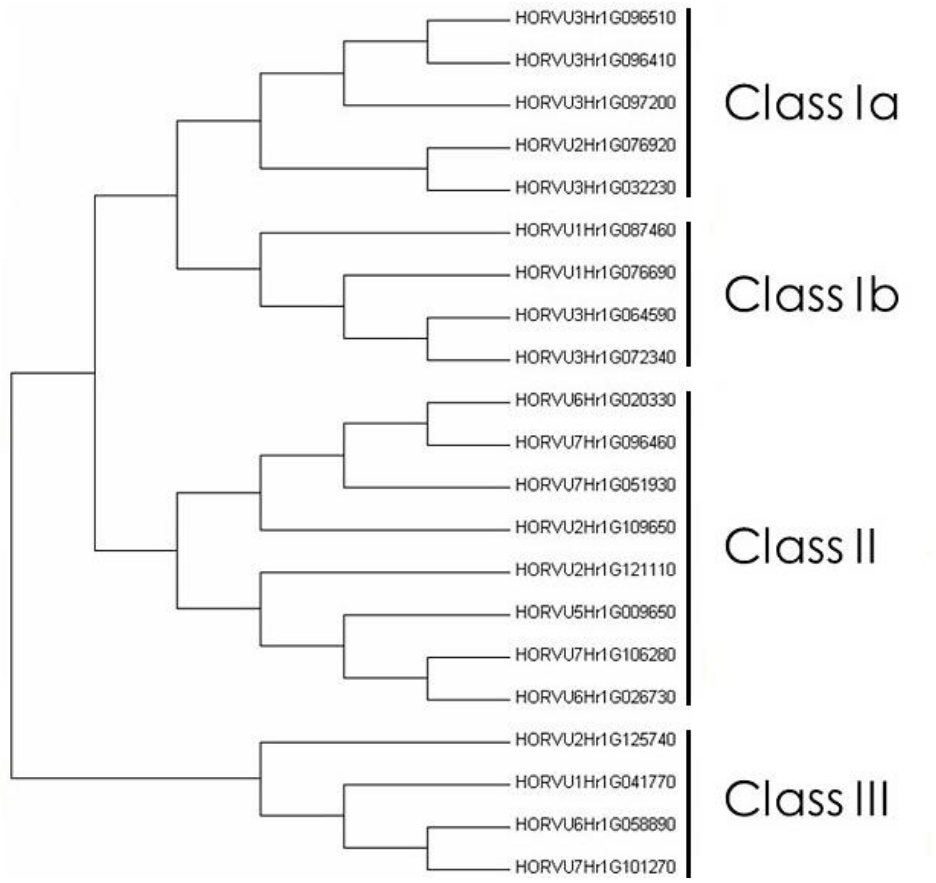

Figure 16 Cladogram of barley ARF proteins. Phylogenetic relations between HvARF proteins was analysed by MEGA7 software. HvARF proteins were separated in classes Ia, Ib, II and III.

4.2 *ARF* gene expression analysis

4.2.1 Analysis of *ARF* gene expression in barley

The overall expression of all 21 *ARF* genes was assessed in 11 samples of barley tissue (Fig. 17). The differential expression pattern of individual *ARF* genes was observed. The main focus was on crown of the barley seedlings 10 days after germination (DAG). In crown, a balanced expression between repressors and activators was observed. Transcripts of *HvARF8* and *HvARF19b* were not detected at all in this tissue. Also, the expression of *HvARF11*, *HvARF13* and *HvARF14* was very low in crown samples.

Most of *ARF* genes were expressed in the majority of tested tissues. The expression level of most *ARF* genes changed between different developmental stages of leaves, grains and inflorescence. Also, the balance between repressors and activators was disturbed in young leaves in favor of repressors. The balance was restored in later development of leaves, when the expression of more activators was observed.

When individual genes were assessed, it was observed that *HvARF4b*, *HvARF4c* and *HvARF15* showed relatively high level of expression among different samples. Very stable expression in all samples was observed for *HvARF4a* or *HvARF21*. On the contrary, transcripts of *HvARF11*, *HvARF13* and *HvARF14* were the least abundant in the tested samples. In the case of *HvARF13*, the highest expression was observed in later stages of inflorescence development.

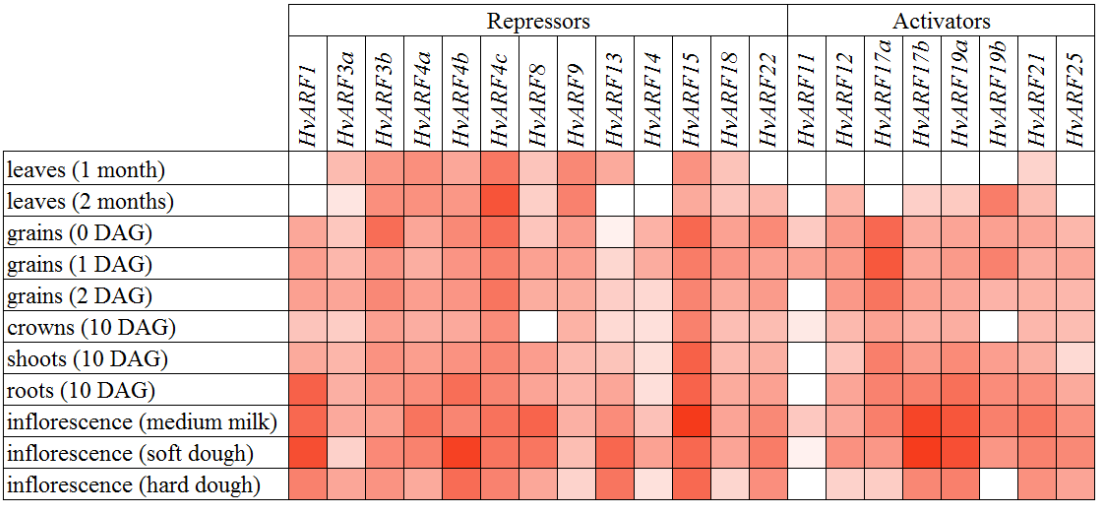

Figure 17 Heat-map analysis of barley *ARF* genes expression (semi-quantitative PCR) in different tissues and stages of development. Each box represents a mean value of three biological replicates. The mean values were normalized to four reference genes: *EF2*, *Malate dehydrogenase*, *E2*, *EF1α*. Expression in different samples is shown as a colored scale with white color representing no gene expression and red color the highest expression score in a specific tissue.

4.2.2 Analysis of repressor *ARF* gene expression

To analyse the expression profile of repressor *ARF* genes in early development of crown-root, qPCR experiment was performed with barley crown samples collected from first to fourth day after germination (1 DAG to 4 DAG). Based on the expression profile, the analysed genes were separated into four groups. *ARF* genes in the first group showed upregulation of gene expression (Fig. 18A) during the analysed period. The upregulation of gene expression was observed for repressor genes *HvARF3a*, *HvARF3b*, *HvARF4a*, *HvARF4c* and *HvARF9*. *HvARF3b* showed to be the most stably upregulated during first four days after germination compared to other genes in this group.

Genes in the second group showed rather downregulation of gene expression from 1 DAG to 4 DAG (Fig. 18B). Downregulation of gene expression was observed for *HvARF1* and *HvARF4b*. Apart from these two groups, *HvARF15* gene did not show any specific pattern on gene expression (Fig. 18C). Expression of *HvARF15* was quite stable from 1 DAG to 4 DAG. This result was in agreement with the heap-map of *ARF* gene expression (Fig. 17), where *HvARF15* also exhibited a relatively stable expression between different tissues or developmental stages. In the case of *HvARF22* the expression was unstable during the analysed period (Fig. 18D), and there was a large variability in *HvARF22* expression between biological replicates. For these reasons, *HvARF22* was not classified into any of the previous groups. The rest of repressor *ARF* genes, including *HvARF8*, *HvARF13*, *HvARF14* and *HvARF18*, were not detected in the conditions of this experiment.

A) Upregulation of gene expression

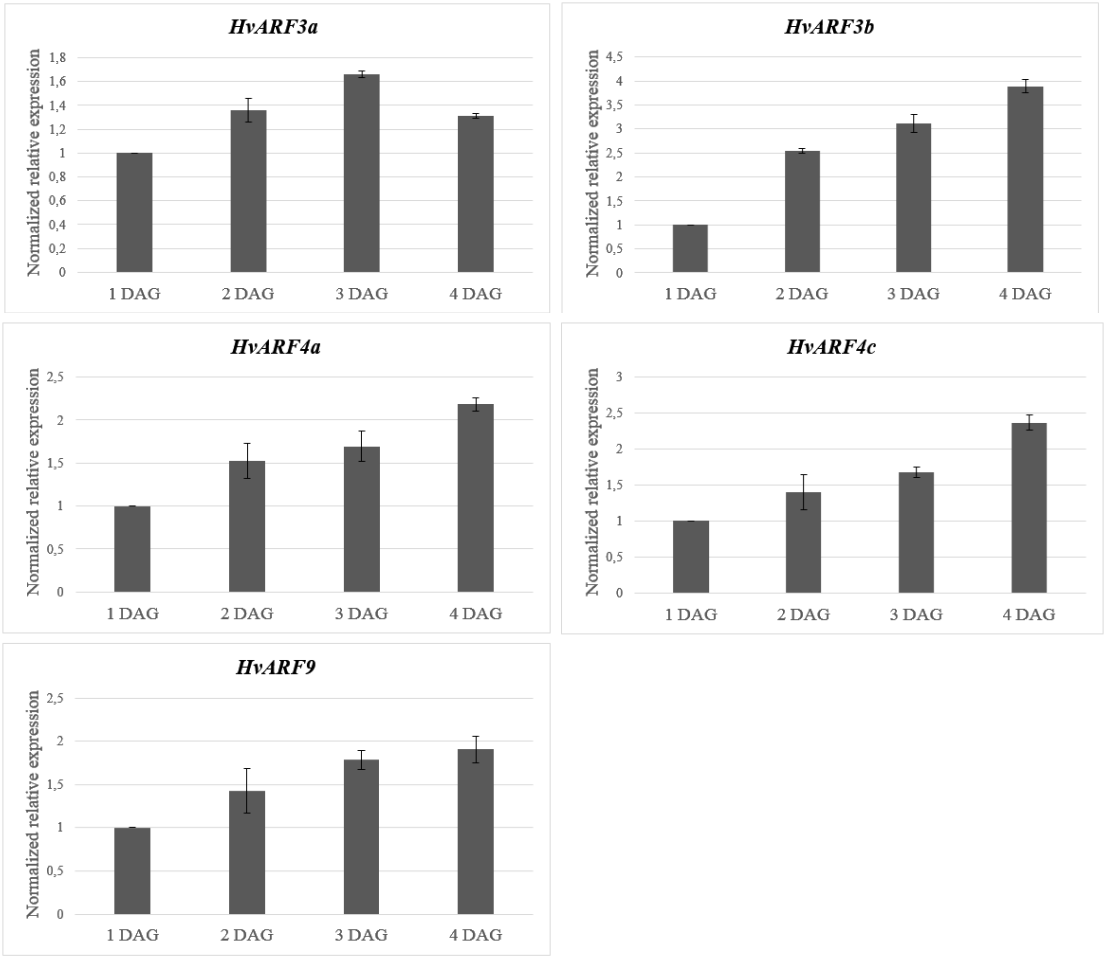

B) Downregulation of gene expression

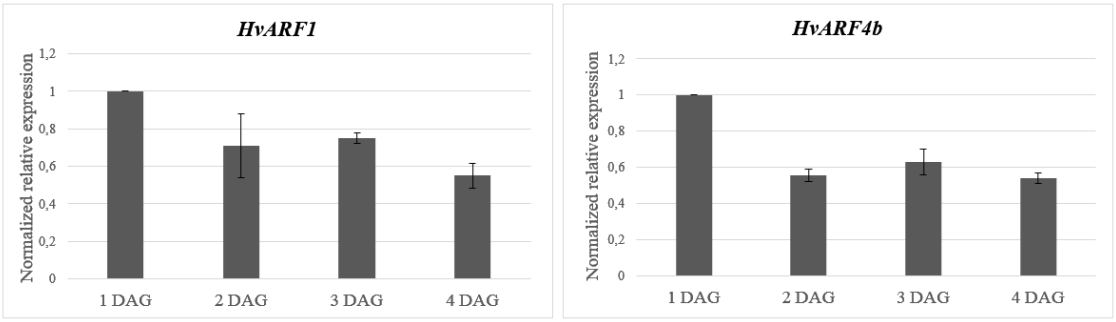

Figure 18 Expression profile of barley repressor *ARF* genes in the crown of barley seedlings from 1 DAG to 4 DAG. The graph represents the mean of three independent biological replicates, with bars showing the standard errors of the means. Normalization was done in relation to three reference genes: *Actin*, *EF2* and *Hv5439*. Results were expressed as fold change relative to the expression in 1 DAG crown samples.

C) No effect **D) No classification**

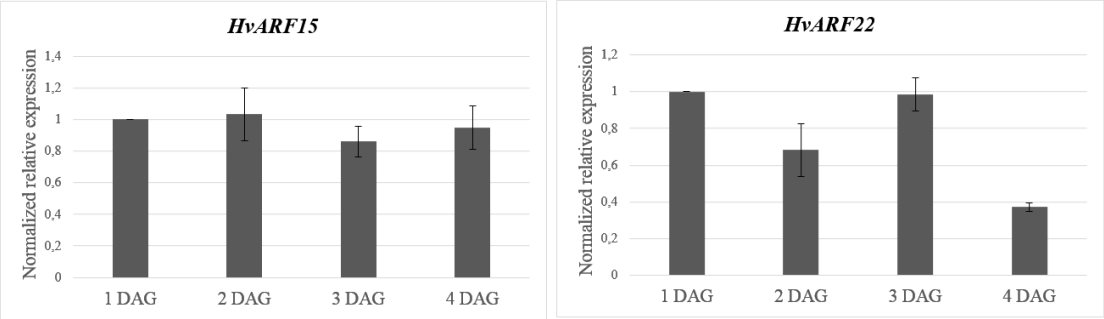

Figure 18 Expression profile of barley repressor *ARF* genes from 1 DAG to 4 DAG in crown. The graph represents the mean of three independent biological replicates, with bars showing the standard errors of the means. Normalization was done in relation to three reference genes: *Actin*, *EF2* and *Hv5439*. Results were expressed as fold change relative to the expression in 1 DAG crown samples (*continuation*).

4.2.3 Gene expression analysis of selected activator *ARF* genes

In Arabidopsis, AtARF6 and AtARF8 are the main activator ARF proteins controlling adventitious rooting (Sorin *et al*., 2005; Gutierrez *et al*., 2009). Closest orthologs of AtARF6 and AtARF8 were searched in barley. Based on BLAST search results and the cladogram in Fig. 24, barley HvARF17a (HORVU6Hr1G026730.8) and HvARF17b (HORVU7Hr1G106280.1) were identified as the closest orthologs of Arabidopsis AtARF8. According to the phylogenetic tree (Fig. 16), HvARF17a and HvARF17b are very closely related. HvARF25 (HORVU5Hr1G009650.17) was identified as the closest ortholog of Arabidopsis AtARF6.

The expression profile of the three selected activator *ARF* genes (*HvARF17a*, *HvARF17b* and *HvARF25*) was analysed from 1 DAG to 4 DAG by qPCR. All three genes exhibit an apparent downregulation of gene expression (Fig. 19). The decrease of gene expression was observed the second day after germination.

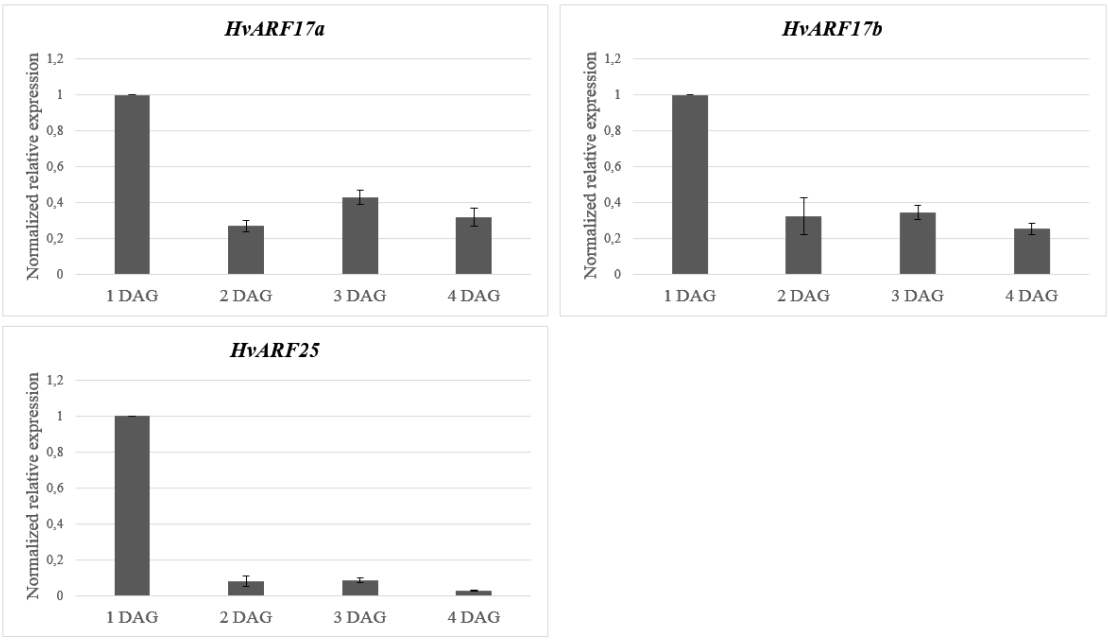

Figure 19 Expression profile of three selected activator *ARF* genes in the crown of barley seedling from 1 DAG to 4 DAG. The graph represents the mean of three independent biological replicates, with bars showing the standard errors of the means. Normalization was done in relation to three reference genes: *Actin*, *EF2* and *Hv5439*. Results were expressed as fold change relative to the expression in 1 DAG crown samples.

4.2.4 Absolute quantification of *HvARF13* in early development

HvARF13 was determined as the candidate gene for CRISPR-Cas9 mediated knock-out in barley (Chapter 4.3.1). To further characterize *HvARF13*, it was desirable to obtain the expression profile of *HvARF13*. As the expression of *HvARF13* could not be analysed in conditions of the relative quantification experiment (Chapter 4.2.2), absolute quantification experiment was performed to assess the number of *HvARF13* copies per µl of sample. The number of copies of *HvARF13* was analysed in 1 DAG to 4 DAG crown samples.

First, a standard sample was prepared by cloning a *HvARF13* fragment into *pDRIVE* vector. Using the formula in Chapter 3.2.4.3, the number of *pDRIVE::HvARF13* copies per 1 µl was determined. qPCR was performed with tenfold serial dilution of a standard sample to obtain the standard curve (Fig. 20). The standard curve was used for determination of the number of *HvARF13* copies per 1 µl in 1 DAG, 2 DAG, 3 DAG and 4 DAG crown samples.

Unfortunately, there were very big differences in the number of copies of *HvARF13* between individual biological replicates of 1 DAG, 2 DAG and 3 DAG crowns (Fig. 21).

Therefore, the overall expression profile of *HvARF13* in the analysed period could not be assessed. However, in 4 DAG crowns the number of *HvARF13* copies was decreased, with the mean value of 87 copies·µl^{-1}.

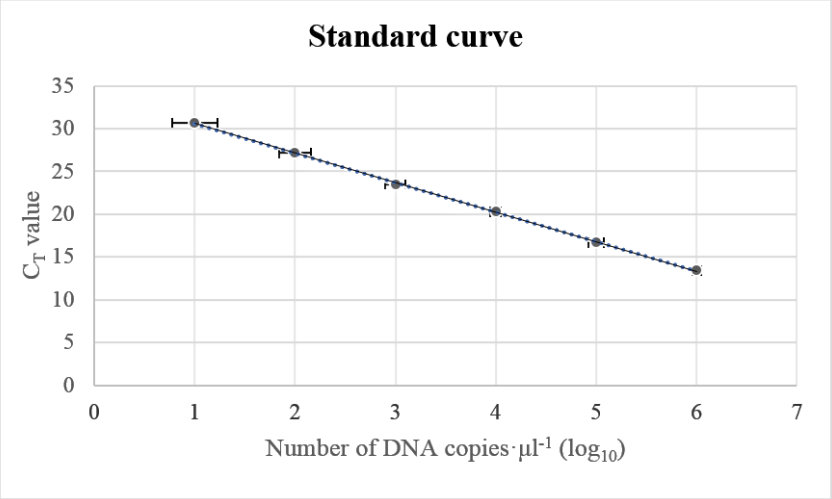

Figure 20 Standard curve for absolute quantification of *HvARF13*. Tenfold serial dilution of the *HvARF13* standard was subjected to qPCR. The C_T values were plotted against log number of DNA copies·µl^{-1}. Data points are means of three replicates, with bars showing the standard errors of the means.

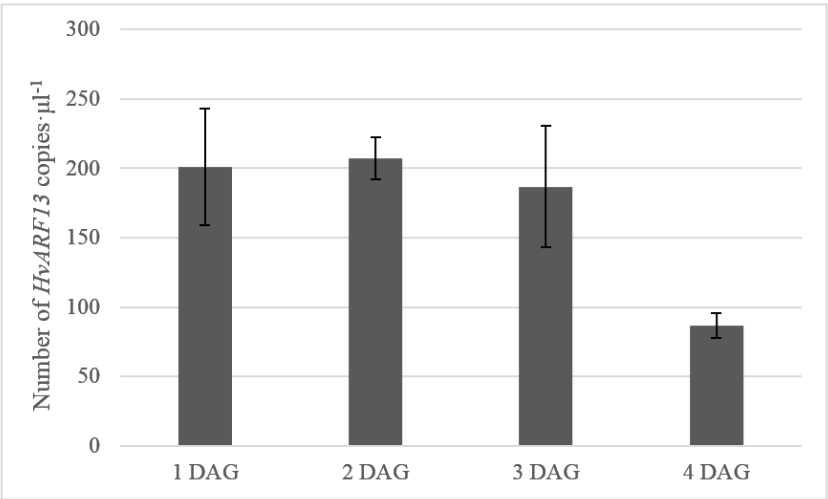

Figure 21 Absolute quantification of *HvARF13* in 1 DAG to 4 DAG barley crowns. The individual samples were subjected to qPCR and C_T values were obtained. The number of transcript copies·µl^{-1} was calculated using the standard curve in Fig. 20. The graph represents the mean of three independent biological replicates, with bars showing the standard errors of the means.

4.2.5 Optimization of *in situ* PCR for barley crown

In situ PCR is a molecular biology technique that allows to detect expression pattern in a target tissue. Athman *et al*. (2014) introduced a simple "in-tube" protocol for *in situ* PCR in plant tissues. The authors stated that the protocol can be adapted to various tissue types. The authors successfully tested the protocol on leaves, roots, flowers or epidermal peel of Arabidopsis, rice, maize or even barley. When this protocol was applied on barley crown samples, several problems were identified. There was a significant amount of positive signal detected in negative controls. Also, using a housekeeping gene *Actin* as a positive control, homogeneous expression in crown samples was expected. But, the positive signal from *Actin* transcripts was missing in cortex cells (Fig. 22A). The same distribution of signal was observed also for samples where oligo dT primers were used in reverse transcription (RT) reaction (Fig. 22B).

Firstly, the suggestions for optimization of the protocol provided by Athman *et al*. (2014) were considered. The overall fixation time was reduced to 4 hours to avoid inconsistent staining due to over-fixation. Secondly, number of sections in the tube was reduced to allow the reagents to reach all the sections in the tube. Additional treatment with 5 $mmol \cdot l^{-1}$ levamisole was performed before incubation with the substrate for alkaline phosphatase to inhibit endogenous alkaline phosphatases. These minor changes in the protocol did not result in any improvement in the detection.

To identify the source of the false positive signal, several negative control samples were included in the experiment. For two types of negative controls, reverse transcription was performed without primers or without reverse transcriptase enzyme. In both, light blue signal with the same distribution as in a positive control was observed (Fig. 22C, 22D). The signal was also missing from cortex cells and CRP. Another negative control was completely excluded from reverse transcription, resulting in slightly reduced light blue signal (Fig. 22E). The last negative control was excluded from both reverse transcription and PCR reaction. It was incubated with the anti-digoxigenin antibody and the endogenous alkaline phosphatases were inhibited by levamisole. In this type of a negative control, no positive signal was observed (Fig. 22F). These results suggest that the positive signal did not come from binding of the antibody to any unspecific epitops or from reaction of the BM substrate with endogenous alkaline phosphatases. Instead, the most probable source of the false positive signal was the amplification of residual genomic DNA in the PCR reaction.

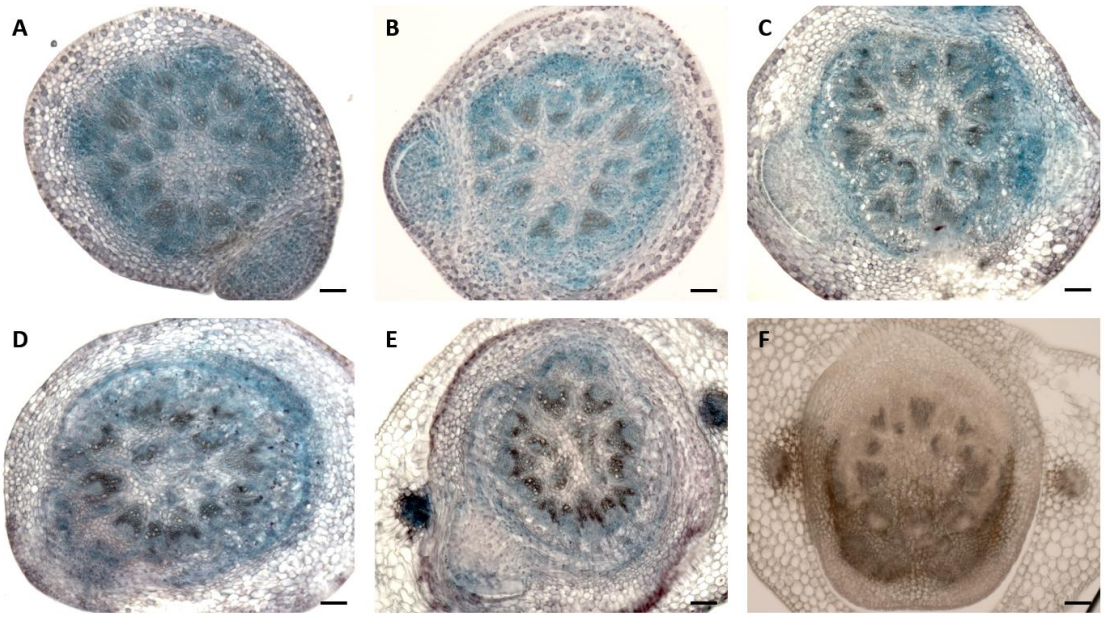

Figure 22 *In situ* PCR results before optimization of the protocol. A, *Actin* positive control, positive signal was detected in ground tissue around vascular bundles, the signal is nonhomogeneous in cortex. B, *Actin* positive control (oligo dT primers were used in RT), the same distribution of signal as in A was observed. C, D, negative controls (without primers in RT, without reverse transcriptase in RT, respectively), distribution of signal is comparable to positive control. E, negative control (without RT), signal is weaker than in C or D. F, negative control (without RT and PCR), no positive signal was detected. Objective: 5x. Scale bar: 100 μm.

According to Przybecki *et al*. (2006) and Urbańczyk-Wochniak *et al*. (2002) an additional step can be included after tissue sectioning, in which cells are permeabilized by proteinase K treatment. Permeabilization of cells then improves penetration of the different reagents. Comparing different protocols for *in situ* PCR in plant sections, it was found that at least 8 units of DNase should be used for overnight treatment to remove all genomic DNA (Urbańczyk-Wochniak *et al*., 2002; Przybecki *et al*., 2006; Wieczorek, 2015). Based on these suggestions, the final protocol included proteinase K treatment, overnight DNase treatment (10 units of DNase I) and overnight incubation with antibody to increase the specificity of detection. Unfortunately, the problem of nonhomogeneous distribution of signal in *Actin* positive control was not solved (Fig. 23A, 23D). Lack of the signal in cortex cells could result from RNA degradation or insufficient fixation. The fixation procedure could be further optimized by adjusting time of fixative infiltration and time for overall fixation. Applying the optimized protocol to negative control samples (a sample without reverse transcriptase enzyme in RT reaction mixture and a sample excluded from reverse transcription reaction) resulted in improved

detection. In both negative controls, only background dark blue signal was detected (Fig. 23B, 23C, 23E, 23F). The background signal is clearly distinguishable from positive light blue signal. Further optimization of the *in situ* PCR protocol will be necessary to reduce the background signal. The unspecific signal from cell walls could be caused by high content of pectins. This type of unspecific signal can be eliminated by pectinase treatment after sample sectioning (Przybecki *et al*., 2006). Considering the unspecific signal from nuclei, a restriction endonuclease could be used instead of DNase I to digest genomic DNA. Choice of the restriction endonuclease depends on the gene amplified during PCR reaction. Such restriction endonuclease should recognize a restriction site in the amplified region of the gene (Pesquet *et al*., 2004).

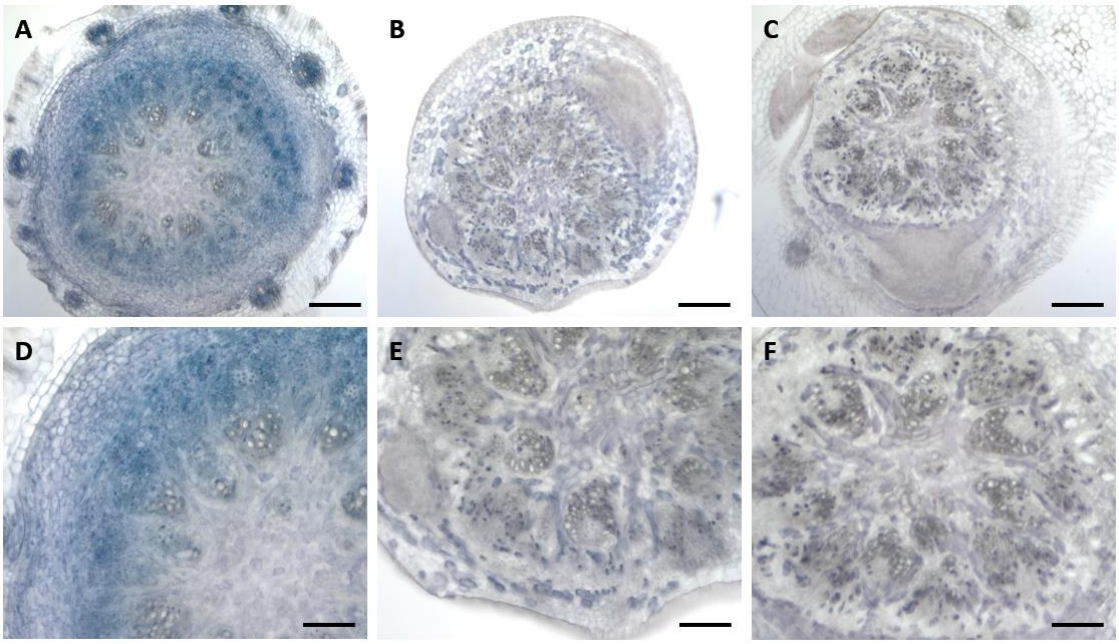

Figure 23 *In situ* PCR results after optimization of the protocol. A, *Actin* positive control, positive signal was detected in ground tissue around vascular bundles, the signal is nonhomogeneous in cortex. B, negative control (without reverse transcriptase in RT), only background dark blue signal was detected. C, negative control (without RT), only background dark blue signal was detected. D, E, F, details of A, B, C, respectively. Objective: 5x (A, B, C), 10x (D, E, F). Scale bar: 200 μm (A, B, C), 100 μm (D, E, F).

4.3 CRISPR-Cas9 mediated gene knock-out in barley

4.3.1 Selection of a candidate for CRISPR-Cas9 mediated knock-out

One of the main aims of this thesis was to design an experiment to study CR initiation in barley. As there is lack of knowledge about the molecular principle of CR initiation in barley, the process of adventitious rooting in Arabidopsis served as a model. The choice of adventitious rooting as a model system was based on the common features of adventitious roots in Arabidopsis and CRs in barley. Both root types are established post-embryonically and they can originate from aerial parts of a plant. During adventitious rooting in Arabidopsis, AtARF17 acts as a negative regulator (Sorin *et al*., 2005; Gutierrez *et al*., 2009).

The closest ortholog of AtARF17 was searched among the members of ARF family in barley. The ortholog of AtARF17 could potentially act as a negative regulator of CR initiation in barley. The main parameter for the choice of a candidate gene was the homology of protein sequences. Protein sequences of Arabidopsis, rice and barley were analysed by Phylogeny.fr and a cladogram was obtained. In the cladogram, there is a group of proteins comprising AtARF17 from Arabidopsis, HvARF13 (HORVU2Hr1G125740) from barley and OsARF13 and OsARF20 from rice (Fig. 24). All of these proteins are truncated, missing the C-terminal PB1 dimerization domain (Guilfoyle and Hagen, 2001; Wang *et al*., 2007). Also, HvARF13 was already predicted to be a repressor in the previous analysis (Table 29). Therefore, HvARF13 was chosen as a candidate for CRISPR-Cas9 mediated knock-out in barley.

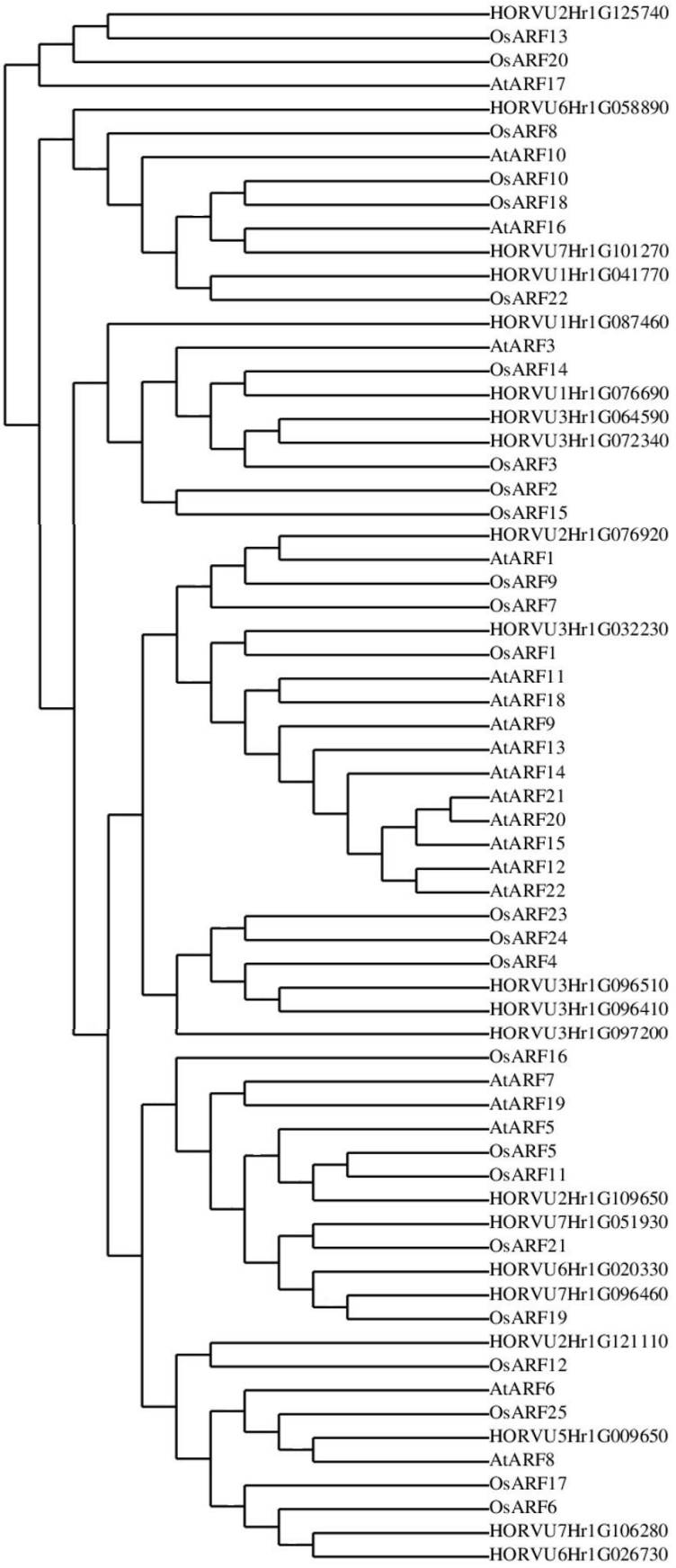

Figure 24 Cladogram of barley, Arabidopsis and rice ARF proteins, generated by Phylogeny.fr online tool.

4.3.2 Test of Cas9 endonuclease activity

A test of endonuclease activity aims to confirm functionality of a prepared construct in a transient expression assay. An assay designed by Budhagatapalli *et al*. (2016) was performed to test the constructs for CRISPR-Cas9 mediated knock-out of *HvARF13* in barley. First, two different *HvARF13*-specific gRNA sequences were designed. gRNA was successfully cloned into *pSH91* vector. In the assay, *pSH91::gRNA-HvARF13* vector was coding for Cas9 endonuclease, specifically targeting *HvARF13* sequence. Also, gRNA together with PAM sequence were successfully cloned into *pNB1* vector, the gRNA was cloned upstream of frameshift *YFP*. Verification of both *pSH91::gRNA-HvARF13* and *pNB1::gRNA-HvARF13* was done by PCR (Fig. 25) and sequencing. Finally, *pSH91::gRNA-HvARF13*, *pNB1::gRNA-HvARF13* and *pNB2* (constitutive expression of mCherry) were co-transformed into barley leaves by bombardment. In theory, mutations caused by DNA-repair mechanisms should result in restoration of YFP reading frame. The ratio of mCherry and YFP-positive cells provides information about the activity of designed Cas9 endonuclease system.

In the final step of this assay, fluorescent signal from mCherry and YFP was analysed in transformed leaves. Weak fluorescent signal from mCherry was observed already one day after transformation. The signal from mCherry was improved by the second and third day after transformation. The mCherry signal served as a control of successful transformation of barley leaves. Unfortunately, the YFP signal was not observed in transformed cells. Therefore, the activity of Cas9 endonuclease could not be analysed.

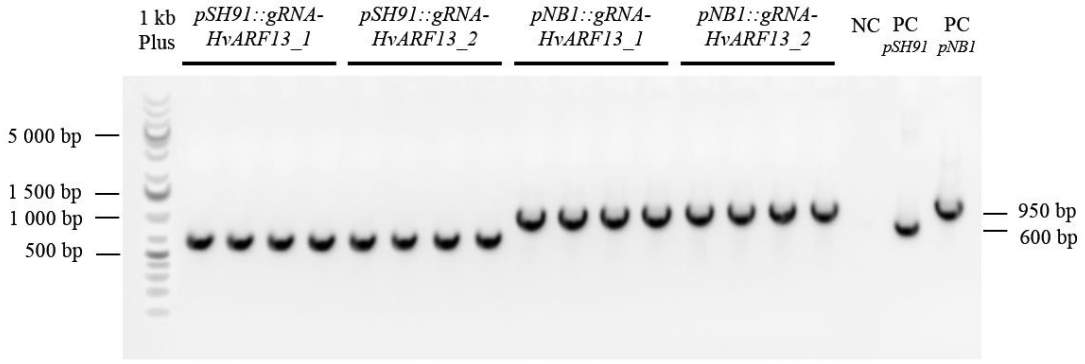

Figure 25 Colony PCR for *pSH91::gRNA-HvARF13* and *pNB1::gRNA-HvARF13* control. For control of each construct, four colonies were subjected to colony PCR. The PCR products were analysed by electrophoresis in 1% agarose gel stained by ethidium bromide. *pSH91::gRNA-HvARF13*-positive colonies provide a DNA band of 600 bp. *pNB1::gRNA-HvARF13*-positive colonies provide a DNA band of 950 bp. NC, negative control; PC, positive control; 1 kb Plus, molecular standard.

4.3.3 Stable transformation and screening of transgenic plants

Based on the prediction described in Chapter 4.3.1, *HvARF13* is a repressor of CR initiation in barley. To test this hypothesis, the CRISPR-Cas9 mediated knock-out of *HvARF13* was designed. The CRISPR-Cas9 cassette was transformed into barley cultivar Golden Promise. To obtain stably transformed barley plants, the protocol for *A. tumefaciens*-mediated transformation of immature barley embryos was followed (Marthe *et al*., 2015).

The CRISPR-Cas9 cassette was successfully cloned into *p6i-d35S-TE9* binary vector. The insert was verified by control restriction with *BsiW*I restriction endonuclease (Fig. 26) and Sanger sequencing. *A. tumefaciens* was transformed with *p6i-d35S-TE9::gRNA-HvARF13* by electroporation.

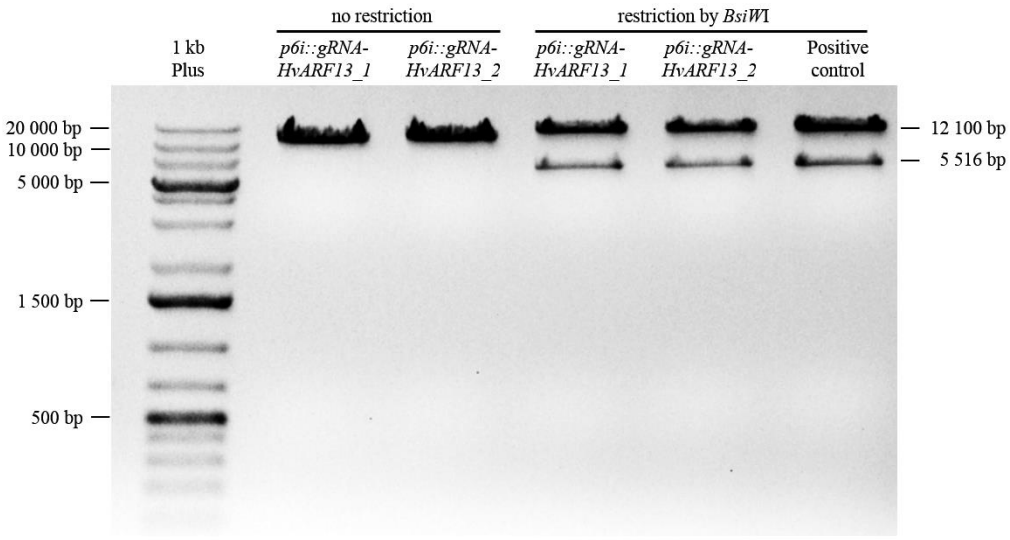

Figure 26 Control restriction of *p6i-d35S-TE9::gRNA-HvARF13* by *BsiW*I enzyme. The restriction fragments were analysed by electrophoresis in 1% agarose gel stained by ethidium bromide. Intact *p6i-d35S-TE9::gRNA-HvARF13* plasmids without restriction were analysed. After restriction, *p6i-d35S-TE9::gRNA-HvARF13* provide two DNA bands of 12 100 bp and 5 516 bp. PC, positive control; 1 kb Plus, molecular standard.

The transformation of barley immature embryos was repeated twice with construct *p6i-d35S-TE9::gRNA-HvARF13_1*. Each time, approximately 250 immature embryos were transformed. Seventeen transgenic plants were obtained at the end of the regeneration procedure. From these, only 13 plants survived the transfer into phytotron conditions.

Presence of the T-DNA insertion was analysed in T_0 barley plants. T_0 plants were analysed for the presence of the *Cas9*, *Hpt* and gRNA scaffold genes. From these, 7 plants were positive for *Cas9* gene (Fig. 27), 6 were positive for *Hpt* (Fig. 28) and gRNA scaffold (Fig. 29) genes. In total, 6 T_0 plants were positive for all *Cas9*, *Hpt* and gRNA scaffold genes. In all transgenic plants, the region surrounding protospacer sequence was amplified by PCR and sequenced by Sanger sequencing. In one of the transgenic plants (plant number 2-1), 1 nucleotide insertion mutation in the protospacer sequence was discovered (Fig. 30). The insertion mutation occurs at position -3 from PAM sequence. The insertion mutation results in reading frame shift.

Transgenic plants with mutation in *HvARF13* sequence will be further analysed after the duration of this master thesis. Also, transformation of barley immature embryos will be performed with the second construct *p6i-d35S-TE9::gRNA-HvARF13_2*.

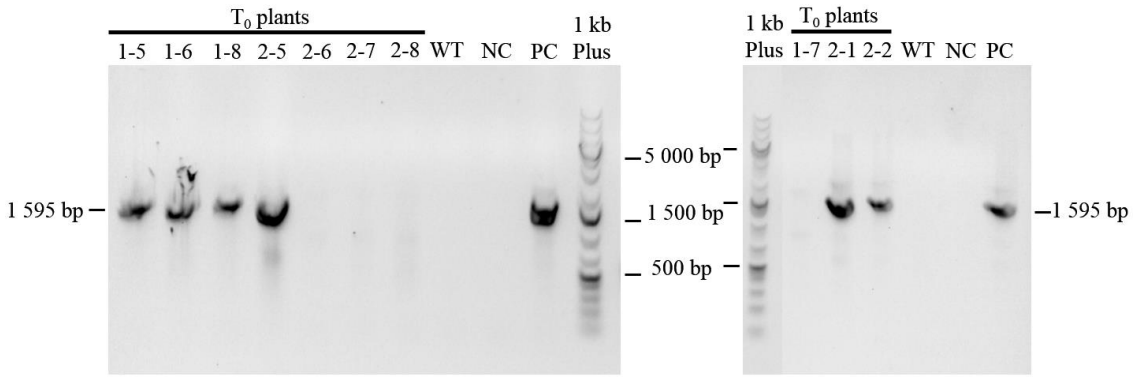

Figure 27 Screening by PCR of different independent barley T_0 lines for the presence of the *Cas9* gene. gDNA of T_0 transgenic plants was used as template in PCR reaction using *Cas9*-specific primers. T_0 plants 1-5, 1-6, 1-7, 1-8 were generated in first set of barley transformation. T_0 plants 2-1, 2-2, 2-5, 2-6, 2-7 and 2-8 were generated in second set of barley transformation. Plants 1-5, 1-6, 1-8, 2-1, 2-2, 2-5 were positive for *Cas9* gene. WT, gDNA of wild type plant was used as template in PCR reaction; NC, gDNA of non-transgenic plant was used as template in PCR reaction in negative control; PC, gDNA of transgenic plant positive for *Cas9* was used as template in PCR reaction in positive control; 1 kb Plus, molecular standard.

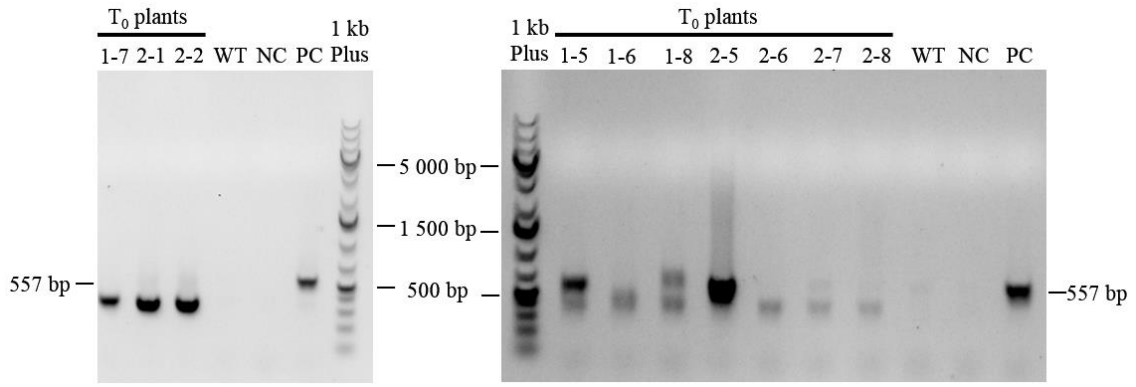

Figure 28 Screening by PCR of different independent barley T_0 lines for the presence of *Hpt* gene. gDNA of T_0 transgenic plants was used as template in PCR reaction using *Hpt*-specific primers. Plants 1-5, 1-8, 2-1, 2-2, 2-5 were positive for *Hpt* gene. Abbreviations were explained in Fig. 27.

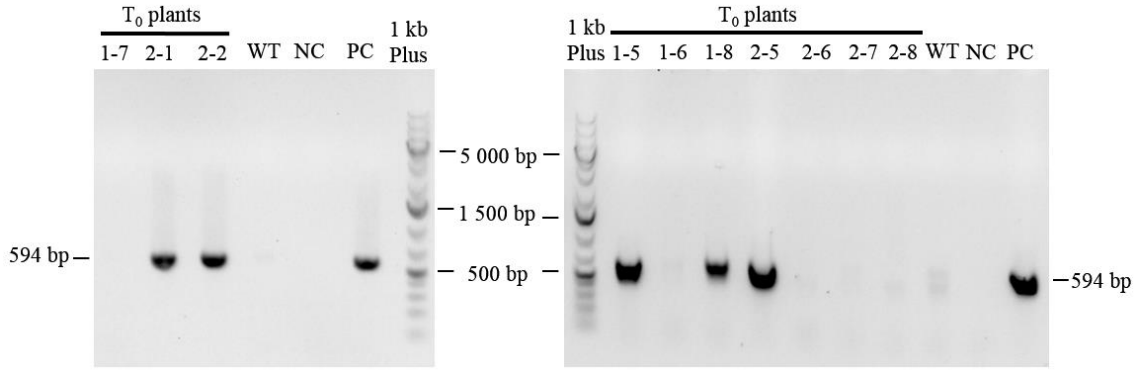

Figure 29 Screening by PCR of different independent barley T_0 lines for the presence of gRNA scaffold gene. gDNA of T_0 transgenic plants was used as template in PCR reaction using gRNA scaffold-specific primers. Plants 1-5, 1-8, 2-1, 2-2, 2-5 were positive for gRNA scaffold gene. Abbreviations were explained in Fig. 27.

```
                                                        *
wild type HvARF13   AATCTACCTG CCTGCAGATA AACTGGGCTG AATCTGTG~G CAGGGTCACT AAACAGGTAT GTCAACGCTT
2-1 plant           AATCTACCTG CCTGCAGATA AACTGGGCTG AATCTGTGAG CAGGGYCACT AAACAGGWAT GTCAACGCTT
protospacer + PAM   ---------- ---------- -ACTGGGCTG AATCTGTG~G CAggg..... .......... ..........
```

Figure 30 Analysis of mutation in *HvARF13* sequence in a transgenic plant. Region of *HvARF13* gene surrounding protospacer sequence was amplified by PCR. PCR product was sequenced by Sanger sequencing. *HvARF13* sequences of wild type (Golden Promise) and transgenic plants were aligned in Bioedit. In transgenic plant (number 2-1) a 1 nucleotide insertion mutation was discovered in position -3 from PAM sequence (asterisk).

5 DISCUSSION

Auxin-dependent processes occur throughout the whole plant life, from very early stages of embryogenesis to plant senescence. Among many different roles in root development, auxin controls crown-root (CR) initiation and formation in monocot plants (Inukai *et al*., 2005). In rice, auxin-dependent root developmental processes are initially regulated by the polar auxin transport, facilitated by auxin transporters. Signal from auxin is then transduced to a complex network of factors, including downstream Aux/IAA inhibitors, ARF transcription factors and finally to auxin-responsive genes (Meng *et al*., 2019). Both Aux/IAA and ARF protein families are represented by high number of members in higher plants. In all studied monocot plants, there were more than 20 members of ARF family, with 25 *ARF* genes in *O. sativa* and 36 *ARF* genes in *Z. mays* (Wang *et al*., 2007; Wang *et al*., 2012). Similar number of *ARF* genes was expected also for barley. Based on the sequence homology with Arabidopsis and rice, 21 *ARF* genes were identified in barley.

A typical full-length ARF protein comprises DNA-binding domain, middle region (MR) and PB1 dimerization domain (Guilfoyle and Hagen, 2001). Analysis of the amino acid composition of the MR can serve as a prediction of ARF regulatory function, where the MR of a transcription activator is rich in glutamine (Tiwari *et al*., 2003). According to these predictions, 8 barley ARFs would act as activators and 13 as repressors of transcription. Further analysis of domain composition revealed that 8 barley repressor ARFs lack PB1 dimerization domain. In comparison, the ratio between activators and repressors is comparable in rice, with 9 activators, 10 full-length repressors and 6 truncated repressors (Shen *et al*., 2010). As in Arabidopsis and rice, the phylogenetic analysis revealed three separate classes of barley ARF proteins. In the phylogenetic tree, activators and repressors form separate classes. However, additional experimental evidence is necessary to confirm predicted functions as activators or repressors.

Genome-wide ARF identification studies very often include gene expression analysis to get first insight into the distribution of gene expression and to predict potential gene function. Expression patterns of *ARF* genes usually overlap among different tissues or developmental stages, suggesting a high level of redundancy between different *ARF* genes (Shen *et al*., 2015; Zhang *et al*., 2017). Similar trend of *ARF* expression was observed also for barley. Abundance of *ARF* transcripts was analysed by semi-quantitative PCR in cDNA samples of different barley tissues. Heat-map of *ARF* expression showed ubiquitous expression in all tissues with low level of tissue-specificity

for individual *ARF* genes. Expression level of most *ARF* genes differed among different barley tissues and changed during tissue development. On the contrary, *HvARF4a* and *HvARF21* showed the most stable expression level among different tissues, while, *HvARF11*, *HvARF13* and *HvARF14* showed the lowest level of expression. Rademacher *et al*. (2011) and Vernoux *et al*. (2011) propose a strictly controlled *ARF* expression pattern resulting in distinct sets of ARF transcription factors in a specific time and place. These specific sets of ARF transcription factors control transcription of target genes and may also affect general sensitivity to auxin. Rademacher *et al*. (2011) also proposed a balance between repressors and activators in Arabidopsis. In barley, this balance was observed for most tissue types with only one exception in 1-month old leaves, however the balance was restored in later development.

In rice, a monocot model plant, OsARF1 is the only ARF isoform which function is described in the process of CR initiation (Inukai *et al*., 2005). To better understand a contribution of individual barley ARFs in crown-rooting, expression profiles of repressor *ARF* genes were analysed by qPCR. Time-course expression profiles of *ARF* repressors were obtained for crowns from 1 DAG to 4 DAG, as CRs initiate soon after germination (data not shown). For *HvARF3a*, *HvARF3b*, *HvARF4a*, *HvARF4c* and *HvARF9* a gradual upregulation of their expression was observed in crowns from 1 DAG to 4 DAG. Opposite effect was observed for *HvARF1* and *HvARF4b*. These genes could potentially have important functions in crown-rooting. While *HvARF8*, *HvARF13*, *HvARF14* and *HvARF18* are either not expressed in crowns during chosen period, or their expression is significantly suppressed. These genes are possibly released from such strict control in later development, as low expression of *HvARF13*, *HvARF14* and *HvARF18* was detected in 10 DAG crowns by semi-quantitative PCR. However, analyzing the *ARF* expression in more biological repliates would be necessary to increase the statistical credibility of the results.

Based on the qPCR data, candidates for further analysis of gene expression by *in situ* PCR could be chosen. After optimization of the protocol for crown tissue, *in situ* PCR could allow detecting even low-abundant transcripts, providing valuable information about the spatial distribution of specific transcripts directly in crown tissue. The detection results could be improved by testing different fixation conditions, performing pectinase treatment after sectioning or improved handling with the sample in strictly RNase-free conditions (Przybecki *et al*., 2006; Athman *et al*., 2014). Also, background signal could

be further eliminated by using a restriction enzyme for genomic DNA digestion instead of DNase I (Pesquet *et al*., 2004).

Due to high number of ARF isoforms in plants, specific functions were described for only few ARFs. For Arabidopsis AtARF17 protein, a specific function was discovered in two distinct processes, pollen development and adventitious rooting (Sorin *et al*., 2005; Yang *et al*., 2013). In Arabidopsis, AtARF17 is a truncated repressor that acts as a negative regulator of adventitious root initiation (Sorin *et al*., 2005). Gutierrez *et al*. (2009) proposed that AtARF17 competes with positive regulators of adventitious rooting, AtARF6 and AtARF8, to regulate auxin-responsive genes. Furthermore, a complex transcriptional and post-transcriptional regulation of *AtARF17* is ensured by miR160, AtARF6 and AtARF8. As both adventitious roots and CRs develop post-embryonically from aerial part of a plant, similar aspects of regulation are expected. Barley HvARF13 was determined as the closest ortholog of Arabidopsis AtARF17, based on phylogenetic analysis and sequence homology. Very low level of *HvARF13* expression was detected in 10 DAG crowns compared to other tissue types. But the time-course *HvARF13* expression profile could not be analysed by relative quantification method. When number of *HvARF13* copies was analysed in cDNA samples of crowns, very big differences were observed for individual biological replicates of 1 DAG to 3 DAG crowns. However, an apparent decrease in *HvARF13* copy number was detected in 4 DAG crowns. These results suggest a strict suppression of *HvARF13* expression in early development of crowns. Similarly, a putative negative regulator of adventitious rooting in *M. truncatula* is suppressed during adventitious rooting (Zhang *et al*., 2017). Next, orthologs of AtARF6 and AtARF8 were searched in barley. Even though HvARF17a, HvARF17b and HvARF25 are predicted activators, expression profile of corresponding genes showed great down-regulation during early development of crowns. Therefore, it is possible that these barley ARF proteins have distinct functions, different from their Arabidopsis orthologs.

If HvARF13 was a negative regulator of CR initiation in barley, a distinct CR phenotype would be expected in *HvARF13*-knock-out barley lines. To examine the role of HvARF13 in the process of crown-rooting in barley, a CRISPR-Cas9 mediated knock-out of *HvARF13* was designed. First, a test of Cas9 endonuclease activity specific for *HvARF13* sequence was performed. In the principal of the test, if Cas9 efficiently recognizes and cuts a target sequence, DNA-repair mechanisms of the cell introduce

mutations to the target sequence, leading to restoration of a reading frame of YFP. However, only mutations of 1 nucleotide deletion or 2 nucleotides insertion in a target sequence can restore the functional reading frame of YFP. Unfortunately, the test of *HvARF13*-specific Cas9 activity was not successful. The most probable reason for non-functionality of the test was an occurrence of a 1 nucleotide insertion mutation, which is more frequent in barley but does not lead to restoration of *YFP* gene reading frame (Budhagatapalli *et al*., 2016).

Despite negative results of Cas9 activity test, stable transformation with construct for CRISPR/Cas9 mediated *HvARF13* knock-out was performed. A method of *A. tumefaciens*-mediated transformation of barley immature embryos was carried out to deliver the construct to barley cells. The overall barley regeneration and transformation efficiency was very low, with only 6 transgenic plants positive for *Cas9*, *Hpt* and gRNA scaffold genes. In comparison, the expected efficiency of the transformation protocol was 25 transgenic plants per 100 cultured immature embryos (Marthe *et al*., 2015). Finally, 1 nucleotide insertion mutation in *HvARF13* sequence was confirmed for 1 T_0 transgenic plant. Whether the mutation leads to *HvARF13* knock-out and potentially affects CR phenotype will be examined after the duration of the thesis.

Together, these results represent first insight into the role of ARF proteins in barley CR development. Results demonstrated in this thesis may be used as a basis for future identification of the most important ARF isoforms in CR initiation. Such knowledge would be useful in molecular breeding aiming for improvement of barley root system.

6 CONCLUSION

In the theoretical part, current knowledge about CR initiation and development of monocot plants was summarized. In the introductory part, root system of monocot plants was characterized, with emphasis on the function and development of CRs. Next, specific roles of individual components of auxin signaling were described in the process of CR development in rice, lateral and adventitious roots in Arabidopsis. Finally, the main focus was on detailed characterization of ARF proteins, the essential regulators of auxin-dependent response in plants.

In the practical part, the research aimed to identify ARF protein family members in barley and to make first step toward understanding ARF function in the process of CR initiation and development in barley. A list of 21 ARF isoforms in barley was obtained, together with general characterization of ARF domain composition, regulatory function and affiliation to a phylogenetic class. For corresponding *ARF* genes, a map of expression among different barley tissues was created, indicating a ubiquitous distribution of ARFs among different barley tissues and changes in *ARF* expression during development. Expression profiles of repressor *ARF* genes and selected activator genes were obtained, in which most *ARF* genes showed either up-regulation, down-regulation or suppression of gene expression during early development of crown, suggesting an important role of these ARFs in crown-rooting.

Further, HvARF13 was determined as a candidate for the main repressor of CR initiation in barley. The choice of this candidate was supported by the fact that *HvARF13* expression was strongly suppressed during early development of crown. Therefore, it would be interesting to assess the level of *HvARF13* expression during longer period and to obtain information concerning the spatial distribution of *HvARF13* transcripts in crown. Repeating the stable transformation of barley with two different constructs will potentially provide independent transgenic lines with different mutations in the *HvARF13* sequence. Transgenic lines with confirmed knock-out of *HvARF13* will be analysed for changes in CR phenotype.

Results of this thesis could contribute to identification of ARF proteins with important function in CR initiation and development. In the future, these findings could be applied in breeding programs, aiming for improved barley root system.

7 REFERENCES

Aida M., Beis D., Heidstra R., Willemsen V., Blilou I., Galinha C., ... Scheres B. (2004): The *PLETHORA* genes mediate patterning of the Arabidopsis root stem cell niche. *Cell* **119**, 109-120.

Athman A., Tanz S., Conn V.M., Jordans C., Mayo G.M., Ng W.W., ... Gilliham M. (2014): Protocol: a fast and simple in situ PCR method for localising gene expression in plant tissue. *Plant Methods* **10**, 29.

Badr A., Müller K., Schäfer-Pregl R., El Rabey H., Effgen S., Ibrahim H., ... Salamini F. (2000): On the Origin and Domestication History of Barley (*Hordeum vulgare*). *Molecular biology and evolution* **17**(4), 499-510.

Barnes E. (2017): *A Cellular and Molecular Characterization of Early Events in Plant Gravitropism*. Bachelor´s thesis, University of South Florida, USA.

Beeckman T., Burssens S., Inze D. (2001): The peri-cell-cycle in Arabidopsis. *Journal of Experimental Botany* **52**, 403-411.

Benjamins R., Scheres B. (2008): Auxin: the looping star in plant development. *Annual Review of Plant Biology* **59**, 443-65.

Benková E., Michniewicz M., Sauer M., Teichmann T., Seifertová D., Jurgens G., Friml J. (2003): Local, efflux-dependent auxin gradients as a common module for plant organ formation. *Cell* **115**, 591-602.

Bennett M.J., Marchant A., Green H.G., May S.T., Ward S.P., Millner P.A., ... Feldmann K.A. (1996): Arabidopsis *AUX1* gene: a permease-like regulator of root gravitropism. *Science* **273**, 948-950.

Berckmans B., Vassileva V., Schmid S.P., Maes S., Parizot B., Naramoto S., ... De Veylder L. (2011): Auxin-Dependent Cell Cycle Reactivation through Transcriptional Regulation of Arabidopsis E2Fa by Lateral Organ Boundary Proteins. *The Plant Cell* **23**, 3671-3683.

Berleth T., Jürgens G. (1993): The role of the *monopteros* gene in organising the basal body region of the Arabidopsis embryo. *Development* **118**, 575-587.

Bezdíčková A., Černý L., Klem K., Křováček J., Kudrna T., Míša P., ... Vašák J. (2005): *Jarní ječmen – základ úspěchu rostlinné výroby ČR v evropském soustátí*. 1st ed., Česká zemědělská univerzita v Praze, Czech Republic, 51 p.

Bian H.W., Xie Y.K., Guo F., Han N., Ma S., Zeng Z., ... Zhu M. (2012): Distinctive expression patterns and roles of the miRNA393/TIR1 homolog module in regulating flag leaf inclination and primary and crown root growth in rice (*Oryza sativa* L.). *The New Phytologist* **196**, 149-161.

Bittner V. (2008): *Škodlivé Organizmy Ječmene: Abiotická Poškození, Choroby, Škůdci*. 1st ed., Kurent, České Budějovice, Czech Republic, 54 p.

Blilou I., Xu J., Wildwater M., Willemsen V., Paponov I., Friml J., ... Scheres B. (2005): The PIN auxin efflux facilitator network controls growth and patterning in Arabidopsis roots. *Nature* **433**, 39-44.

Boer D.R., Freire-Rios A., van den Berg W.A., Saaki T., Manfield I.W., Kepinski S., ... Coll M. (2014): Structural Basis for DNA Binding Specificity by the Auxin-Dependent ARF Transcription Factors. *Cell* **156**(3), 577-589.

Bonoli M., Verardo V., Marconi E., Caboni M.F. (2004): Antioxidant phenols in barley (*Hordeum vulgare* L.) flour: comparative spectrophotometric study among extraction methods of free and bound phenolic compounds. *Journal of agricultural and food industry* **52**(16), 5195-5200.

Budhagatapalli N., Schedel S., Gurushidze M., Pencs S., Hiekel S., Rutten T., ... Hensel G. (2016): A simple test for the cleavage activity of customized endonucleases in plants. *Plant Methods* **12**, 71-83.

Causier B., Ashworth M., GuoW., Davies B. (2012): The TOPLESS interactome: a framework for gene repression in Arabidopsis. *Plant Physiology* **158**, 423-438.

Chandler J.W. (2016): Auxin response factors. *Plant, Cell and Environment* **39**, 1014-1028.

Chapman E.J., Estelle M. (2009): Mechanism of Auxin-regulated gene expression in plants. *Annual review of genetics* **43**, 265-285.

Cho H., Ryu H., Rho S., Hill K., Smith S., Audenaert D. (2014): A secreted peptide acts on BIN2-mediated phosphorylation of ARFs to potentiate auxin response during lateral root development. *Nature Cell Biology* **16**, 66-76.

Christian F., Krause E., Houslay M.D., Baillie G.S. (2014): PKA phosphorylation of p62/SQSTM1 regulates PB1 domain interaction partner binding. *Biochimica et Biophysica Acta (BBA) - Molecular Cell Research* **1843**(11), 2765-2774.

Ckurshumova W., Krogan N.T., Marcos D., Caragea A.E., Berleth T. (2012): Irrepressible, truncated auxin response factors. *Plant Signaling & Behavior* **7**(8), 1027-1030.

Clowes F.A.L. (1975): The quiescent centre. In: *The development and function of roots*. (Torrey J.G., Clarkson D.T., eds.), Academic, London, U.K., 3-19.

Coudert Y., Bès M., Le T.V., Pré M., Guiderdoni E., Gantet P. (2011): Transcript profiling of *crown rootless1* mutant stem base reveals new elements associated with crown root development in rice. *BMC Genomics* **12**, 1-12.

Coudert Y., Le V.A., Adam H., Bes M., Vignols F., Jouannic S., Guiderdoni E., Gantet P. (2015): Identification of CROWN ROOTLESS1-regulated genes in rice reveals specific and conserved elements of postembryonic root formation. *The New Phytologist* **206**, 243-254.

De Rybel B., Vassileva V., Parizot B., Demeulenaere M., Grunewald W., Audenaert D., ... Beeckman T. (2010): A novel Aux/IAA28 signaling cascade activates GATA23-dependent specification of lateral root founder cell identity. *Current Biology* **20**, 1697-1706.

De Smet I., Lau S., Voss U., Vanneste S., Benjamins R., Rademacher E..H, ... Beeckman T. (2010): Bimodular auxin response controls organogenesis in Arabidopsis. *Proceedings of the National Academy of Sciences of the USA* **107**, 2705-2710.

Dereeper A., Audic S., Claverie J.M., Blanc G. (2010): BLAST-EXPLORER helps you building datasets for phylogenetic analysis. *BMC Evolutionary Biology* **10**, 8.

Dereeper A., Guignon V., Blanc G., Audic S., Buffet S., Chevenet F., ... Gascuel O. (2008): Phylogeny.fr: robust phylogenetic analysis for the non-specialist. *Nucleic Acids Research* **36**, W465-W469.

Deskgen: https://www.deskgen.com/landing/#/ (29/4/2019).

Dharmasiri N., Dharmasiri S., Estelle M. (2005): The F-box protein TIR1 is an auxin receptor. *Nature* **435**, 441-445.

Die J.V., Gil J., Millan T. (2018): Genome-wide identification of the auxin response factor gene family in *Cicer arietinum*. *BMC Genomics* **19**(1), 301.

Diplock A.T., Aggett P.J., Ashwell M., Bornet F., Fern E.B., Roberfroid M.B. (1999): Scientific concepts of functional foods in Europe: Concensus document. *British Journal of Nutrition* **81**(S1), S1-S27.

Ensembl Plants Home: http://plants.ensembl.org/index.html (4/3/2019).

Fahn A. (1990): The Root. In: *Plant anatomy*. 4th ed., Pergamon Press, New York, U.S.A., 270-307.

Falasca G., Altamura M.M. (2003): Histological analysis of adventitious rooting in *Arabidopsis thaliana* (L.) Heynh seedlings. *Plant Biosystems* **137**(3), 265-273.

Feng Z., Zhu J., Du X., Cui X. (2012): Effects of three auxin-inducible LBD members on lateral root formation in *Arabidopsis thaliana*. *Planta* **236**(4), 1227-1237.

Fenster C.R., Boosalis M.G., Weihing, J.L. (1972): Date of planting studies of winter wheat and winter barley in relation to root and crown rot grain yields and quality. *Historical Research Bulletins of the Nebraska Agricultural Experiment Station* **250**, 153.

Fukaki H, Taniguchi N, Tasaka M. (2006): PICKLE is required for SOLITARY-ROOT/IAA14-mediated repression of ARF7 and ARF19 activity during Arabidopsis lateral root initiation. *Plant Journal* **48**, 380-389.

Geisler M., Murphy A.S. (2006): The ABC of auxin transport: the role of p-glycoproteins in plant development. *FEBS Letters* **580**, 1094-1102.

Gray W.M., Kepinski S., Rouse D., Leyser O., Estelle M. (2001): Auxin regulates SCF(TIR1)-dependent degradation of AUX/IAA proteins. *Nature* **414**, 271-276.

Guilfoyle T.J. (2015): The PB1 domain in auxin response factor and Aux/IAA proteins: a versatile protein interaction module in the auxin response. *The Plant Cell* **27**(1), 33-43.

Guilfoyle T.J., Hagen G. (2001): Auxin response factors. *Journal of Plant Growth Regulation* **20**, 281-291.

Guilfoyle T.J., Hagen G. (2007): Auxin response factors. *Current Opinion in Plant Biology* **10**(5), 453-460.

Gutierrez L., Bussell J.D., Pacurar D.I., Schwambach J., Pacurar M., Bellini C. (2009): Phenotypic plasticity of adventitious rooting in Arabidopsis is controlled by complex regulation of AUXIN RESPONSE FACTOR transcripts and microRNA abundance. *The Plant Cell* **21**, 3119-3132.

Gutierrez L., Mongelard G., Floková K., Pacurar D.I., Novák O., Staswick P., ... Bellini C. (2012): Auxin controls Arabidopsis adventitious root initiation by regulating jasmonic acid homeostasis. *The Plant Cell* **24**(6), 2515-2527.

Ha C.V., Le D.T., Nishiyama R., Watanabe Y., Sulieman S., Tran U.T., ... Tran L.S. (2013): The auxin response factor transcription factor family in soybean: genome-wide identification and expression analyses during development and water stress. *DNA Research* **20**, 511-524.

Hackett C. (1968): A study of the root system of barley. *New Phytologist* **67**, 287-299.

Hackett C., Rose D.A. (1972): A model of the extension and branching of a seminal root of barley, and its use in studying relations between root dimensions. *Australian journal of biological sciences* **25**, 669-677.

Hall T.A. (1999): BioEdit: a user-friendly biological sequence alignment editor and analysis program for Windows 95/98/NT. *Nucleic acids symposium series* **41**, 95-98.

Hardtke C.S., Ckurshumova W., Vidaurre D.P., Singh S.A., Stamatiou G., Tiwari S.B., ... Berleth T. (2004): Overlapping and non-redundant functions of the Arabidopsis auxin response factors MONOPTEROS and NONPHOTOTROPIC HYPOCOTYL 4. *Development* **131**, 1089-1100.

Harper R.M., Stowe-Evans E.L., Luesse D.R., Muto H., Tatematsu K., Watahiki M.K., Yamamoto K., Liscum E. (2000): The NPH4 locus encodes the auxin response factor ARF7, a conditional regulator of differential growth in aerial Arabidopsis tissue. *The Plant Cell* **12**(5), 757-770.

Hecht V.L., Temperton V.M., Nagel K.A., Rascher U., Pude R., Postma J.A. (2018): Plant density modifies root system architecture in spring barley (*Hordeum vulgare* L.) through a change in nodal root number. *Plant and Soil*, 1-22.

Himanen K., Boucheron E., Vanneste S., De Almeida Engler J., Inze D., Beeckman T. (2002): Auxin-mediated cell cycle activation during early lateral root initiation. *The Plant Cell* **14**, 2339-2351.

HMMER: https://www.ebi.ac.uk/Tools/hmmer/ (29/4/2019).

Hochholdinger F., Tuberosa R. (2009): Genetic and genomic dissection of maize root development and architecture. *Current Opinion in Plant Biology* **12**(2), 172-177.

Husbands A., Bell E.M., Shuai B., Smith H.M., Springer P.S. (2007): LATERAL ORGAN BOUNDARIES defines a new family of DNA-binding transcription factors and can interact with specific bHLH proteins. *Nucleic acids research* **35**(19), 6663-6671.

ICARDA (2005): Food barley: Importance, Uses and Local Knowledge. Proceedings of the International Workshop on Food Barley Improvement, International Center for Agricultural Research in the Dry Areas, Aleppo, Syria, 156 p.

Idehen E., Tang Y., Sang S. (2017): Bioactive phytochemicals in barley. *Journal of food and drug analysis* **25**(1), 148-161.

Inukai Y., Sakamoto T., Ueguchi-Tanaka M., Shibata Y., Gomi K., Umemura I., ... Matsuoka M. (2005): *CROWN ROOTLESS1*, which is essential for crown root formation in rice, is a target of an AUXIN RESPONSE FACTOR in auxin signaling. *The Plant Cell* **17**, 1387-1396.

Itoh J., Nonomura K., Ikeda K., Yamaki S., Inukai Y., Yamagishi H., ... Nagato Y. (2005): Rice Plant Development: from Zygote to Spikelet. *Plant & Cell Physiology* **46**(1), 23-47.

Jain M., Kaur N., Garg R., Thakur J.K., Tyagi A.K., Khurana J.P. (2006): Structure and expression analysis of early auxin-responsive Aux/IAA gene family in rice (*Oryza sativa*). *Functional and Integrative Genomics* **6**, 47-59.

Jansen L., Roberts I., De Rycke R., Beeckman T. (2012): Phloem-associated auxin response maxima determine radial positioning of lateral roots in maize. *Philosophical Transactions of The Royal Society B* **367**, 1525-1533.

Kepinski S., Leyser O. (2005): The Arabidopsis F-box protein TIR1 is an auxin receptor. *Nature* **435**, 446-451.

Kitomi Y., Ogawa A., Kitano H., Inukai Y. (2008): CRL4 regulates crown root formation through auxin transport in rice. *Plant Root* **2**, 19-28.

Krogan N.T., Marcos D., Weiner A.I., Berleth T. (2016): The auxin response factor MONOPTEROS controls meristem function and organogenesis in both the shoot and root through the direct regulation of PIN genes. *The New Phytologist* **212**(1), 42-50.

Kumar S., Stecher G., Tamura K. (2016): MEGA7: Molecular Evolutionary Genetics Analysis Version 7.0 for Bigger Datasets. *Molecular biology and evolution* **33**(7), 1870-1874.

Lazo G.R., Stein P.A., Ludwig R.A. (1991): A DNA-transformation-competent Arabidopsis genomic library in *Agrobacterium*. *Nature Biotechnology* **9**, 963-967.

Lee C., Kim J., Shin S.G., Hwang S. (2006): Absolute and relative QPCR quantification of plasmid copy number in Escherichia coli. *Journal of Biotechnology* **123**(3), 273-280.

Lee H.W., Cho C., Kim J. (2015): Lateral Organ Boundaries Domain16 and 18 Act Downstream of the AUXIN1 and LIKE-AUXIN3 Auxin Influx Carriers to Control Lateral Root Development in Arabidopsis. *Plant Physiology* **168**(4), 1792-1806.

Lee H.W., Kim N.Y., Lee D.J., Kim J. (2009): LBD18/ASL20 regulates lateral root formation in combination with LBD16/ASL18 downstream of ARF7 and ARF19 in Arabidopsis. *Plant Physiology* **151**, 1377-1389.

Li S., Xue L., Xu S., Feng H., An L. (2009): Mediators, Genes and Signaling in Adventitious Rooting. *The Botanical Review* **75**(2), 230-247.

Liu H., Wang S., Yu X., Yu J., He X., Zhang S., ... Wu P. (2005): ARL1, a LOB domain protein required for adventitious root formation in rice. *The Plant Journal* **43**, 47-56.

Liu P., Montgomery T.A., Fahlgren N., Kasschau K.D., Nonogaki H., Carrington J. (2007): Repression of AUXIN RESPONSE FACTOR10 by microRNA160 is critical for seed germination and post-germination stages. *The Plant Journal* **52**, 133-146.

Liu S., Wang J., Wang L., Wang X., Xue Y., Wu P., Shou H. (2009): Adventitious root formation in rice requires OsGNOM1 and is mediated by the OsPINs family. *Cell Research* **19**,1110-1119.

Livak K.J., Schmittgen T.D. (2001): Analysis of relative gene expression data using realtime quantitative PCR and 2(-Delta Delta C(T)) Method. *Methods* **25**, 402-408.

Ljung K., Bhalerao R.P., Sandberg G. (2001): Sites and homeostatic control of auxin biosynthesis in Arabidopsis during vegetative growth. *The Plant Journal* **28**, 465-474.

Ljung K., Hull A.K., Celenza J., Yamada M., Estelle M., Normanly J., Sandberg G. (2005): Sites and regulation of auxin biosynthesis in Arabidopsis roots. *The Plant Cell* **17**, 1090-1104.

Ludwig-Müller J. (2000): Indole-3-butyric acid in plant growth and development. *Plant Growth Regulation* **32**, 219-230.

Nagpal P., Ellis C.M., Weber H., Ploense S.E., Barkawi L.S., Guilfoyle T.J., ... Reed J.W. (2005): Auxin response factors ARF6 and ARF8 promote jasmonic acid production and flower maturation. *Development* **132**(18), 4107-4118.

Negi S., Ivanchenko M.G., Muday G.K. (2008): Ethylene regulates lateral root formation and auxin transport in Arabidopsis thaliana. *The Plant Journal* **55**, 175-187.

Niu J., Bi Q., Deng S., Chen H., Yu H., Wang L., Lin S. (2018): Identification of AUXIN RESPONSE FACTOR gene family from *Prunus sibirica* and its expression analysis during mesocarp and kernel development. *BMC Plant Biology* **18**(1), 21.

Mallory A.C., Bartel D.P., Bartel B. (2005): MicroRNA-directed regulation of Arabidopsis AUXIN RESPONSE FACTOR17 is essential for proper development and modulates expression of early auxin response genes. *Plant Cell* **17**, 1360-1375.

Marthe C., Kumlehn J., Hensel G. (2015): Barley (*Hordeum vulgare* L.) transformation using immature embryos. In: *Agrobacterium Protocols*, Vol. 1. *Methods in Molecular Biology*, Vol. 1223 (Wang K., ed.), Springer Science+Business Media, New York, U.S.A., p. 71-83.

Martínez M., Motilva M.J., López de Las Hazas M.C., Romero M.P., Vaculova K., Ludwig I.A. (2018): Phytochemical composition and β-glucan content of barley genotypes from two different geographic origins for human health food production. *Food chemistry* **245**, 61-70.

Meng F., Xiang D., Zhu J., Li Y., Mao C. (2019): Molecular Mechanisms of Root Development in Rice. *Rice (New York, N.Y.)* **12**(1), 1.

Mun J.H., Yu H.J., Shin J.Y., Oh M., Hwang H.J., Chung H. (2012): Auxin response factor gene family in *Brassica rapa*: genomic organization, divergence, expression, and evolution. *Molecular Genetics and Genomics* **287**, 765-784.

Okushima Y., Fukaki H., Onoda M., Theologis A., Tasaka M. (2007): ARF7 and ARF19 regulate lateral root formation via direct activation of LBD/ASL genes in Arabidopsis. *The Plant Cell* **19**, 118-130.

Okushima Y., Overvoorde P.J., Arima K., Alonso J.M., Chan A., Chang C., ... Theologis A. (2005): Functional genomic analysis of the AUXIN RESPONSE FACTOR gene family members in *Arabidopsis thaliana*: unique and overlapping functions of ARF7 and ARF19. *The Plant Cell* **17**(2), 444-463.

Overvoorde P., Fukaki H., Beeckman T. (2010): Auxin Control of Root Development. *Cold Spring Harbor Perspectives in Biology* **2**(6), a001537.

Pallotta M.A., Graham R.D., Langridge P., Sparrow D.H.B., Barker S.J. (2000): RFLP mapping of manganese efficiency in barley. *Theoretical and Applied Genetics* **101**, 1100-1108.

Pesquet E., Barbier O., Ranocha P., Jauneau A., Goffner D. (2004): Multiple gene detection by *in situ* RT-PCR in isolated plant cells and tissues. *The plant journal* **39**(6), 947-959.

Petrásek J., Mravec J., Bouchard R., Blakeslee J.J., Abas M., Seifertová D., ... Friml J. (2006): PIN proteins perform a rate-limiting function in cellular auxin efflux. *Science* **312**, 914-918.

Pfaffl M.W. (2001): A new mathematical model for relative quantification in real-time RT-PCR. *Nucleic Acids Research* **29**(9), e45.

Piya S., Shrestha S.K., Binder B., Stewart C.N., Hewezi T. (2014): Protein-protein interaction and gene co-expression maps of ARFs and Aux/IAAs in Arabidopsis. *Frontiers in Plant Science* **5**, 744.

Plant Transcription Factor Database: http://planttfdb.cbi.pku.edu.cn/ (29/4/2019).

Porco S., Larrieu A., Du Y., Gaudinier A., Goh T., Swarup K., ... Bennett M.J. (2016): Lateral root emergence in Arabidopsis is dependent on transcription factor LBD29 regulation of auxin influx carrier LAX3. *Development* **143**(18), 3340-3349.

Przybecki Z., Siedlecka E., Filipecki M., Urbanczyk-Wochniak E. (2006): *In situ* reverse transcription PCR on plant tissues. *Methods in molecular biology* **334**, 181-198.

Rademacher E.H., Möller B., Lokerse A.S., Llavata-Peris C.I., van den Berg W., Weijers D. (2011): A cellular expression map of the Arabidopsis AUXIN RESPONSE FACTOR gene family. *The Plant Journal* **68**(4), 597-606.

Remington D.L., Vision T.J., Guilfoyle T.J., Reed, J.W. (2004): Contrasting modes of diversification in the Aux/IAA and ARF gene families. *Plant Physiology* **135**, 1738-1752.

Romberger J.A., Hejnowicz Z., Hill J.F. (1993): The Root. In: *Plant Structure: Function and Development*. Springer-Verlag, Berlin, Germany, 315-351.

Rozen S., Skaletsky H.J. (2000): Primer3 on the WWW for general users and for biologist programmers. In: *Bioinformatics Methods and Protocols: Methods in Molecular Biology* (Krawetz S., Misener S., eds.), Humana Press, Totowa, New Jersey, U.S.A., p. 365-386.

Saini S., Sharma I., Kaur N., Pati P.K. (2013): Auxin: a master regulator in plant root development. *Plant Cell Reports* **32**(6), 741-757.

Schlereth A., Möller B., Liu W., Kientz M., Flipse J., Rademacher E.H., ... Weijers D. (2010): MONOPTEROS controls embryonic root initiation by regulating a mobile transcription factor. *Nature* **464**(7290), 913-916.

SCQ – The science creative quarterly: www.scq.ubc.ca/image-bank/ (22. 4. 2019).

Sedláček T., Svobodová L., Psota V., Matušinsky P. (2017): *Šlechtění jarního ječmene na kvalitu pro výrobu CHZO "České pivo" a rezistenci vůči hlavním houbovým chorobám*. 1st ed., MSD, Brno, Czech Republic, 27 p.

Shen C., Wang S., Bai Y., Wu Y., Zhang S., Chen M., ... Qi Y. (2010): Functional analysis of the structural domain of ARF proteins in rice (*Oryza sativa* L.). *Journal of Experimental Botany* **61**(14), 3971-3981.

Shen C., Yue R., Sun T., Zhang L., Xu L., Tie S., ... Yang Y. (2015): Genome-wide identification and expression analysis of auxin response factor gene family in *Medicago truncatula*. *Frontiers in plant science* **6**, 73.

Shi Z.H., Zhang C., Xu X.F., Zhu J., Zhou Q., Ma L.J., Niu J., Yang Z.N. (2015): Overexpression of AtTTP affects ARF17 expression and leads to male sterility in Arabidopsis. *PloS one* **10**(3), e0117317.

Singh V.K., Rajkumar M.S., Garg R., Jain M. (2017): Genome-wide identification and co-expression network analysis provide insights into the roles of auxin response factor gene family in chickpea. *Scientific Reports* **7**(1), 10895.

Smith A.M., Coupland G., Dolan L., Harberd N., Jones J., Martin C., ... Amey A. (2010): Development. In: *Plant Biology*. (Hill S., Powis H., Strange L. eds.), Garland Science, New York, U.S.A., p. 301-376.

Sorin C., Bussell J.D., Camus I., Ljung K., Kowalczyk M., Geiss G., ... Bellini C. (2005): Auxin and light control of adventitious rooting in Arabidopsis require ARGONAUTE1. *The Plant Cell* **17**(5), 1343-1359.

Statista – The Statistics Portal: https://www.statista.com/ (20/8/2018).

Stepanova A.N., Robertson-Hoyt J., Yun J., Benavente L.M., Xie D.Y., Dolezal K., ... Alonso J.M. (2008): TAA1-mediated auxin biosynthesis is essential for hormone crosstalk and plant development. *Cell* **133**, 177-191.

Stepanova A.N., Yun J., Robles L.M., Novak O., He W., Guo H., ... Alonso J.M. (2011): The Arabidopsis YUCCA1 flavin monooxygenase functions in the indole-3-pyruvic acid branch of auxin biosynthesis. *The Plant Cell* **23**, 3961-3973.

Sullivan P., Arendt E., Gallagher E. (2013): The increasing use of barley and barley by-products in the production of healthier baked goods. *Trends in Food Science and Technology* **29**, 124-134.

Swarup K., Benková E., Swarup R., Casimiro I., Peret B., Yang Y., ... Bennett M.J. (2008): The auxin influx carrier LAX3 promotes lateral root emergence. *Nature Cell Biology* **10**, 946-954.

Swarup R., Friml J., Marchant A., Ljung K., Sandberg G., Palme K., Bennett M. (2001): Localization of the auxin permease AUX1 suggests two functionally distinct hormone transport pathways operate in the Arabidopsis root apex. *Genes & Development* **15**, 2648-2653.

Tang Y., Bao X., Liu K., Wang J., Zhang J., Feng Y., ... Li C. (2018): Genome-wide identification and expression profiling of the auxin response factor (ARF) gene family in physic nut. *PLoS One* **13**(8), e0201024.

Tiwari S.B., Hagen G., Guilfoyle T.J. (2003): The roles of auxin response factor domains in auxin-responsive transcription. *The Plant Cell* **15**, 533-543.

Tiwari S.B., Hagen G., Guilfoyle T.J. (2004): Aux/IAA proteins contain a potent transcriptional repression domain. *Plant Cell* **16**, 533-543.

Ulmasov T., Hagen G., Guilfoyle T.J. (1997): ARF1, a Transcription Factor That Binds to Auxin Response Elements. *Science* **276**(5320), 1865-1868.

Urbańczyk-Wochniak E., Filipecki M., Przybecki Z. (2002): A useful protocol for *in situ* RT-PCR on plant tissues. *Cellular and molecular biology letters* **7**(1), 7-18.

USDA (2018): World Agricultural Production. WAP 8-18, United States Department of Agriculture, U.S.A., 34 p.

Varaud E., Brioudes F., Szécsi J., Leroux J., Brown S., Perrot-Rechenmann C., Bendahmane M. (2011): AUXIN RESPONSE FACTOR8 regulates Arabidopsis petal growth by interacting with the bHLH transcription factor BIGPETALp. *The Plant Cell* **23**(3), 973-983.

Vernoux T., Brunoud G., Farcot E., Morin V., Van den Daele H., Legrand J., Traas J. (2011): The auxin signalling network translates dynamic input into robust patterning at the shoot apex. *Molecular Systems Biology* **7**, 508.

Vernoux T., Truskina J., Han J., Galvan-Ampudia C.S., Lainé S., Brunoud G., ... Bishopp A. (2018): A network of transcriptional repressors mediates auxin response specificity. *bioRxiv*, 448860.

Vert G., Walcher C.L., Chory J., Nemhauser J.L. (2008): Integration of auxin and brassinosteroid pathways by Auxin Response Factor 2. *Proceedings of the National Academy of Sciences of the USA* **105**, 9829-9834.

Vlamis J., Williams D.E. (1962): Ion Competition in Manganese Uptake by Barley Plants. *Plant Physiol* **37**, 650-655.

Wan S., Li W., Zhu Y., Liu Z., Huang W., Zhan J. (2014): Genome-wide identification, characterization and expression analysis of the auxin response factor gene family in *Vitis vinifera*. *Plant Cell Reports* **33**(8), 1365-1375.

Wang D., Pei K., Fu Y., Sun Z., Li S., Liu H., Tao Y. (2007): Genome-wide analysis of the auxin response factors (ARF) gene family in rice (*Oryza sativa*). *Gene* **394**(1-2), 13-24.

Wang J.W., Wang L.J., Mao Y.B., Cai W.J., Xue H.W., Chen X.Y. (2005): Control of root cap formation by microRNA-targeted auxin response factors in Arabidopsis. *Plant Cell* **17**, 2204-2216.

Wang Y., Deng D., Shi Y., Miao N., Bian Y., Yin Z. (2012): Diversification, phylogeny and evolution of auxin response factor (ARF) family: insights gained from analyzing maize ARF genes. *Molecular Biology Reports* **39**, 2401-2415.

Wang Y., Wang D., Gan T., Liu L., Long W., Wang Y., ... Wan J. (2016): CRL6, a member of the CHD protein family, is required for crown root development in rice. *Plant Physiology and Biochemistry* **105**, 185-194.

Wieczorek K. (2015): Detection and Visualization of Specific Gene Transcripts by *in situ* RT-PCR in Nematode-Infected Arabidopsis Root Tissue. *Bio-protocol* **5**(18), pii:e1597.

Willems E., Leyns L., Vandesompele J. (2008): Standardization of real-time PCR gene expression data from independent biological replicates. *Analytical Biochemistry* **379**, 127-129.

Williams L., Carles C.C., Osmont K.S., Fletcher J.C. (2005): A database analysis method identifies an endogenous trans-acting short-interfering RNA that targets the Arabidopsis ARF2, ARF3, and ARF4 genes. *Proceedings of the National Academy of Sciences of the U.S.A.* **102**, 9703-9708.

Wilmoth J.C., Wang S., Tiwari S.B., Joshi A.D., Hagen G., Guilfoyle T.J., ... Reed J.W. (2005): NPH4/ARF7 and ARF19 promote leaf expansion and auxin-induced lateral root formation. *The Plant Journal: for cell and molecular biology* **43**(1), 118-130.

Wu M.F., Tian Q., Reed J.W. (2006): Arabidopsis micro-RNA167 controls patterns of ARF6 and ARF8 expression, and regulates both female and male reproduction. *Development* **133**, 4211-4218.

Yang J., Tian L., Sun M.X., Huang X.Y., Zhu J., Guan Y.F., Jia Q.S., Yang Z.N. (2013): AUXIN RESPONSE FACTOR17 is essential for pollen wall pattern formation in Arabidopsis. *Plant physiology* **162**(2), 720-731.

Zhang H., Cao N., Dong C., Shang Q. (2017): Genome-wide Identification and Expression of ARF Gene Family during Adventitious Root Development in Hot Pepper (*Capsicum annuum*). *Horticultural Plant Journal* **3**(4), 151-164.

Zolman B.K., Yoder A., Bartel B. (2000): Genetic analysis of indole-3-butyric acid responses in *Arabidopsis thaliana* reveals four mutant classes. *Genetics* **156**, 1323-1337.

Zou Y., Liu X., Wang Q., Chen Y., Liu C., Qiu Y., Zhang W. (2014): OsRPK1, a novel leucine-rich repeat receptor-like kinase, negatively regulates polar auxin transport and root development in rice. *Biochimica et Biophysica Acta* **1840**, 1676-1685.

Zouine M., Fu Y., Chateigner-Boutin A.L., Mila I., Frasse P., Wang H., Bouzayen M. (2014): Characterization of the tomato ARF gene family uncovers a multi-levels post-transcriptional regulation including alternative splicing. *PLoS One* **9**, e84203.

8 LIST OF ABBREVIATIONS

ARF	AUXIN RESPONSE FACTOR proteins
AUX	AUXIN RESISTANT auxin transporter
Aux/IAA	AUXIN/INDOLE-3-ACETIC ACID proteins
CR	crown-root
CRISPR	clustered regularly interspaced short palindromic repeats
CRL	CROWN ROOTLESS proteins
CRP	crown-root primordium
DAG	day after germination
DBD	DNA-binding domain
DD	Dimerization domain
GH	*Gretchen Hagen* genes
gRNA	guide RNA
IAA	indole-3-acetic acid
LBD	LATERAL ORGAN BOUNDARIES transcription factor
LR	lateral root
LRP	lateral root primordium
MR	middle region in ARF structure
PAT	polar auxin transport
PB1	Phox and Bem1 protein domain
PIN	PIN-FORMED auxin transporters